Spectroscopic methods for
Protein structure determination
Protein folding mechanism, kinetics, thermodynamics
Ligand binding studies
Measuring Catalytic activity and carry out mechanistic studies of enzymes
Detect (transient) Conformational changes

Spectroscopic methods:

Absorbance spectroscopy
Fluorescence spectroscopy
Infrared Spectroscopy
Nuclear magnetic resonance
Electron paramagnetic spectroscopy
.....

General Mode of Action of Proteins:

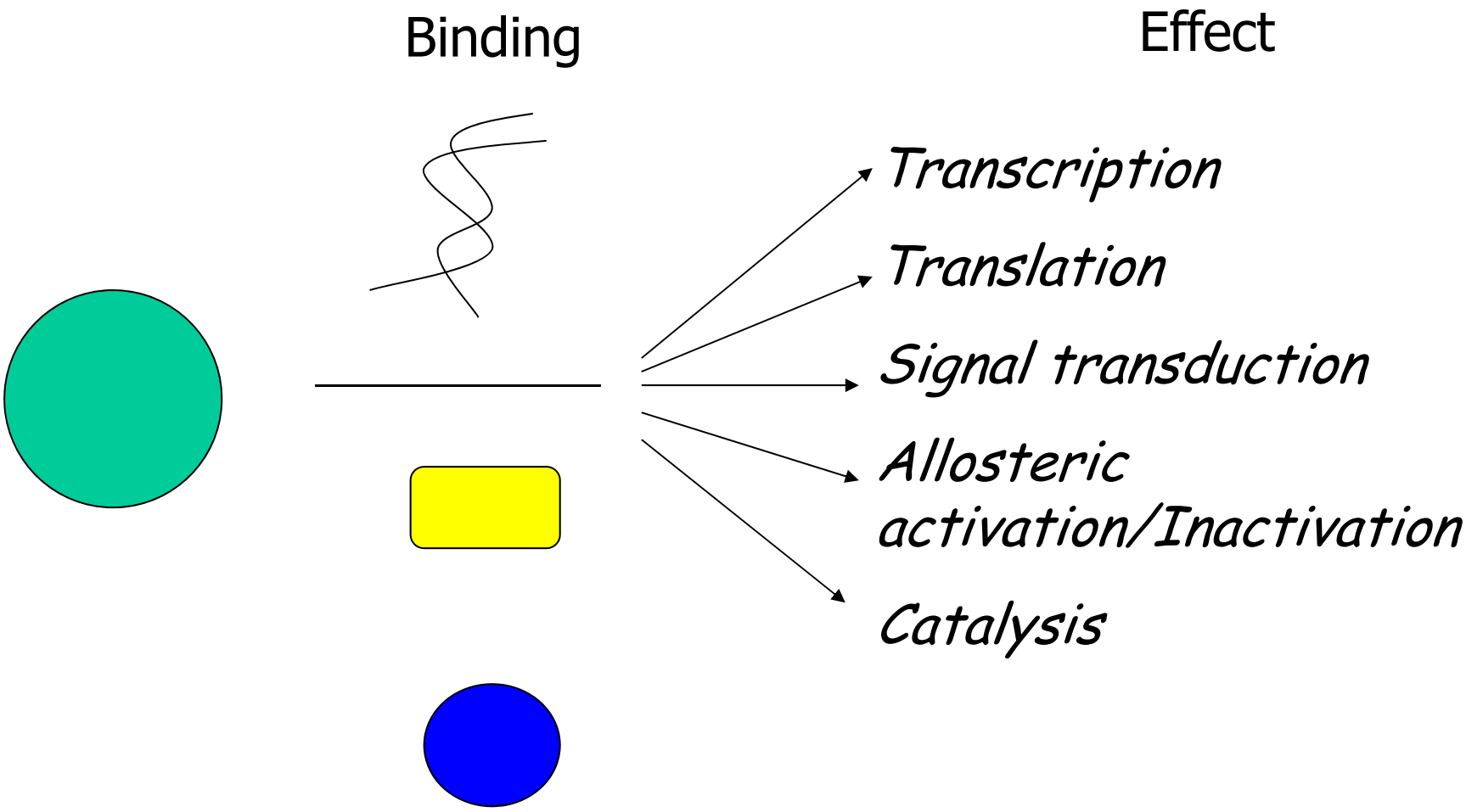

The description of a biological process includes the description of how the energy of the system changes during the process, which requires equilibrium (steady-state) and kinetic studies

$$A + B \underset{k_r}{\overset{k_f}{\rightleftharpoons}} C + D$$

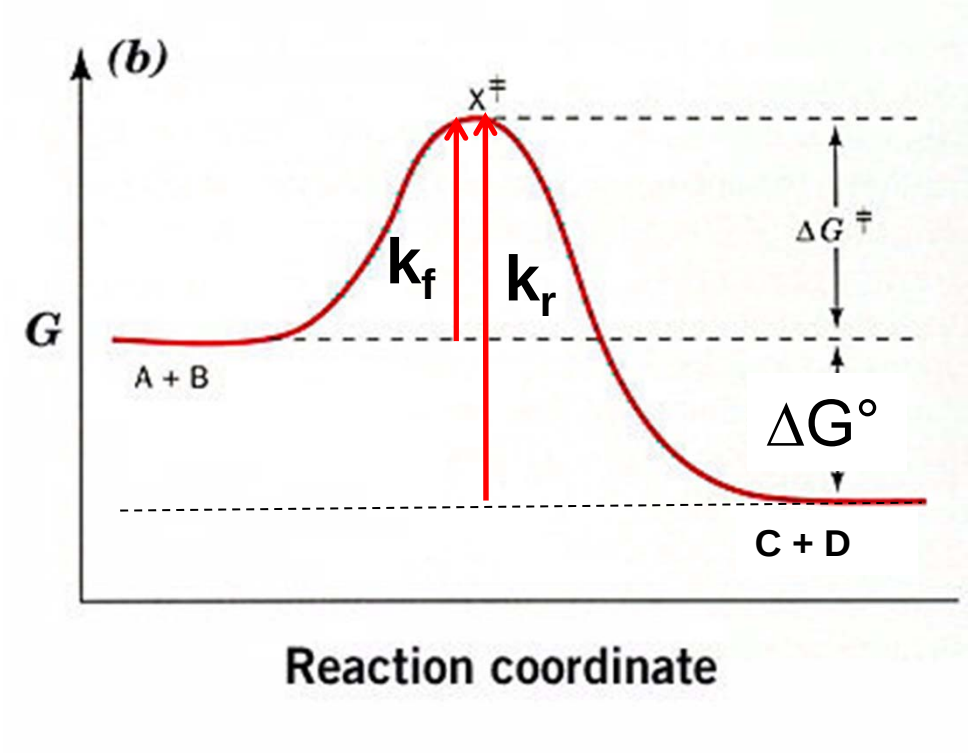

At equilibrium:

$$K_{eq} = \frac{[C]_{eq} * [D]_{eq}}{[A]_{eq} * [B]_{eq}} = \frac{k_f}{k_r}$$

$$\Delta G^\circ = - RT \, ln \, K_{eq}$$

Rate constants

$$k = \frac{\kappa k_B T}{h} e^{\frac{-\Delta G^\ddagger}{RT}}$$

Free energy profile and kinetic scheme of enzyme-catalyzed reactions: multistep processes

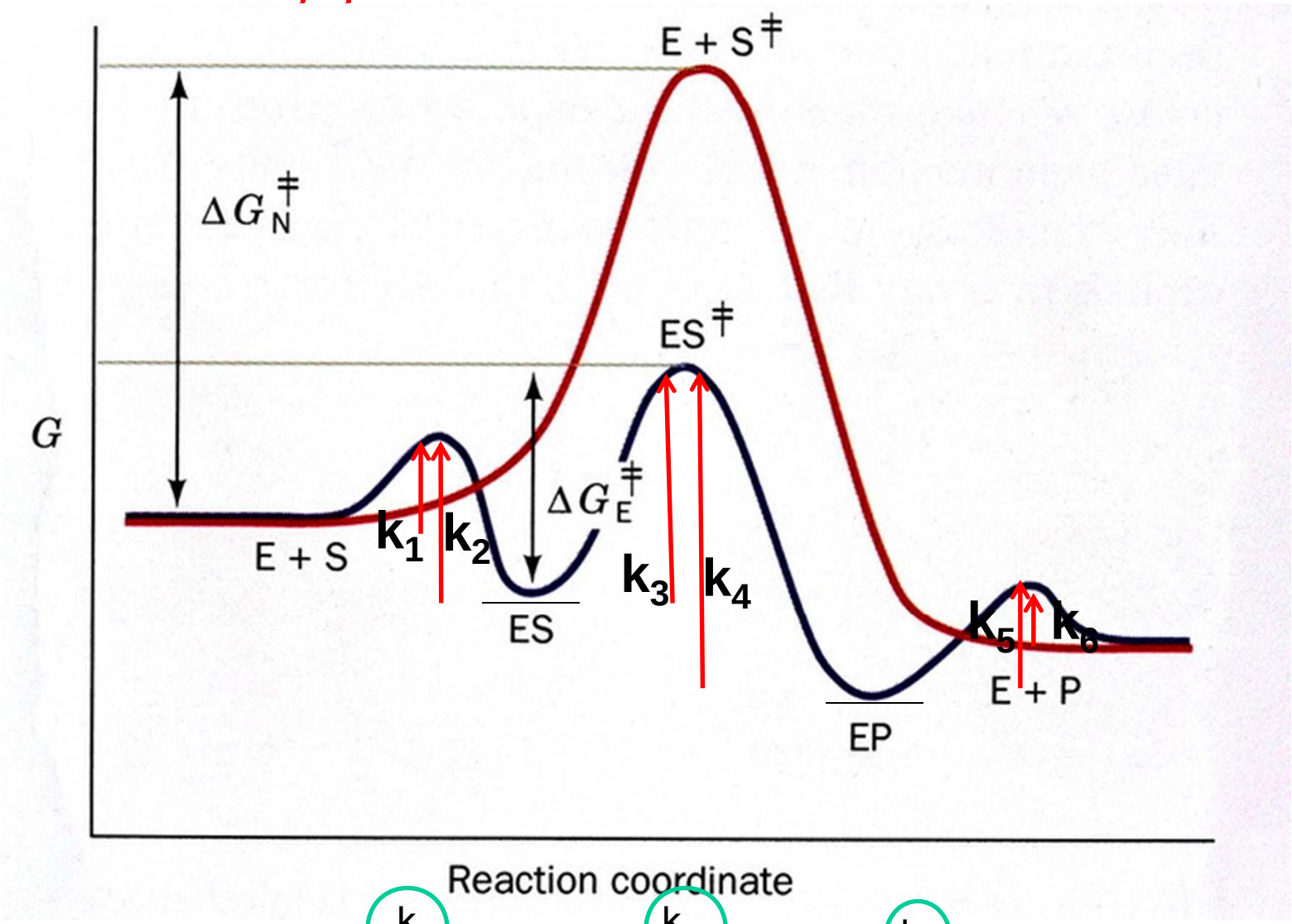

Discontinuous methods for the Detection and Quantitation of the reagents are time-consuming, and they often require:

- Chromatographic separation of the reaction components at different times followed by:

- Detection and Quantitation of the reaction components by UV, Vis Absorbance, Fluorescence; Conductivity; Radioactivity, ...

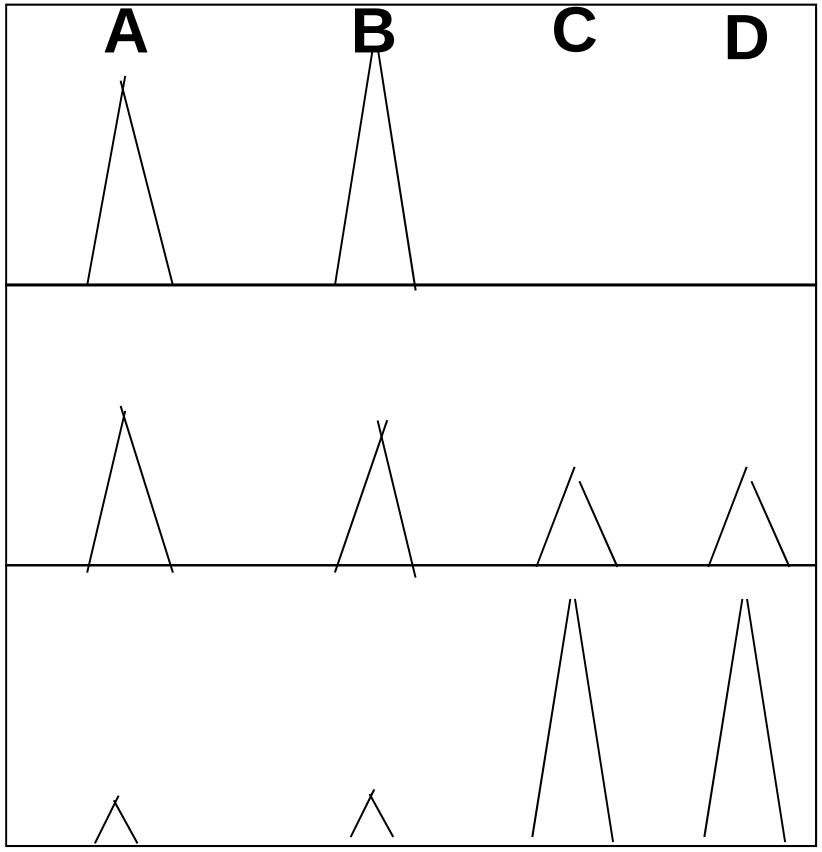

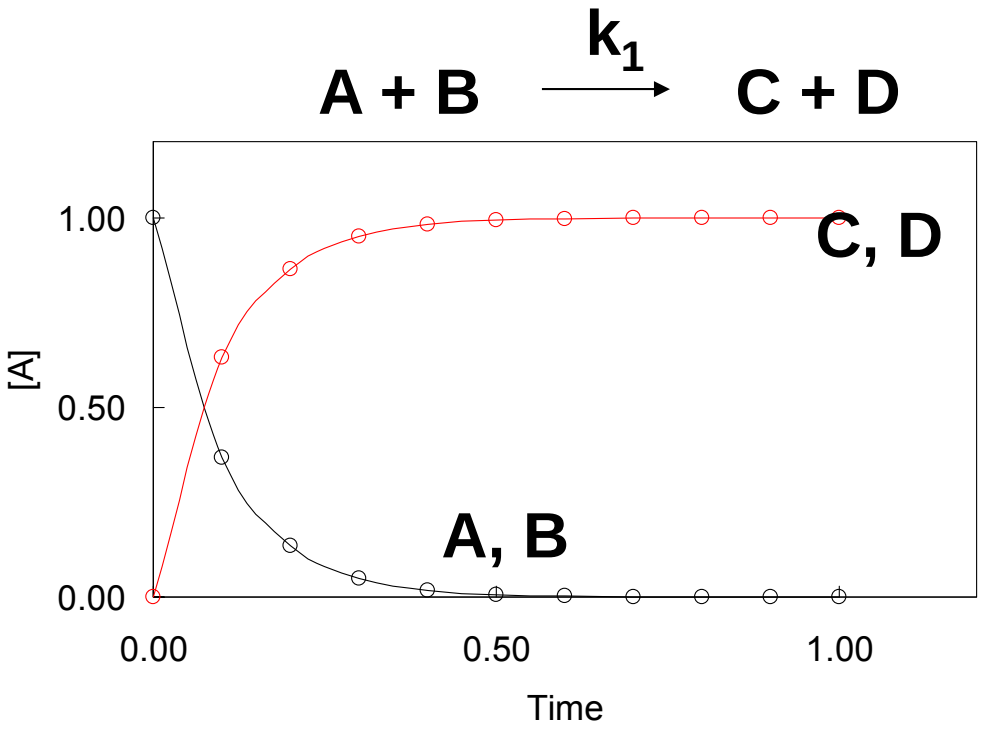

Discontinuous methods may not allow the isolation and identification of (unstable) intermediates or products including protein-protein, protein-ligand complexes, etc.

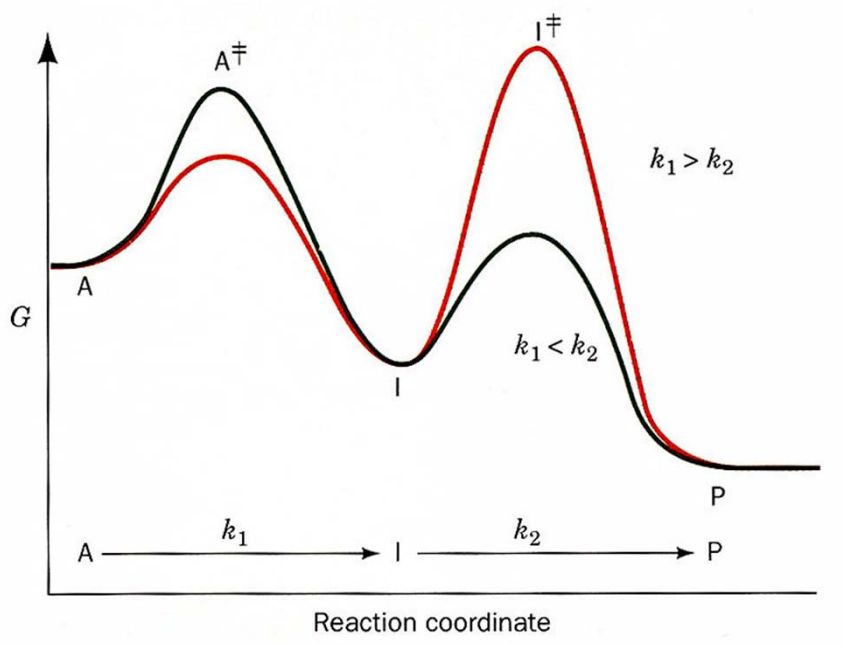

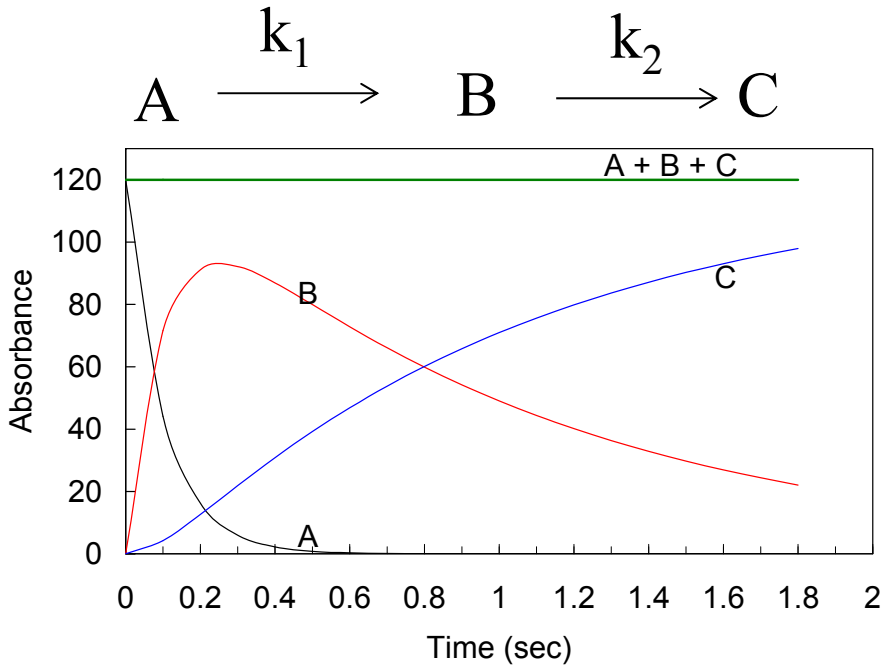

Continuous methods that do not require sample manipulation are:

- less time consuming,
- (usually) less expensive and more precise (lower number of steps where experimental error can be introduced)

Spectroscopic methods may allow the direct observation of the species present in solution IF

- the signals (spectra) of A, B, C, etc. can be distinguished from each other
- the intensity of the signals can be related to the concentrations of A, B, C, etc.
- the signals can be acquired very rapidly to monitor changes over time

Absorbance and fluorescence spectroscopies can allow the rapid acquisition of signals with high sensitivity.

The absorption and fluorescence spectra often allow to identify and quantify the chemical species in solution

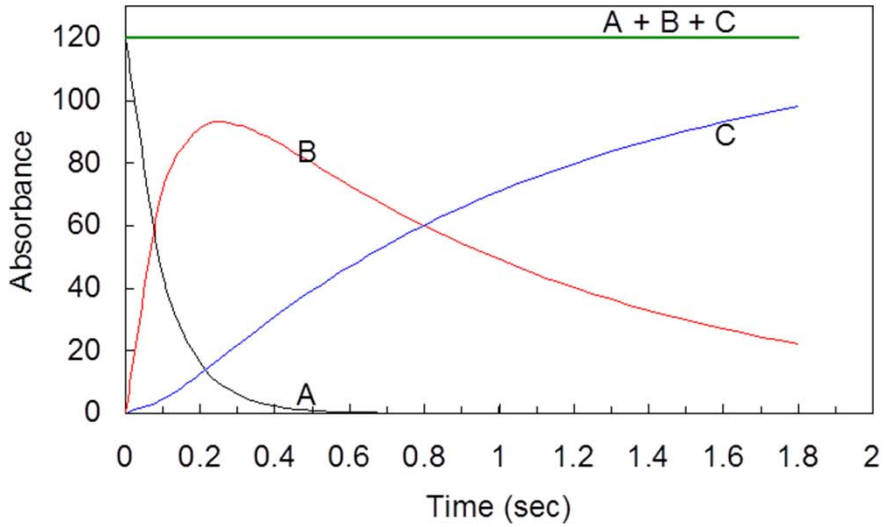

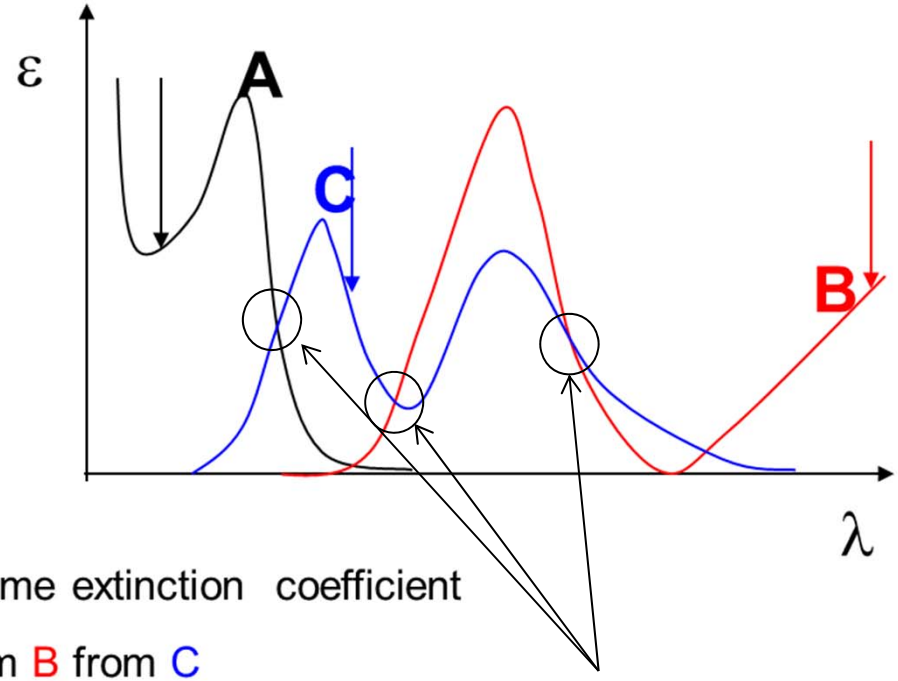

Green: At a given wavelength A, B, C have the same extinction coefficient

At different wavelengths: we can distinguish A from B from C

Isosbestic points

Protein folding and conformational changes can be described through equilibrium and kinetic approaches

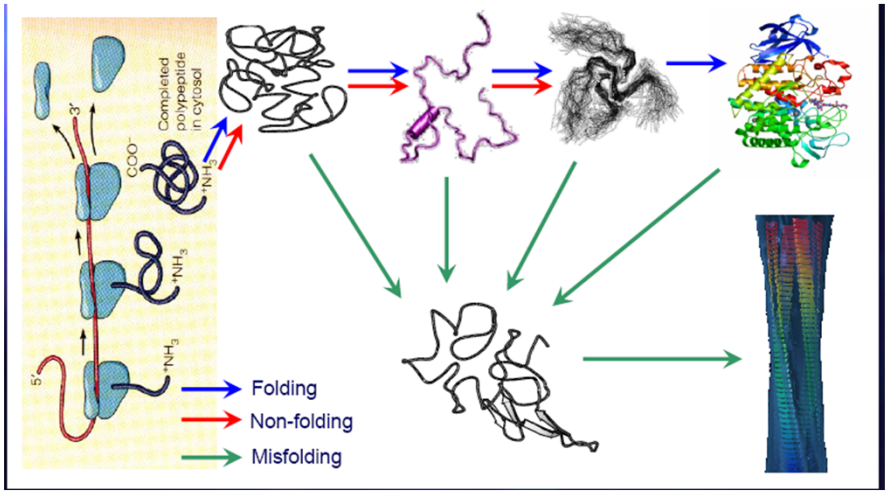

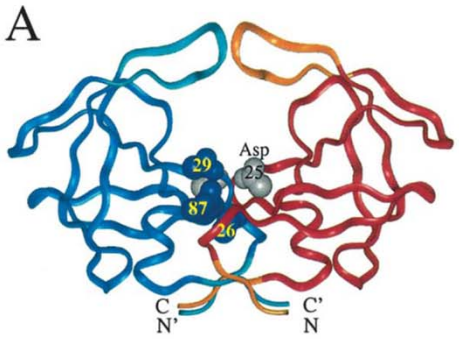

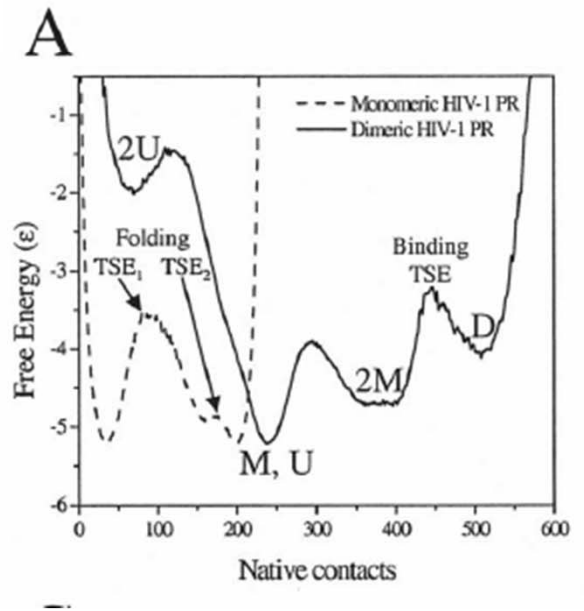

Outline

- Basic principles of absorbance and fluorescence spectroscopies
- Applications of absorbance and fluorescence spectroscopies to study the properties of proteins with special reference to the characterization of enzyme reactions

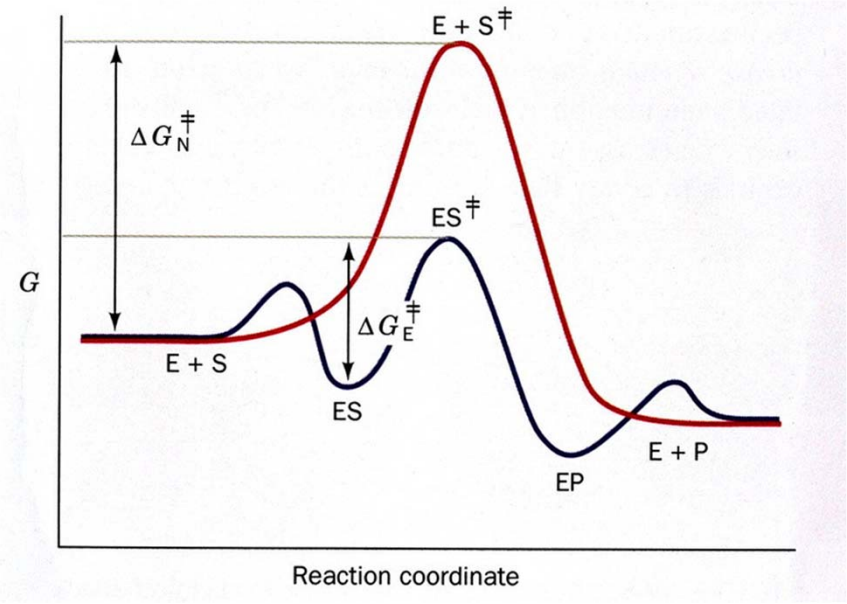

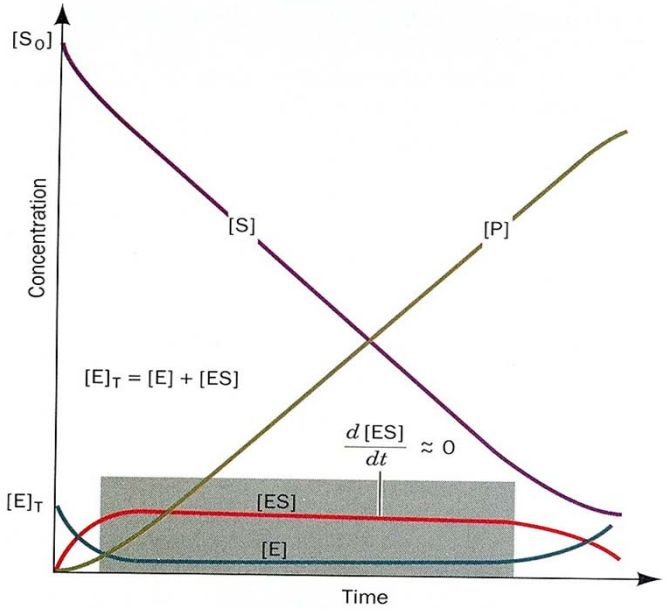

$$E + S \underset{k_2}{\overset{k_1}{\rightleftharpoons}} ES \underset{k_4}{\overset{k_3}{\rightleftharpoons}} EP \underset{k_6}{\overset{k_5}{\rightleftharpoons}} E+P$$

Absorbance and fluorescence spectroscopies use a narrow (200-800 nm) region of the electromagnetic spectrum

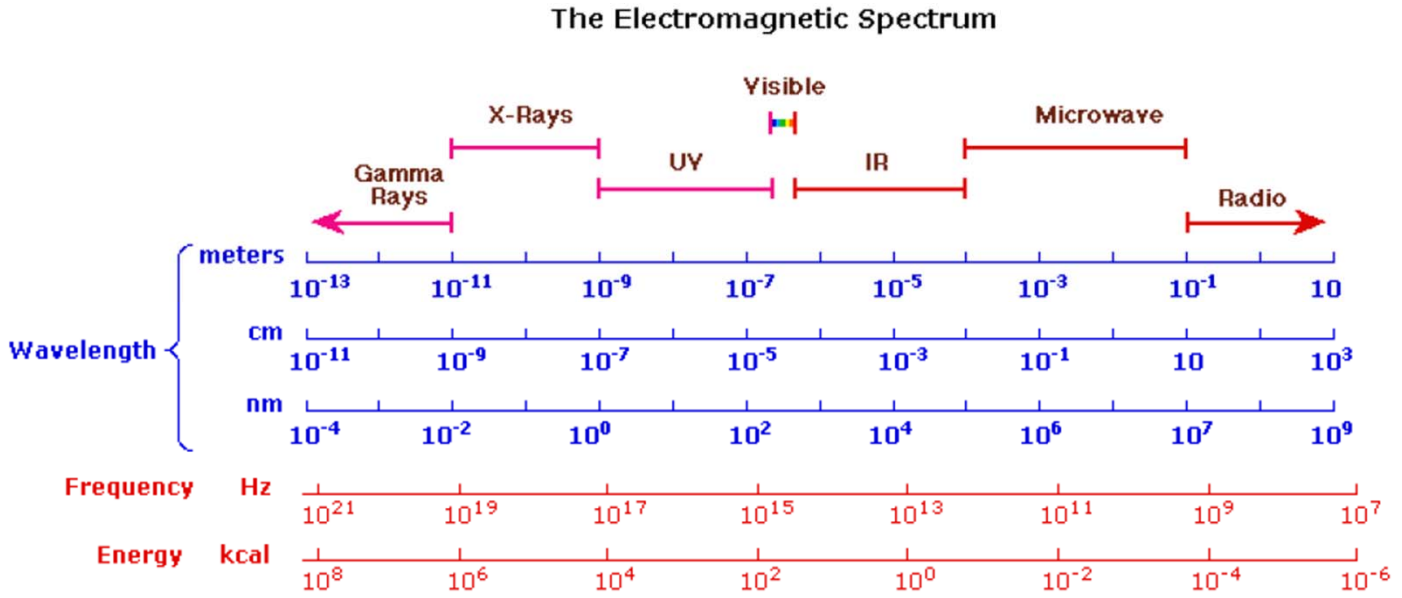

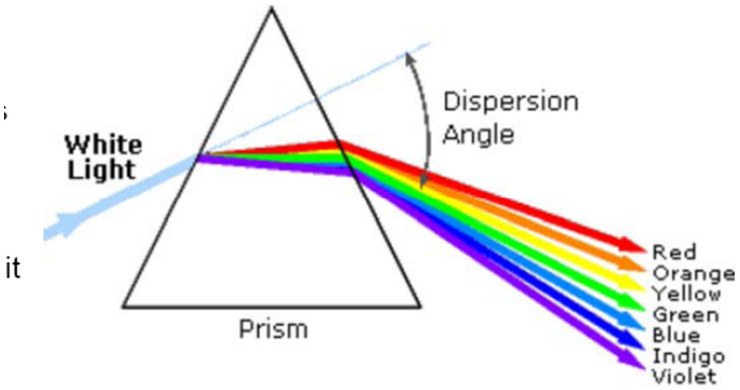

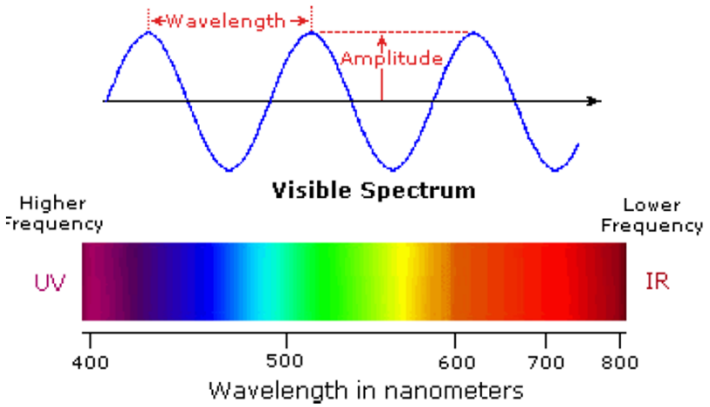

- **Violet:** 400 - 420 nm
- **Indigo:** 420 - 440 nm
- **Blue:** 440 - 490 nm
- **Green:** 490 - 570 nm
- **Yellow:** 570 - 585 nm
- **Orange:** 585 - 620 nm
- **Red:** 620 - 780 nm

Basic principles of absorbance and fluorescence spectroscopies

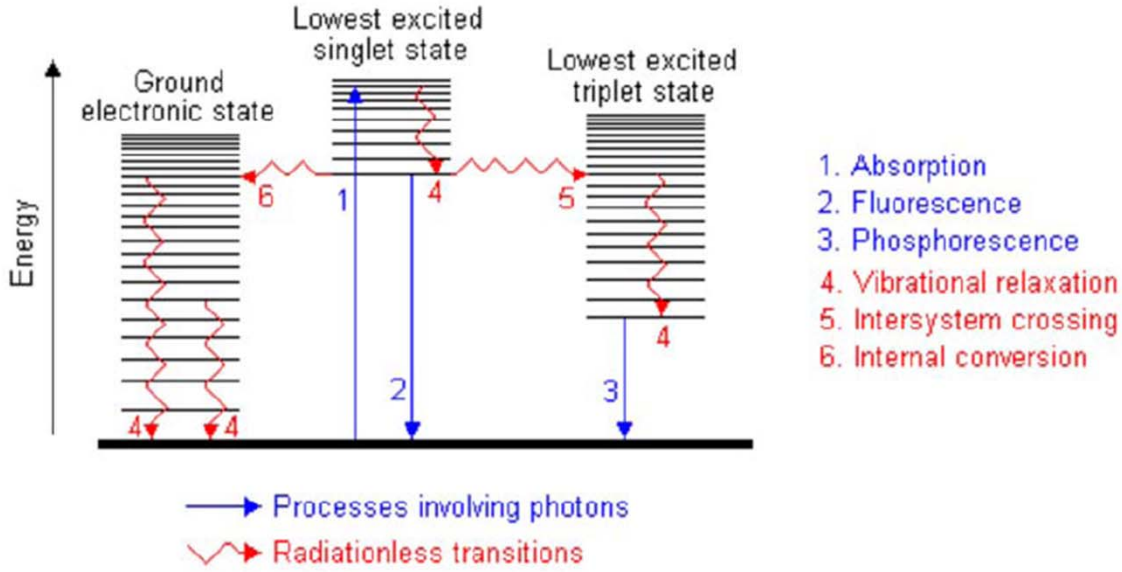

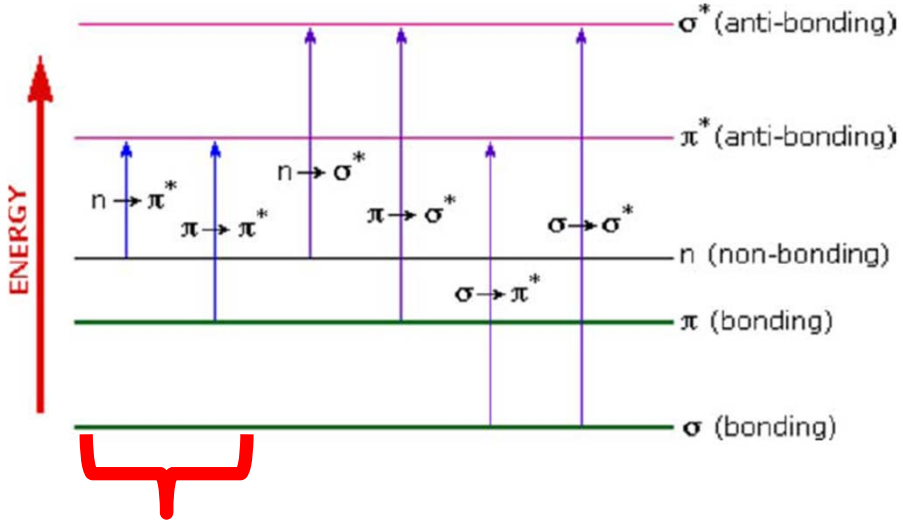

Only some electronic transitions are possible when a sample is irradiated with near UV – visible light

- A light absorbing compound is called a «chromophore»

- A large number of compounds absorb in the near UV region

- Compounds with (several) conjugated double bonds yield complex absorbance spectra, with absorption also in the visible region

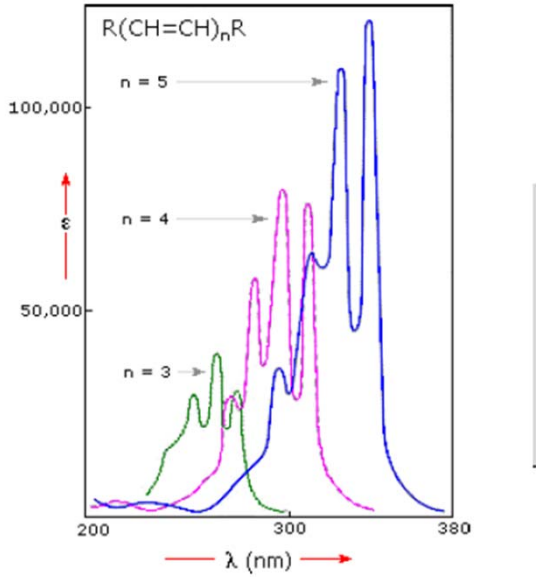

- The absorption spectrum of a compound (especially in the visible region) allows its identification and quantitation

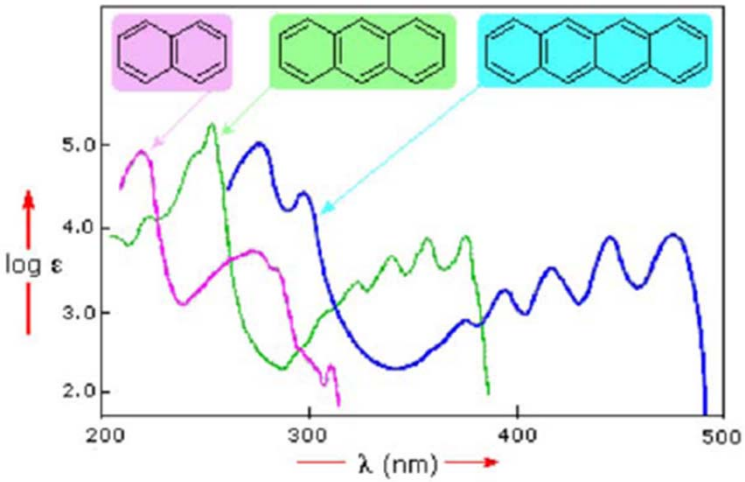

Several natural compounds absorb light in the visible region of the spectrum

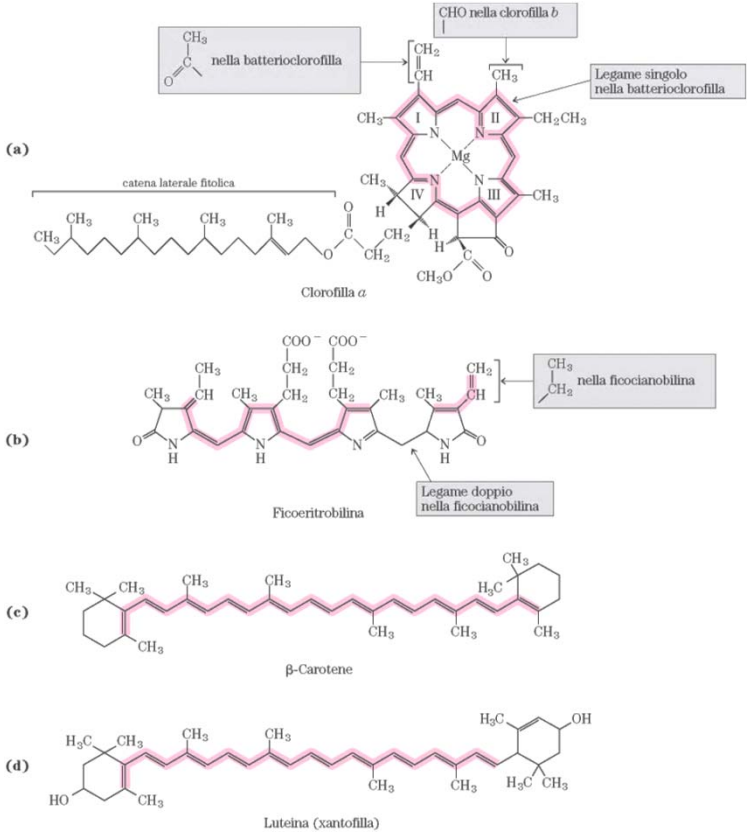

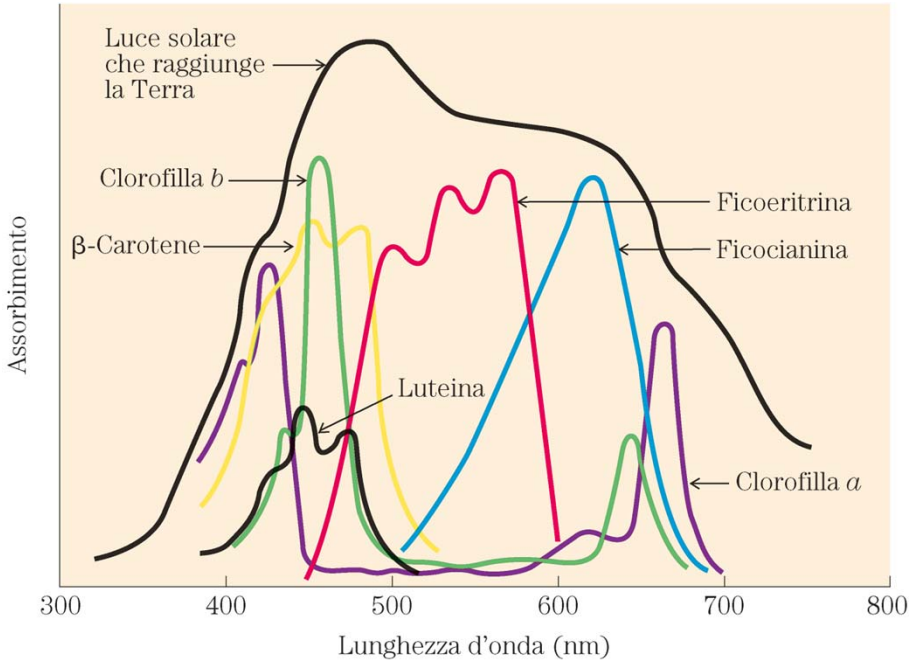

Light-absorbing pigments in photosystems

Several biological compounds are also fluorescent

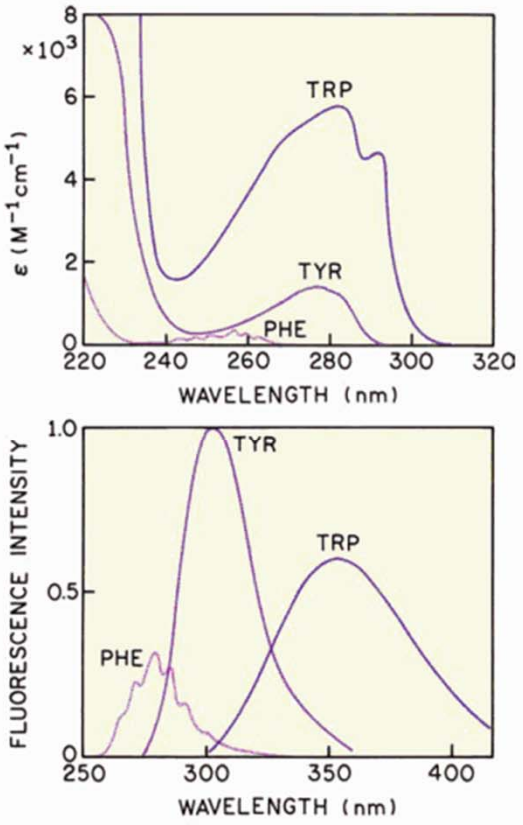

Figure 3.2. Absorption and emission spectra of the fluorescent amino acids in water of pH 7.0.

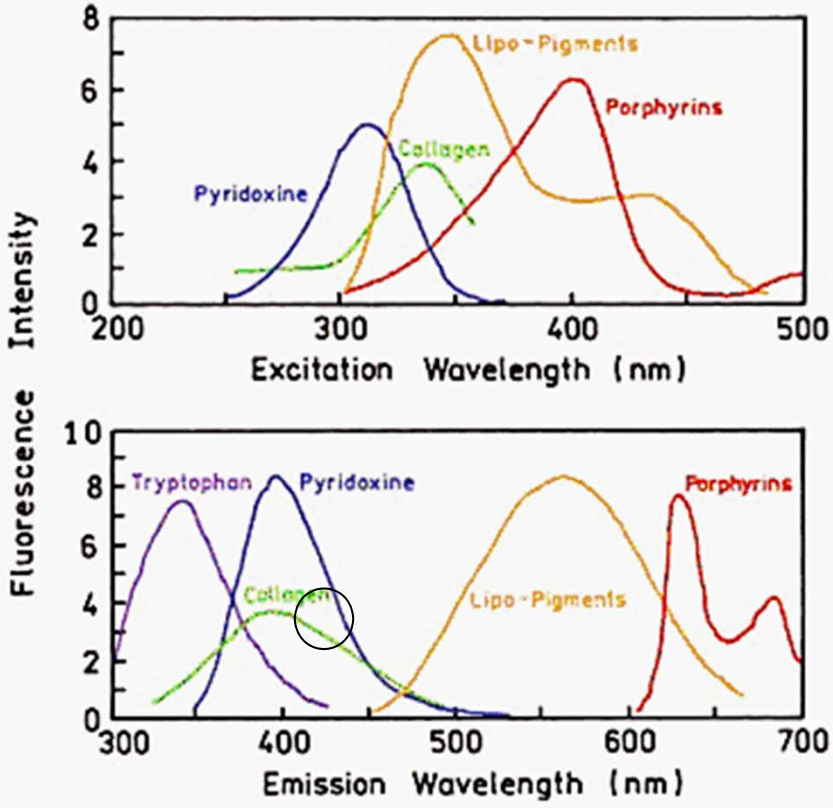

Figure 3.4. Emission spectra from intrinsic tissue fluorophores. Revised from [25].

Fluorescence

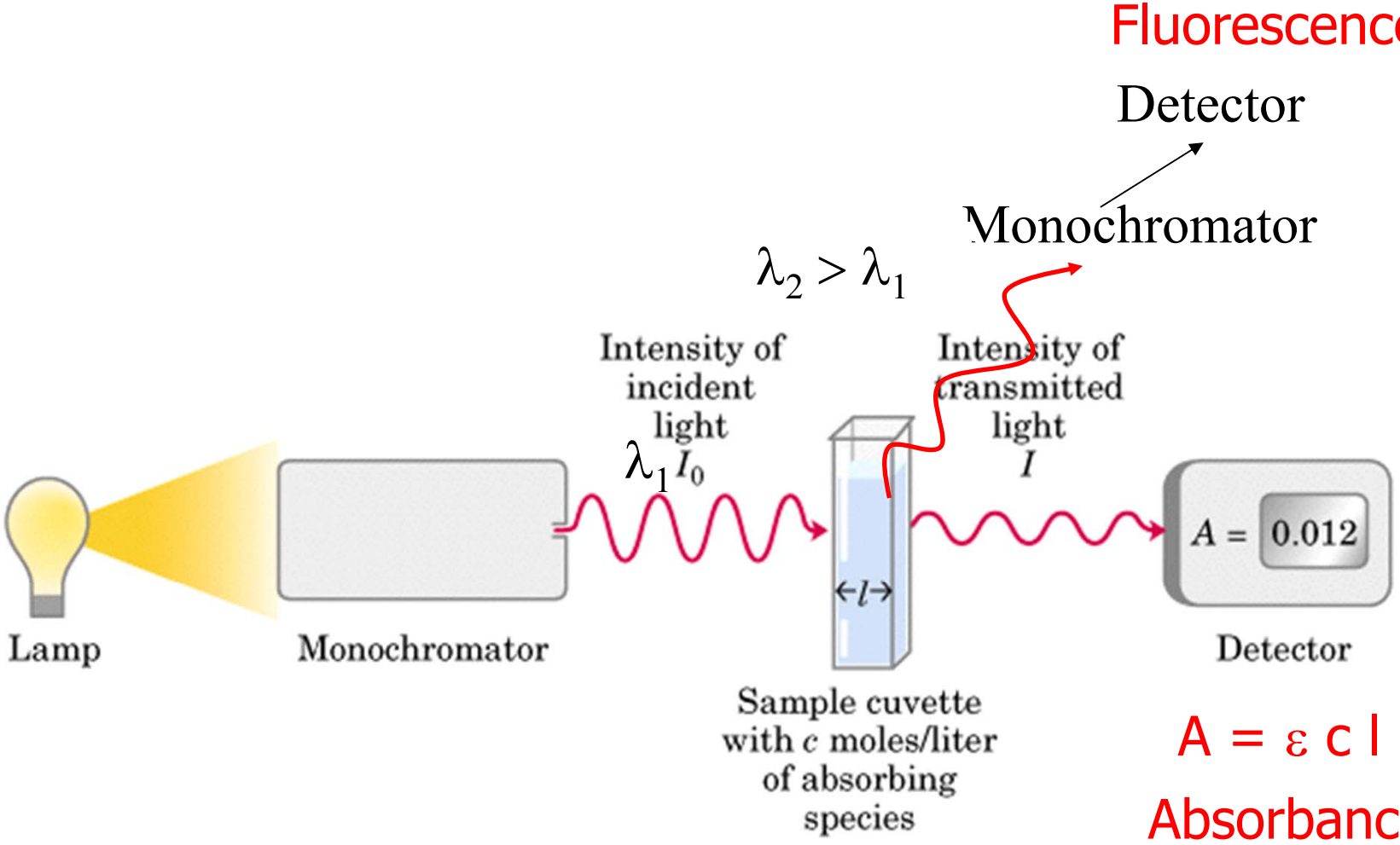

$A = \varepsilon c l$

Absorbance

2 different instruments (or 1 instrument but different setup in stopped-flow)

Scheme of a dual (double) beam spectrophotometer

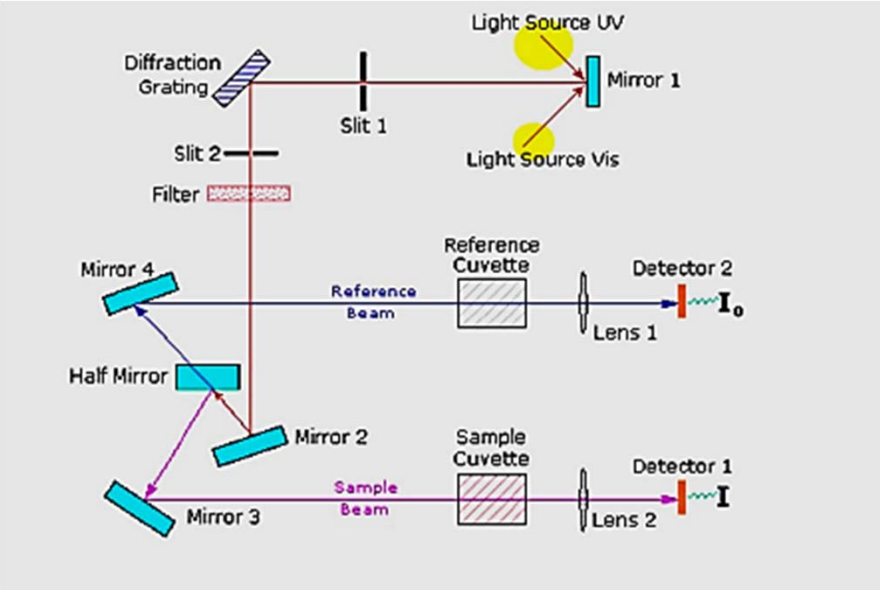

Scheme of a (photo)diode array spectrophotometer

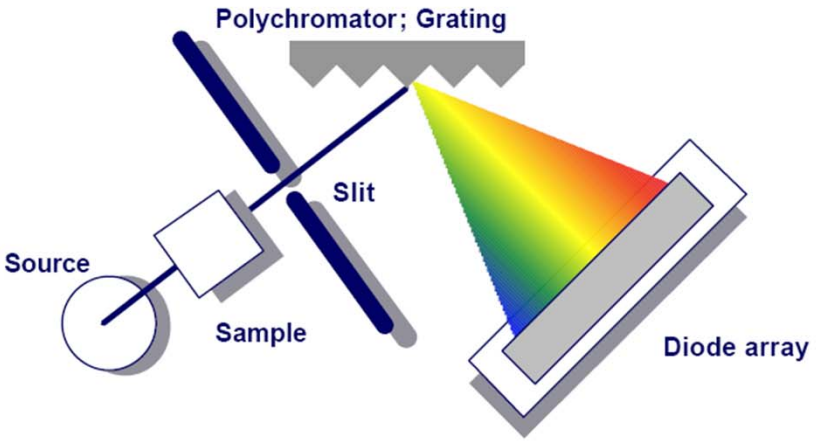

Figure 1. Schematic of photodiode array spectrophotometer

Differences:

Stability
Resolution
Signal-to-noise
Linearity of response
Artifacts (e.g.:photoreactions/degradation)
Speed

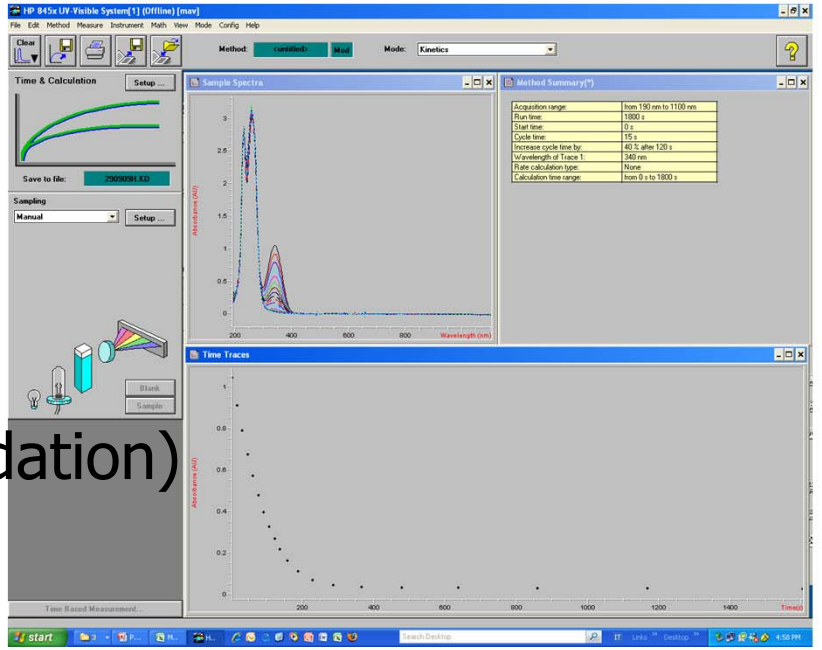

Intrinsic Chromophores in proteins

Amide bond (220 nm)

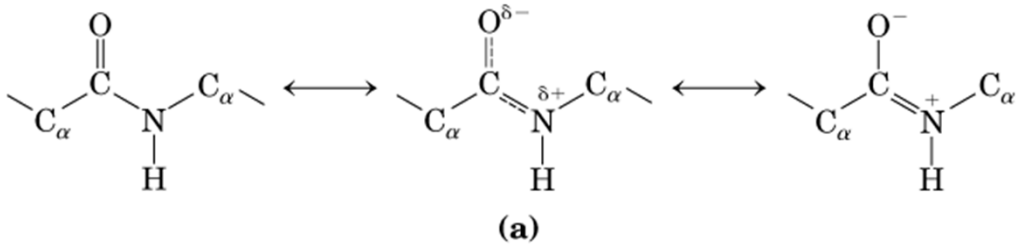

- Use to detect peptides and proteins when concentration is low
- Several other compounds absorb at 220 nm

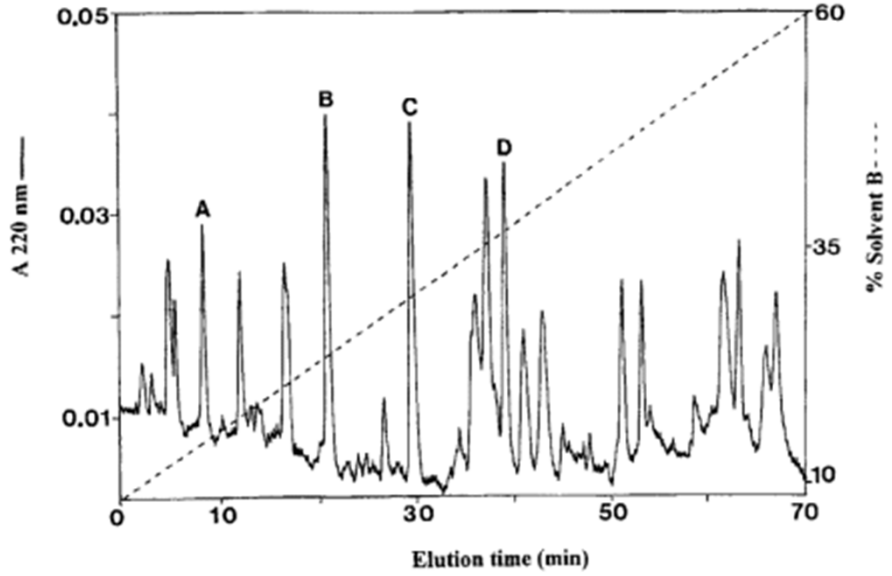

Intrinsic Chromophores /Fluorophors in proteins: Aromatic amino acids

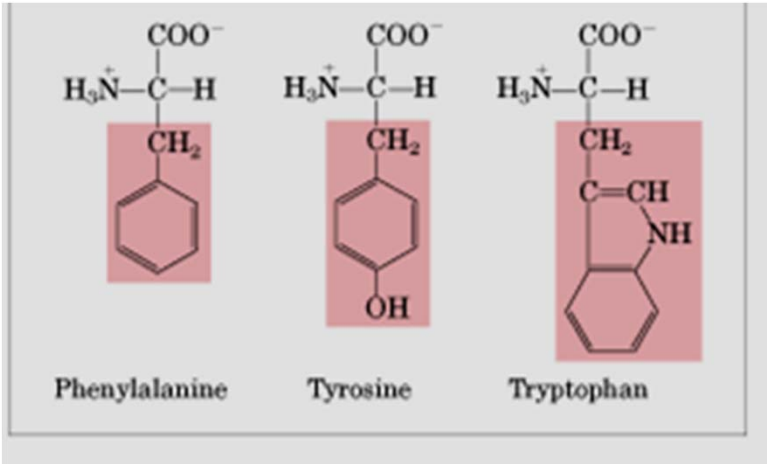

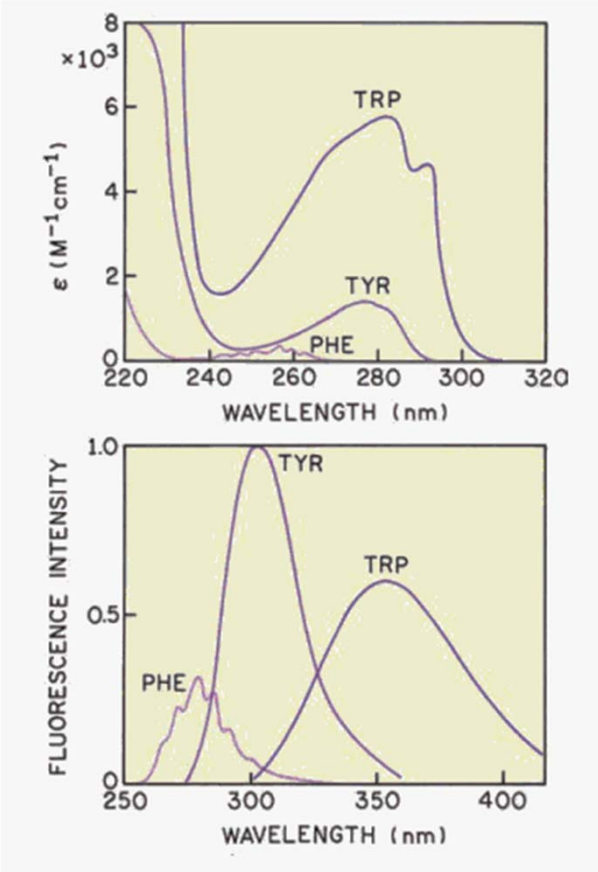

Use absorbance at 280 nm to detect/quantify proteins.

If the number of aromatic amino acids is limited, monitoring their fluorescence changes can help study protein folding/unfolding; protein-ligand, Protein-protein interactions; conformational changes. Otherwise, the data can be difficult to interpret.

Protein unfolding exposes Trp to solvent leading to fluorescence emission increase and shift of lambda max

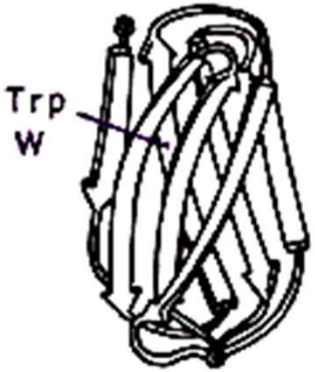

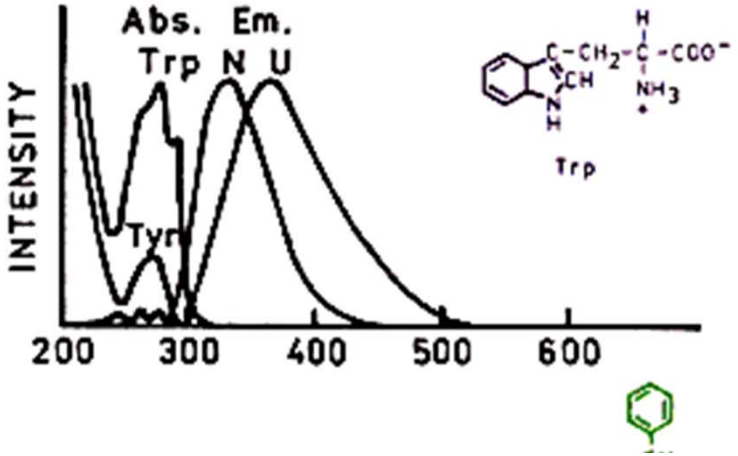

If Protein oligomerization buries Trp the process can be monitored through Trp fluorescence changes

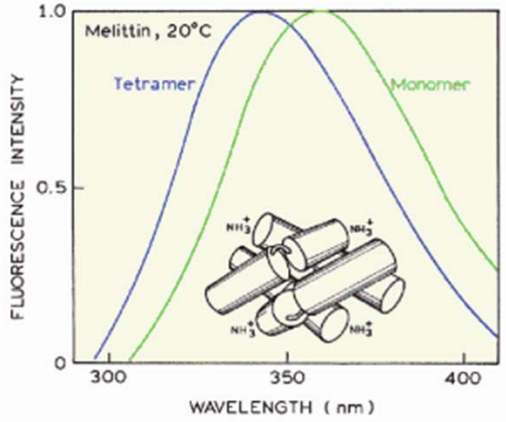

Figure 1.25. Emission spectra of melittin monomer and tetramer. Excitation was at 295 nm. In the schematic structure, the tryptophans are located in the center between the four helices. From [23].

Intrinsic Chromophores in proteins with absorbance in the visible region: several coenzymes and cofactors.

Some are also fluorescent.

Modifications of the compounds or their environment alter the absorption (and fluorescence) spectrum.

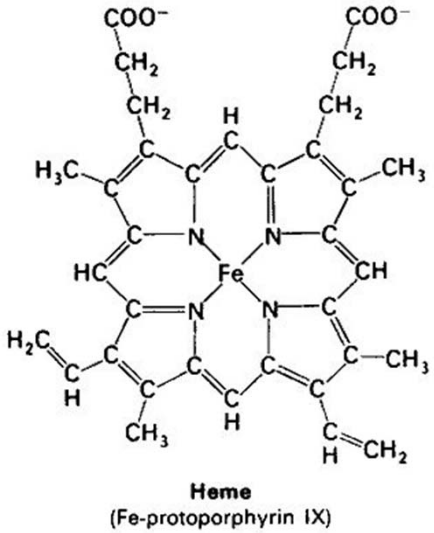

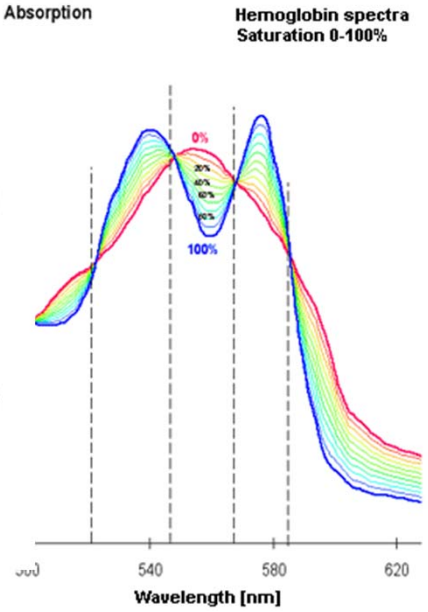

Hemoglobin oxygenation

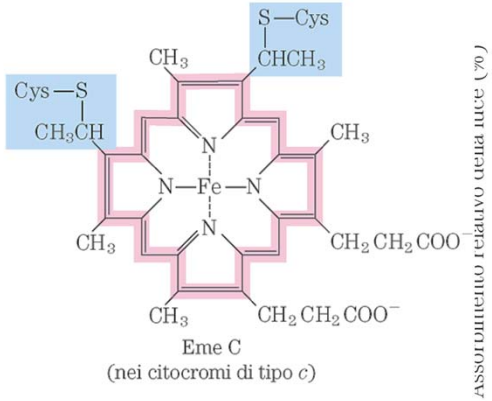

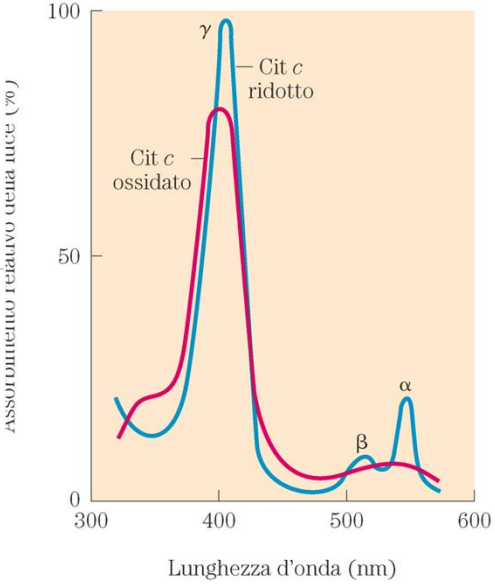

Cytochrome c reduction

Cobalamins (vit B12 derivatives)

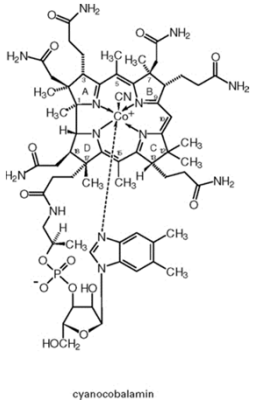

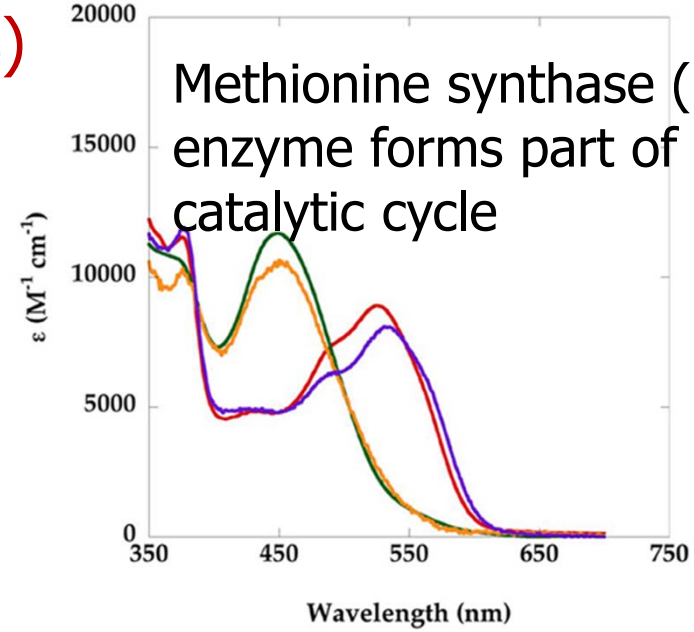

Pyridoxal phosphate (PLP)

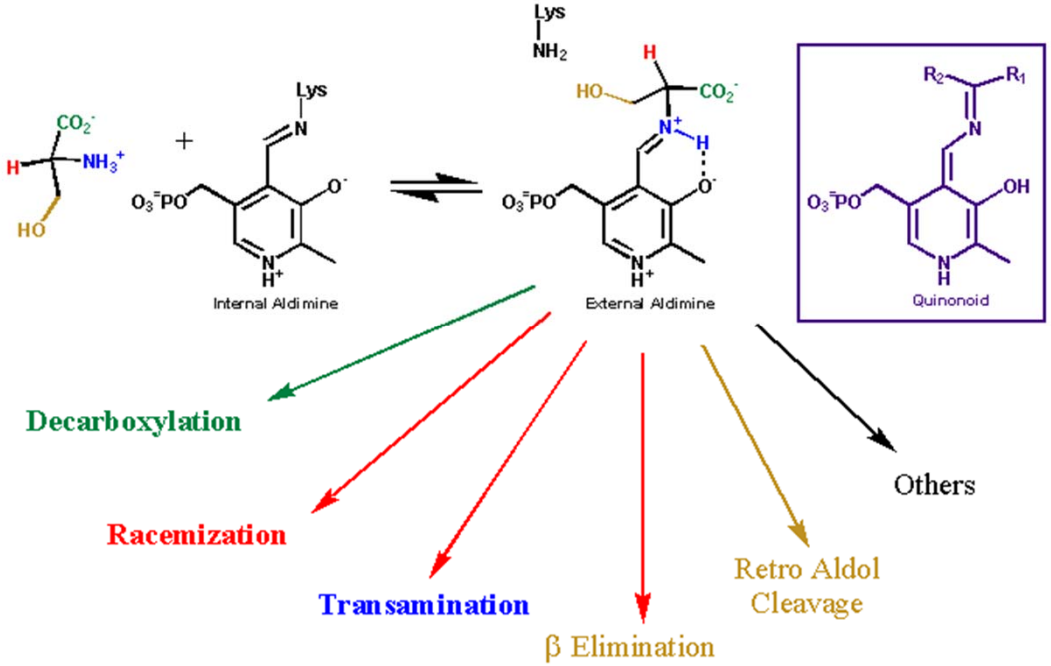

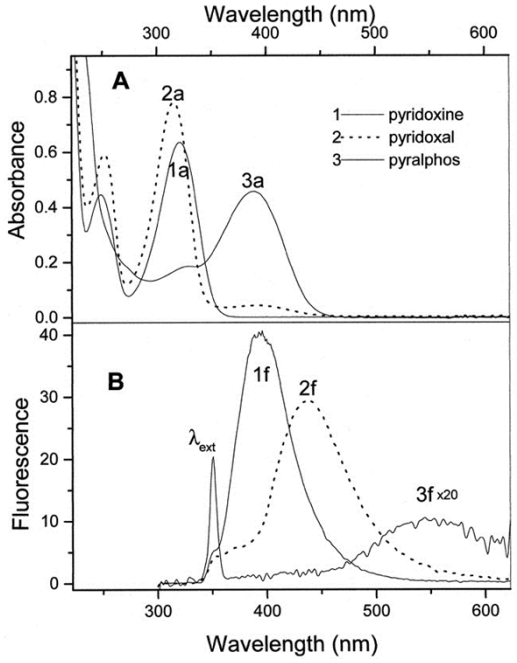

The flavin coenzymes FMN and FAD are derivatives of riboflavin (vitamine b2) and participate in oxidoreduction reactions

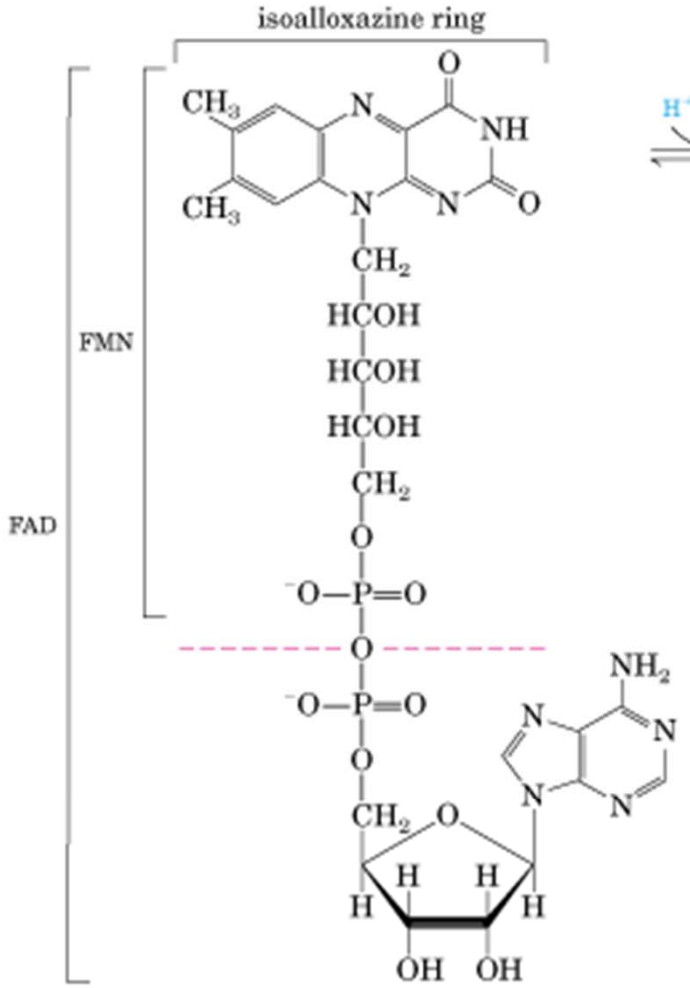

Flavin adenine dinucleotide (FAD) and flavin mononucleotide (FMN)

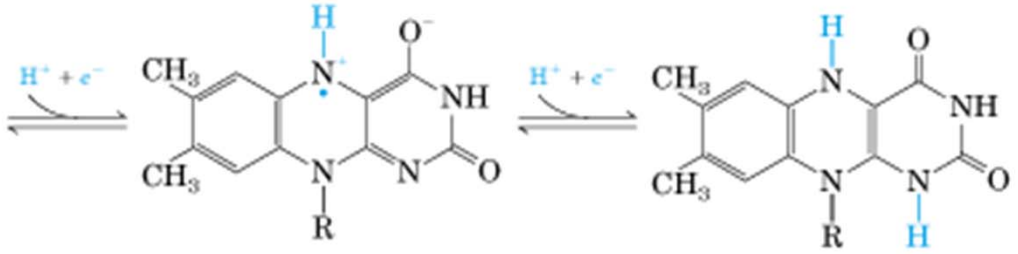

Figure 3

Spectra of glucose oxidase in the oxidized, semi-quinone and fully reduced states

Data are from [23].

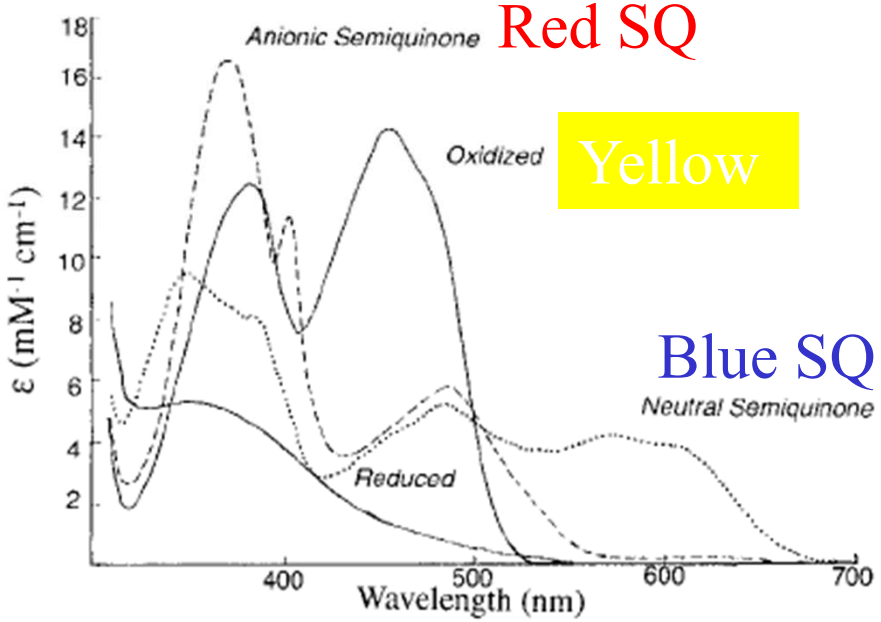

Flavoproteins catalyze a large number of different reactions

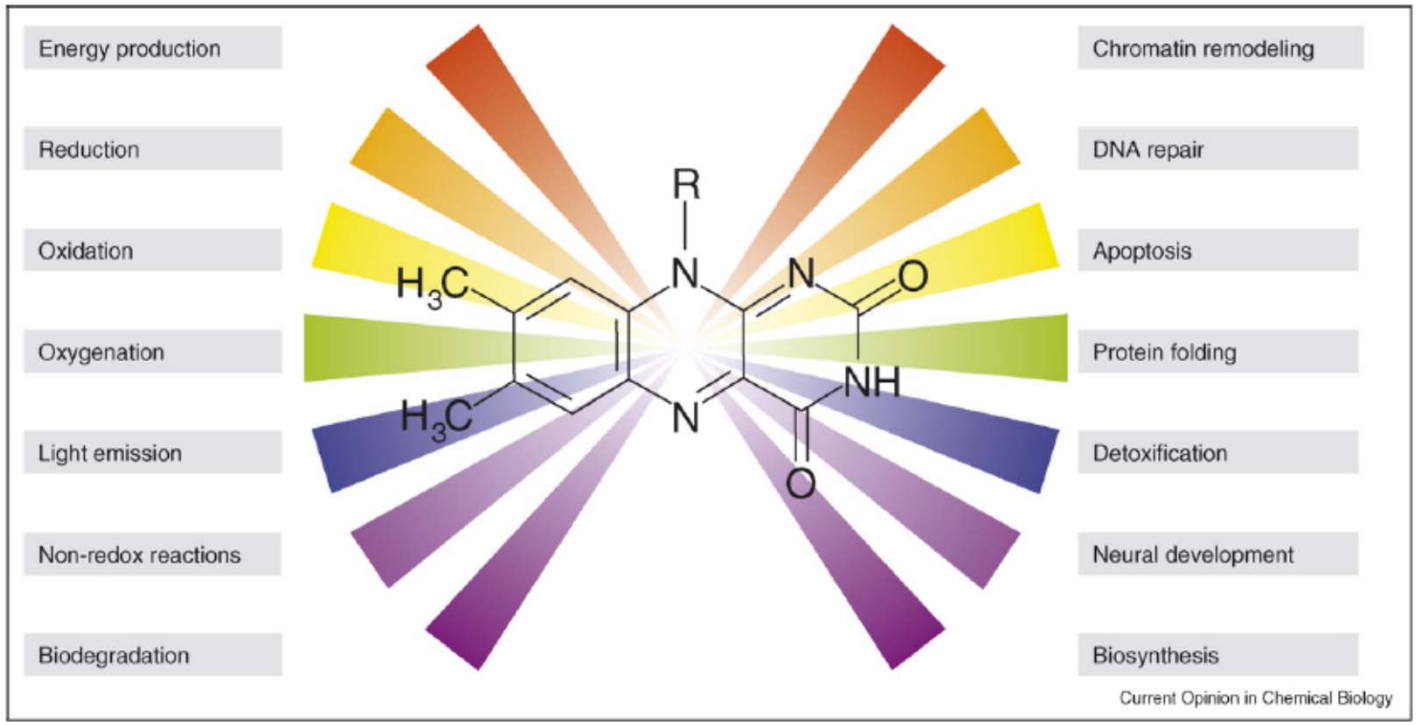

Flavoenzymes classes:

- Dehydrogenase
- Electrontransferases
- Dioxygenases
- Oxidases
- Monooxygenases

Absorption versus fluorescence spectroscopy

	Absorbance	Fluorescence
Detection limits	μM – mM	≤ μM
Linearity of signals	2 orders of magnitude (e.g.: 1 – 100 μM)	≈Narrow (e.g.: 0.1 – 1 μM) inner filter effects
Quantification of solute	ε, extinction coefficient M^{-1} cm^{-1}	$F \propto c*l$, in arbitrary units
Sensitivity to: - Temperature - Solvent - Other solutes	≈	- Very high
Return to ground state	Very fast	(Relatively) slow (can measure fluorescence decay over time after flash of exciting light)

The measured Fluorescence intensity and emission spectrum is very sensitive to compound(s) concentration (inner filter effects; overlapping of emission/absorbance spectra; presence of quenchers, other solutes, FRET).

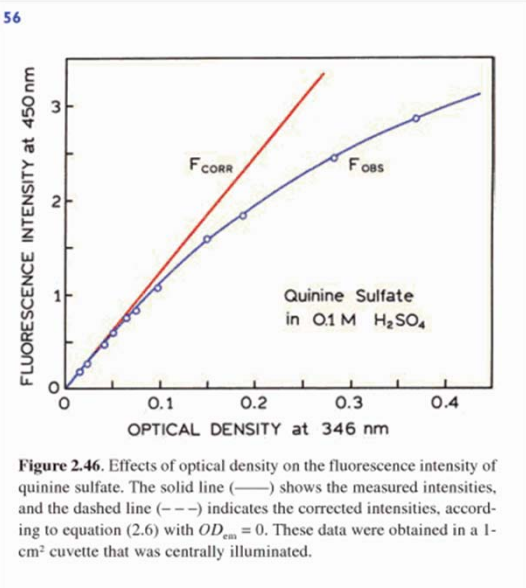

Figure 2.46. Effects of optical density on the fluorescence intensity of quinine sulfate. The solid line (——) shows the measured intensities, and the dashed line (– – –) indicates the corrected intensities, according to equation (2.6) with $OD_{em} = 0$. These data were obtained in a 1-cm² cuvette that was centrally illuminated.

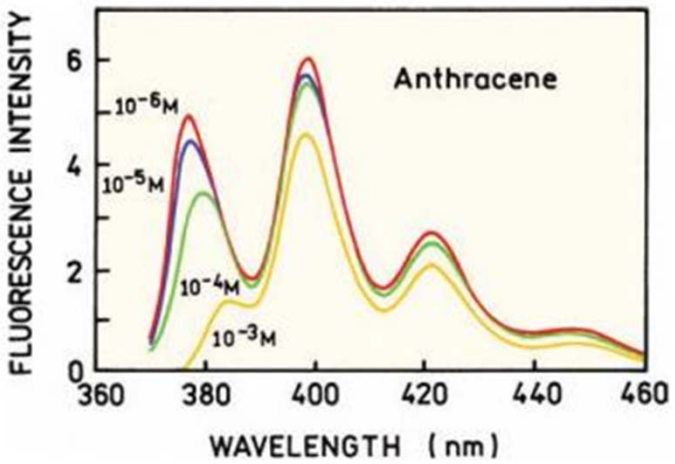

Figure 2.48. Effects of self-absorption of anthracene on its emission spectrum. A 1-cm² cuvette was used with right-angle observation. Revised from [61].

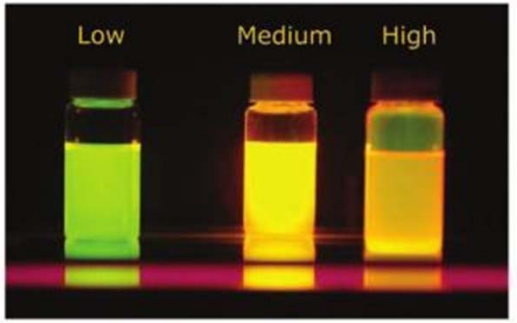

Rhodamine

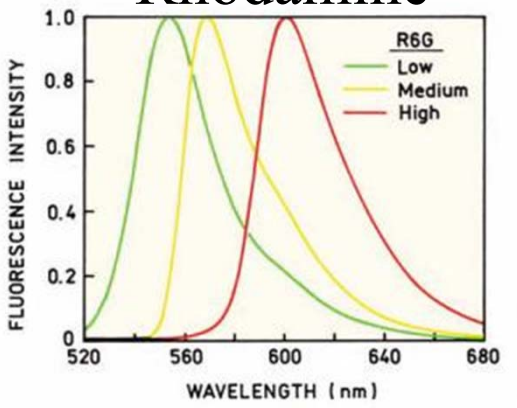

Figure 2.49. Effect of concentrations on the color and emission spectra of rhodamine 6G. The concentrations of R6G are 5 x 10^{-6}, 1.6 x 10^{-4}, and 5.7 x 10^{-3} M. From [64].

Check linearity of signal, minimize unwanted interferences, but also exploit these properties

Fluorescence quenchers by collision such as acrylamide can be used to monitor the location of a Trp residue:

<u>if buried</u>: no effect of quencher; <u>if solvent exposed</u>: effect of quencher

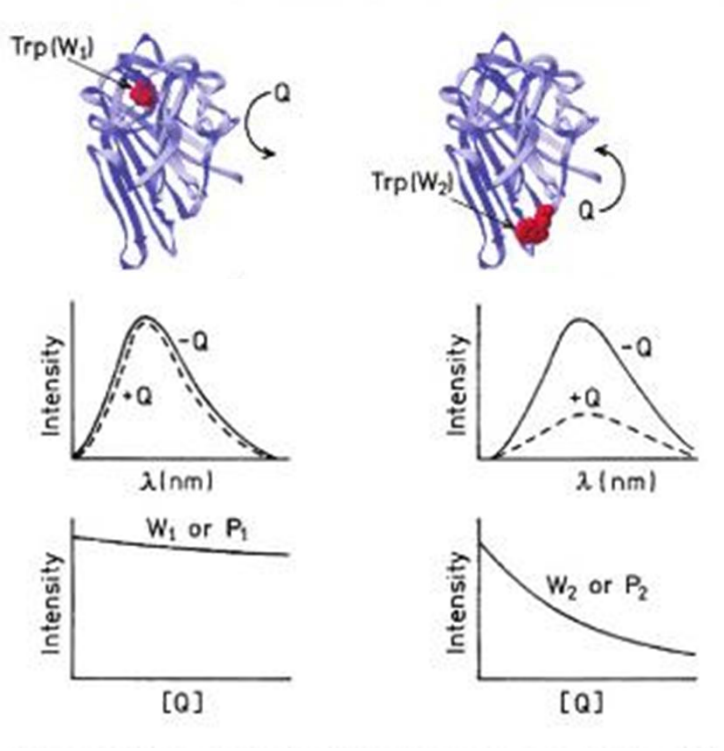

The sensitivity of fluorescence emission to the environment is exploited to study protein folding: ANS, various dyes (see Thermofluor)

ANS fluorescence increases when it interacts with hydrophobic residues.

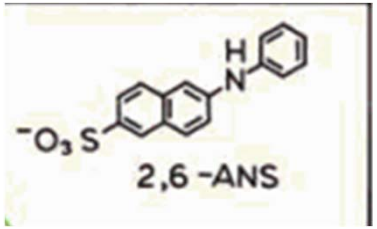

ANS can be used to monitor the exposure or burial of hydrophobic residues in proteins during unfolding, dissociation of oligomer, and conformational changes in general.

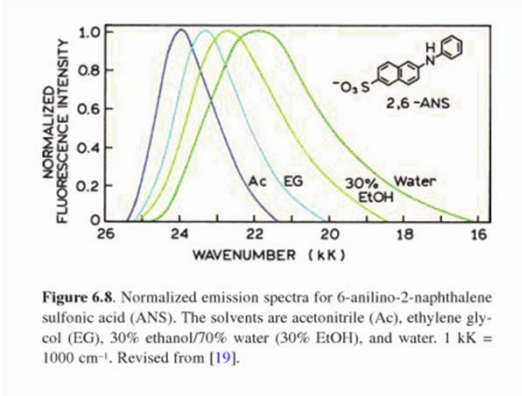

Figure 6.8. Normalized emission spectra for 6-anilino-2-naphthalene sulfonic acid (ANS). The solvents are acetonitrile (Ac), ethylene glycol (EG), 30% ethanol/70% water (30% EtOH), and water. 1 kK = 1000 cm^{-1}. Revised from [19].

6392 *J. Med. Chem.* **2004,** *47,* 6392−6400

New Constrained "Molecular Tongs" Designed To Dissociate HIV-1 Protease Dimer

Naïma Merabet,[†] Julien Dumond,[‡] Bruno Collinet,[‡] Laurence Van Baelinghem,[†] Nicole Boggetto,[‡] Sandrine Ongeri,[†] Fariza Ressad,[‡] Michèle Reboud-Ravaux,[‡] and Sames Sicsic*[,†]

Biocis, UMR-CNRS 8076, Faculté de Pharmacie, Université de Paris-Sud, 5 rue J. B. Clément, F-92296 Châtenay-Malabry Cedex, France, and Laboratoire d'Enzymologie Moléculaire et Fonctionnelle, Institut Jacques Monod, UMR 7592, CNRS-Universités de Paris VI et VII, 2 place Jussieu, F-75251 Paris Cedex 05, France

Received April 30, 2004

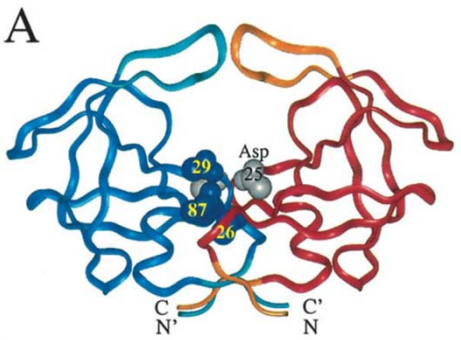

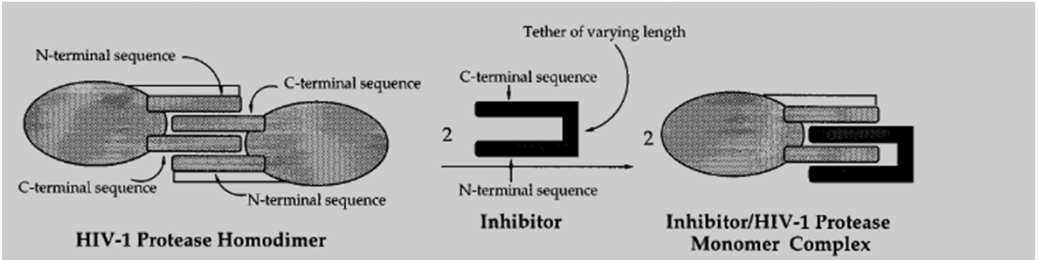

schematic of the strategy employed for dimerization inhibition.

The monomeric (inactive) HIV1 protease exposes hydrophobic patches to which ANS binds: monitor stabilization of monomer in the presence of the compound through increase of ANS fluorescence

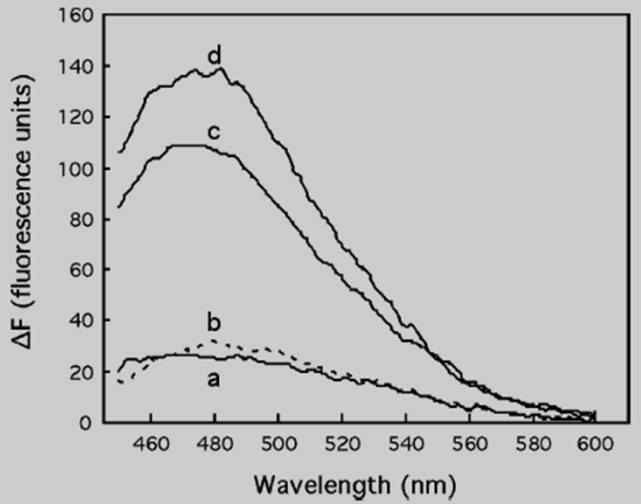

Figure 8. ANS emission spectra at pH 4.7 and 25 °C (λ_{ex} = 376 nm): PR (0.35 μM) was incubated in the absence of inhibitor (a), or in the presence of 0.1 μM acetylpepstatin (b), 3.75 μM **23** (c), or 1.66 μM **32** (d). The fluorescence intensity was corrected from the fluorescence due to the same concentration of ANS (30 μM) without enzyme (a) and without enzyme and inhibitor (b−d).

Example : Use absorbance and fluorescence spectroscopies to quantify and identify the bound coenzyme as FAD exploiting flavin fluorescence quenching by protein + by stacking between isoalloxazine ring and adenylate moiety.

The case of MICAL: a multidomain cytoplasmic protein participating in actin cytoskeleton dynamics through its N-terminal monooxygenase or oxidase flavoprotein domain

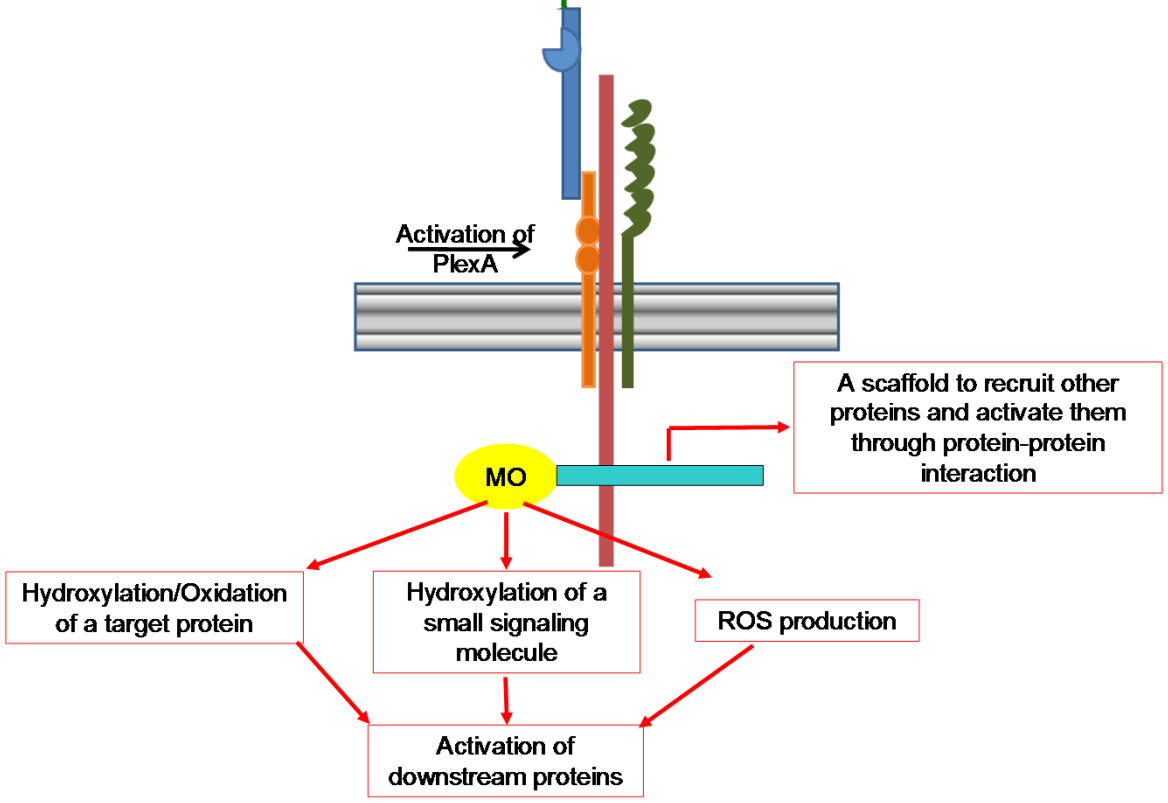

Absorption spectrum of the purified N-terminal domain of h-MICAL

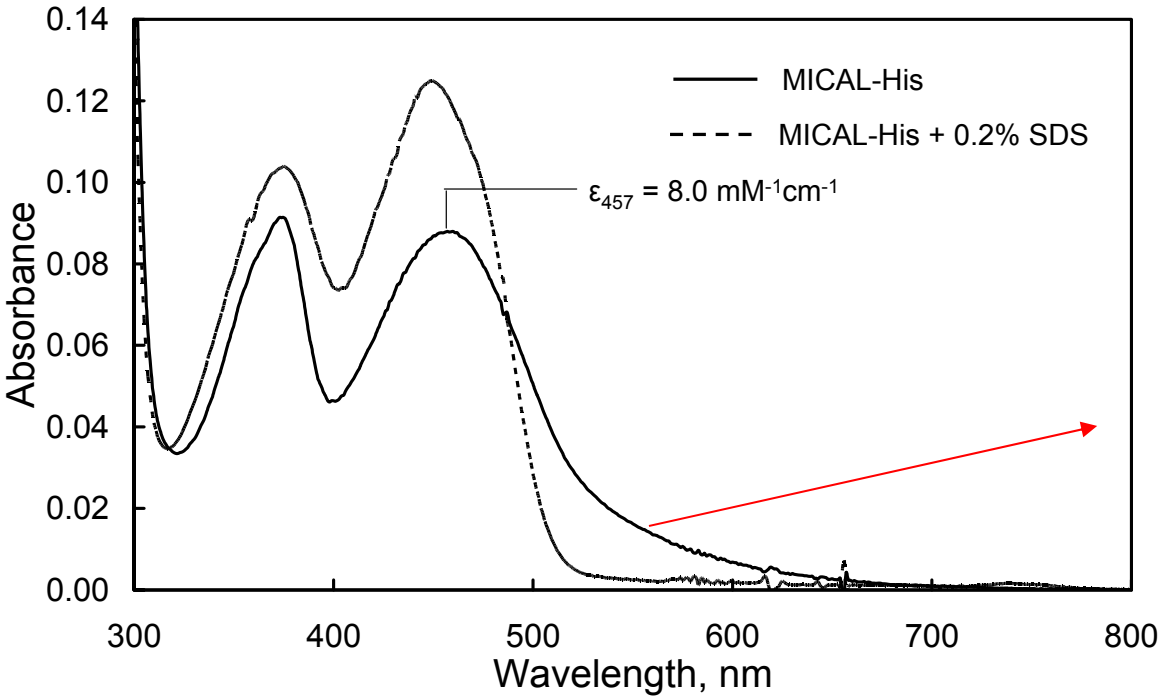

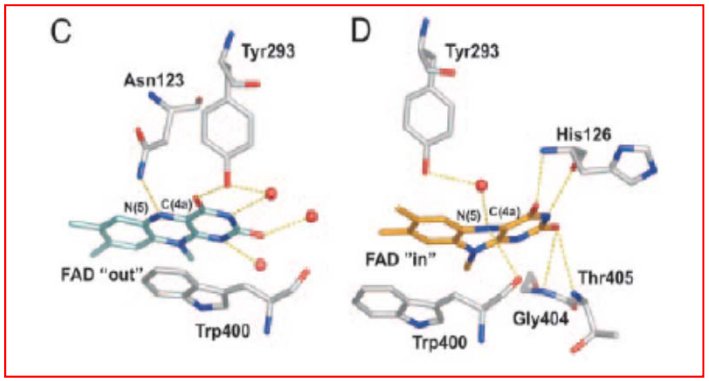

1) The spectrum of the «as isolated» MICAL indicates the presence of a flavin coenzyme, but the spectrum differs from that of authentic flavin, FAD or FMN.
2) Release of the coenzyme by denaturation yields the spectrum of authentic FAD or FMN
(1) A charge-transfer complex between the flavin and Trp400 from X-ray structure
(2) The extinction coefficient of free FAD is known: Use the information to determine the stoichiometry and the extinction coefficient of the bound coenzyme

Still Need to determine if the coenzyme is FAD or FMN

B

Excitation and emission spectra of flavin coenzymes

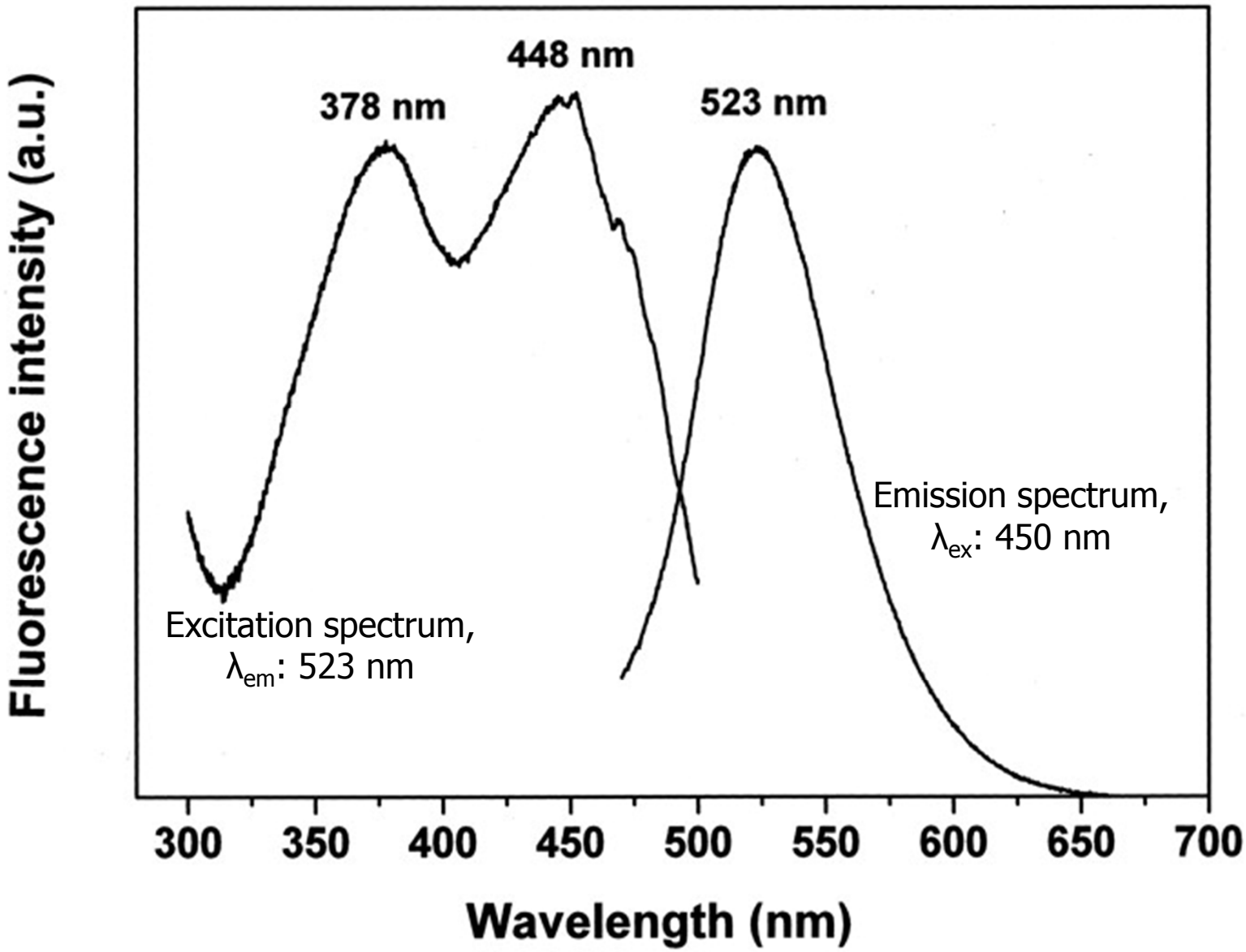

Fluorimetric Indentification of the cofactor bound to MICAL as FAD

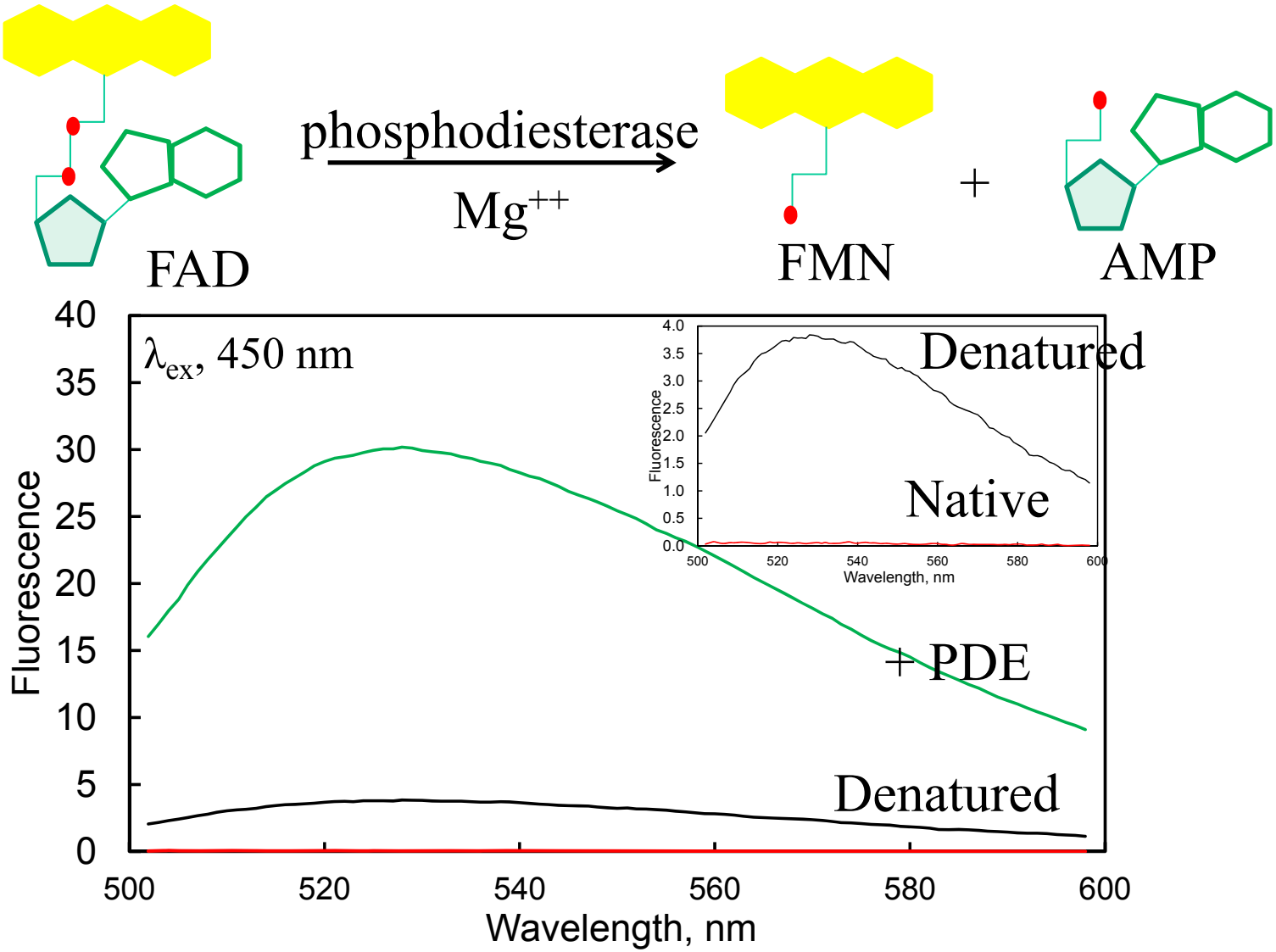

1) The fluorescence of the bound coenzyme is quenched
2) If FAD, PDE will bring along a 10x increase of fluorescence due to conversion into FMN, and removal of internal quenching of fluorescence by the AMP moiety.

Effect of MICAL-MO on F-actin depolymerization

(monitor pyrene-actin polymerization and depolymerization by fluorescence)
http://mullinslab.ucsf.edu/Protocols%20HTML/pyrene.html)

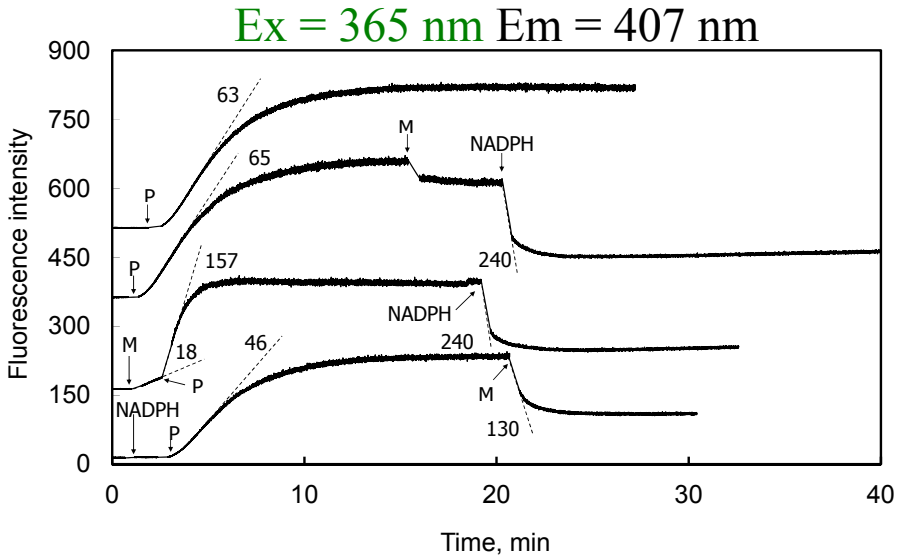

G-Actin, 3.6 μM MICAL,
0.66 μM NADPH 91 μM
P, 10x polymerization buffer

MICAL-MO + NADPH causes decrease of fluorescence of pyrene-labelled Factin

How much of the fluorescence changes are due to NADPH addition and later decrease of NADPH concentration/ absorbance???

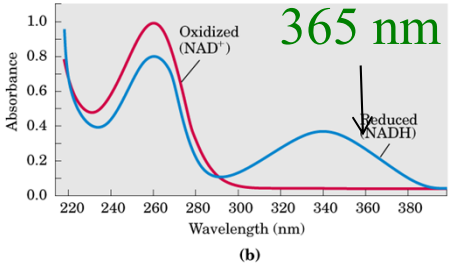

Use DLS (and Ultracentrifugation) to monitor actual polymerization / depolymerization of actin

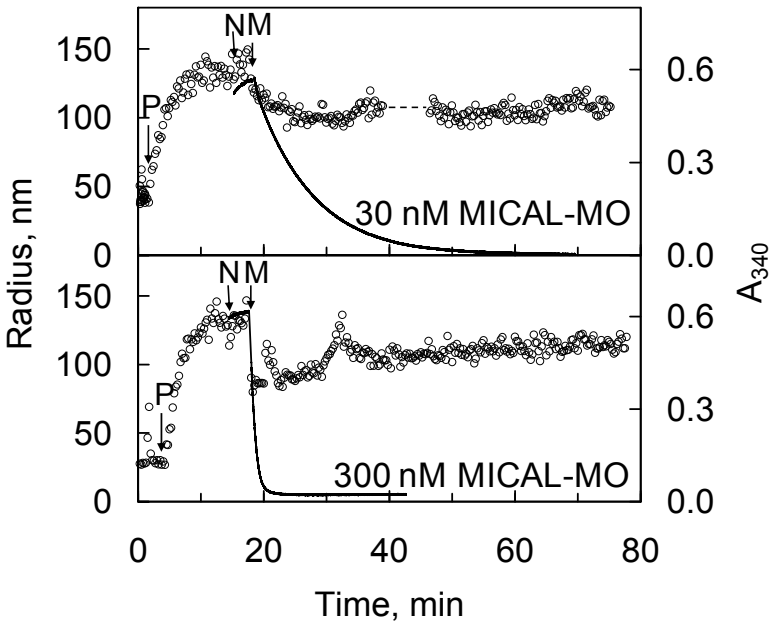

Monitor F-actin polymerization state by DLS and NADPH consumption by absorption spectroscopy at 340 nm:

- F-actin stimulates NADPH oxidation
- F-actin is (partially) depolymerized
- More NADPH is oxidized than total actin present.

MICAL depolymerizing effect on actin may be reversible or may be due to combination of MO activity + H_2O_2 production

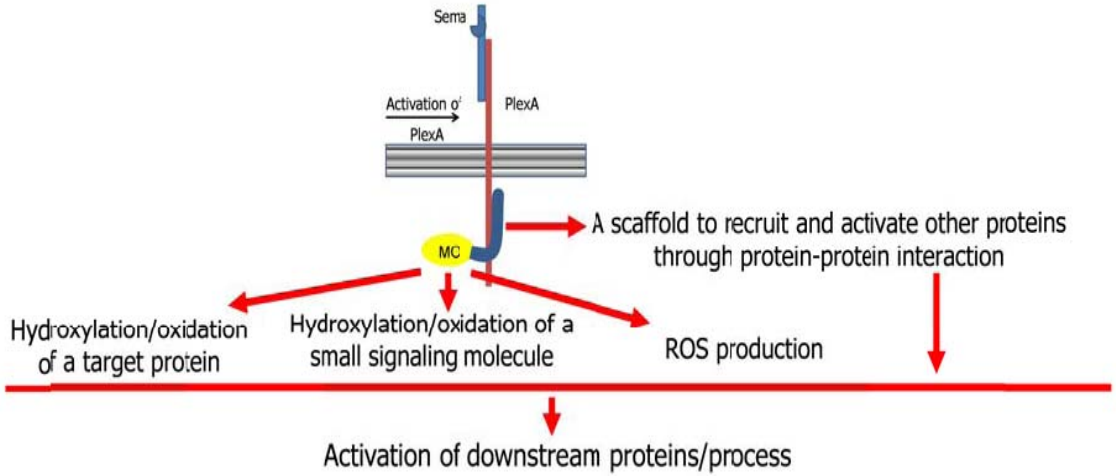

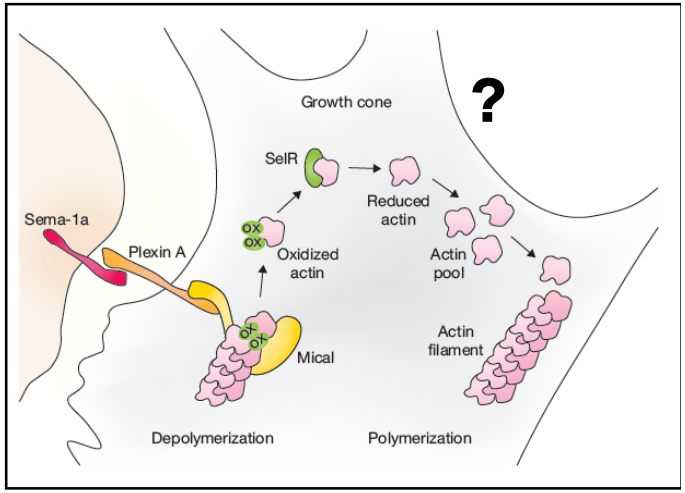

Measured Fluorescence intensity and emission spectrum is very sensitive to compound(s) concentration: inner filter effects; overlapping of emission/absorbance spectra; presence of quenchers, other solutes, FRET.

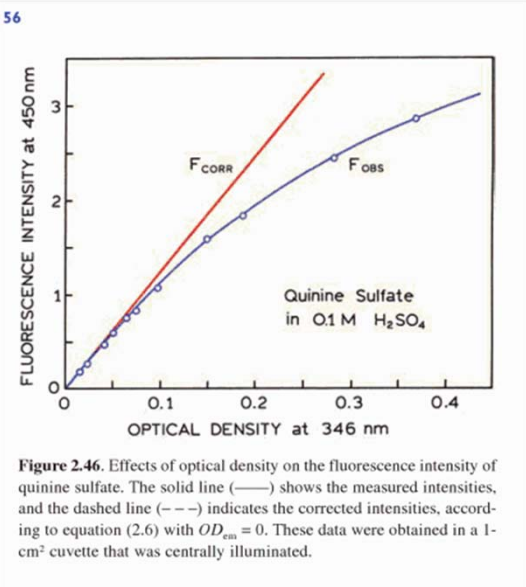

Figure 2.46. Effects of optical density on the fluorescence intensity of quinine sulfate. The solid line (——) shows the measured intensities, and the dashed line (– – –) indicates the corrected intensities, according to equation (2.6) with $OD_{em} = 0$. These data were obtained in a 1-cm² cuvette that was centrally illuminated.

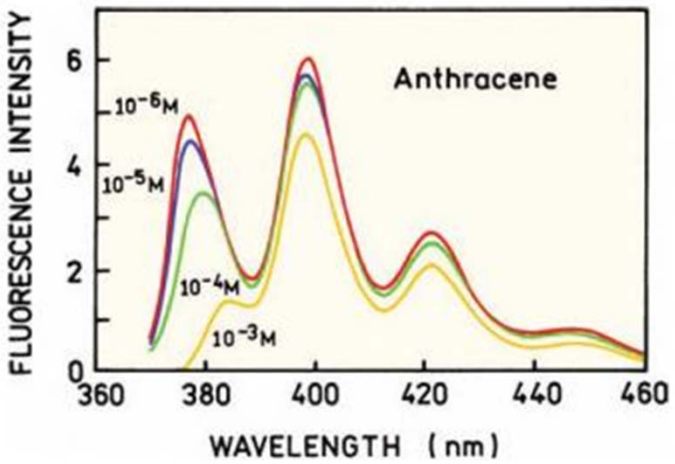

Figure 2.48. Effects of self-absorption of anthracene on its emission spectrum. A 1-cm² cuvette was used with right-angle observation. Revised from [61].

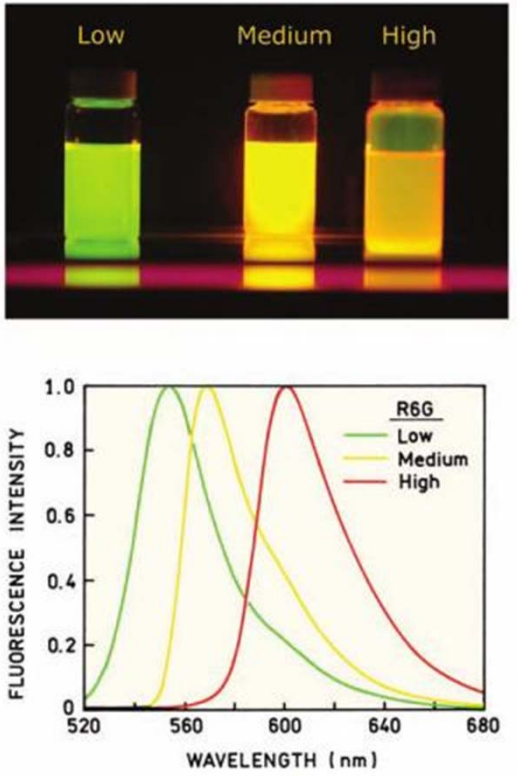

Figure 2.49. Effect of concentrations on the color and emission spectra of rhodamine 6G. The concentrations of R6G are 5 x 10^{-6}, 1.6 x 10^{-4}, and 5.7 x 10^{-3} M. From [64].

Check linearity of signal, minimize unwanted interferences, but also exploit these properties

FRET: Foerster (Fluorescence) resonance energy transfer occurs when the emission spectrum of the «Donor» overlaps with the absorption spectrum of the «Acceptor» without emission of photon from donor.

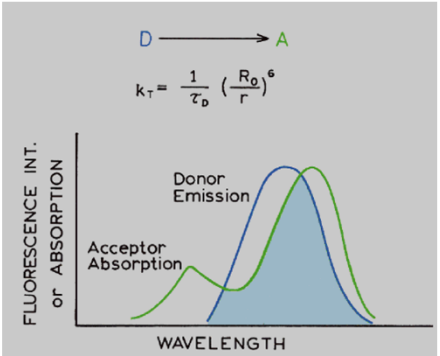

Figure 1.16. Spectral overlap for fluorescence resonance energy transfer (RET).

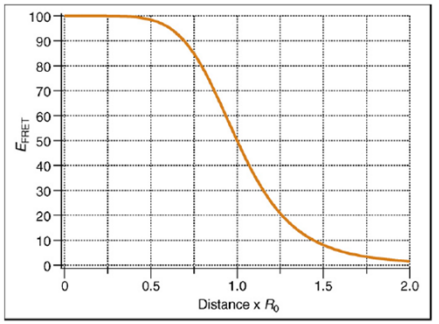

Figure 1. FRET efficiency versus distance. The FRET efficiency (E_{FRET}) varies with the sixth power of distance between donor and acceptor. As a result, there is a steep fall in E_{FRET} with increasing distance. The Förster radius (R_0) is the distance at which 50% FRET occurs. Owing to the strong distance dependence, FRET is usually detected only when the two fluorophores are closer than $1.5R_0$.

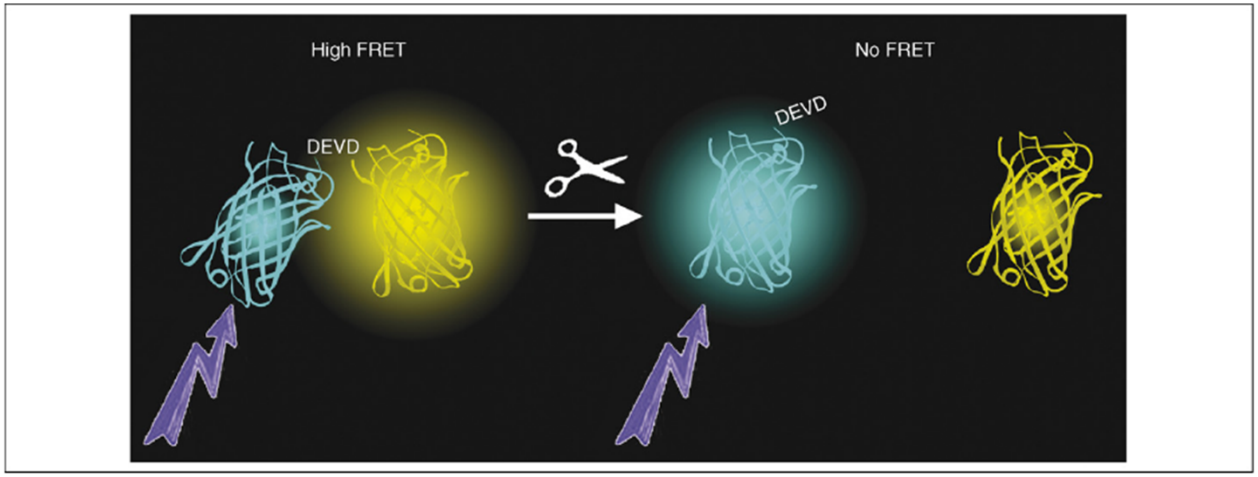

Figure 5. Biosensor for caspase-3 protease activity. FRET-based biosensors for protease activity can be constructed by directly fusing the donor and acceptor FPs through a

The efficiency of FRET depends on the distance between Donor and Acceptor. FRET can be used to monitor distances between Donor and Acceptor

Use of FRET to measure interaction between yellow fluorescent protein and cyan fluorescent protein

Review TRENDS in Biochemical Sciences Vol.32 No.9

Fluorescent protein FRET: the good, the bad and the ugly

David W. Piston and Gert-Jan Kremers

Department of Molecular Physiology and Biophysics, Vanderbilt University, 702 Light Hall, Nashville, TN 37232-0615, USA

Use of FRET to measure enzyme activities

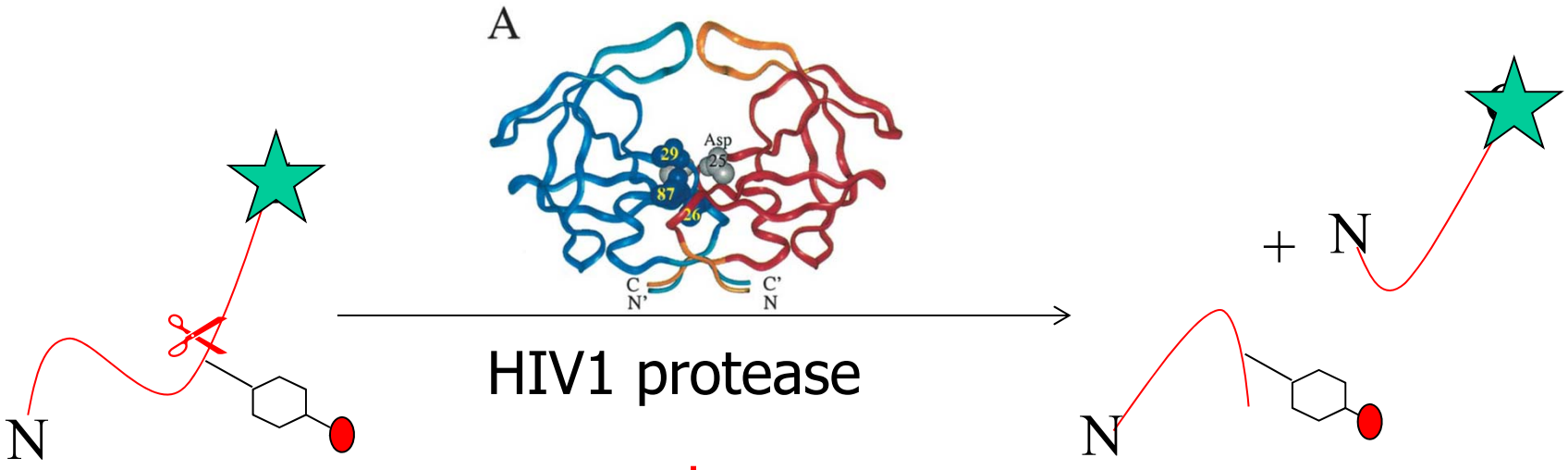

Ser-Nle-Ala-Glu-pNitro-Phe-Leu-Val-Arg-Ala-Lys-His-Abz

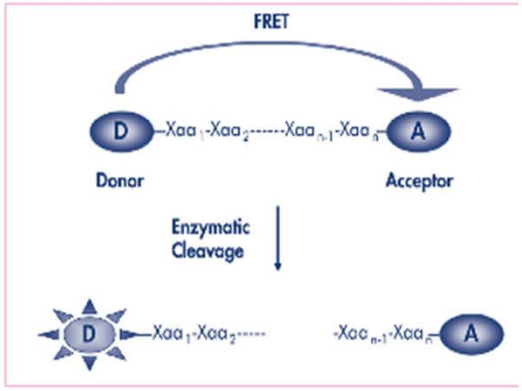

Fig. 2: Fluorescence Resonance Energy Transfer (FRET)

Abz (2-Aminobenzoyl or Anthraniloyl) Substrates

Abz substrates are generally used in connection with number of quenchers (Q) such as Dnp (2,4-dinitroph nyl), EDDnp (N-(2,4-dinitrophenyl)ethylenediamine) 4-nitro-phenylalanine and 3-nitro-tyrosine. Substra cleavage can be detected at 420 nm using an excitatio wavelength of 320 nm.

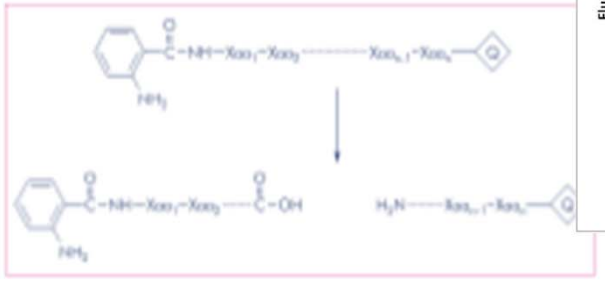

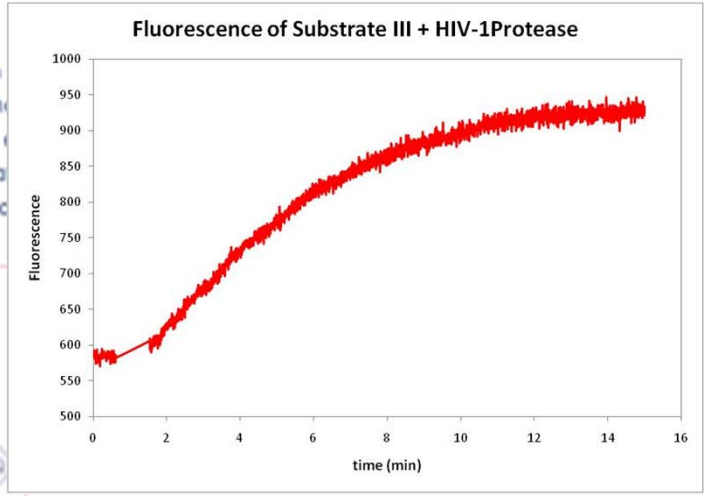

Also absorption of a given compound is often sensitive to environment but absorbance changes are smaller than fluorescence changes

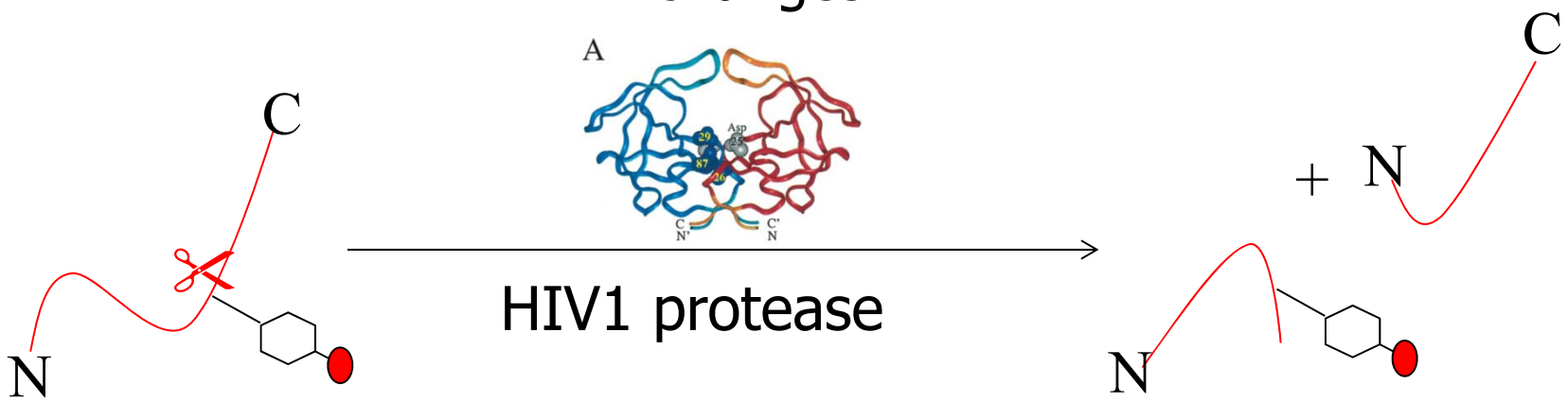

Ser-Nle-Ala-Glu-pNitro-Phe-Leu-Val-Arg-Ala-Lys-His

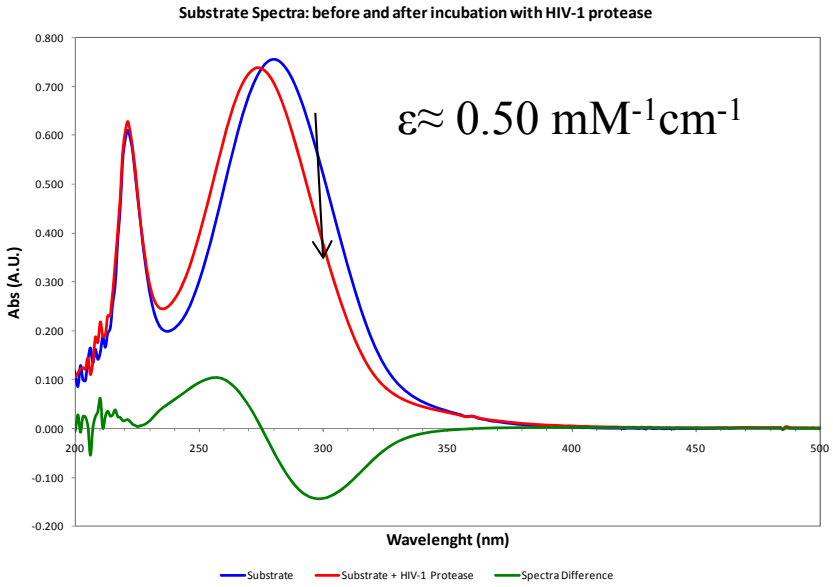

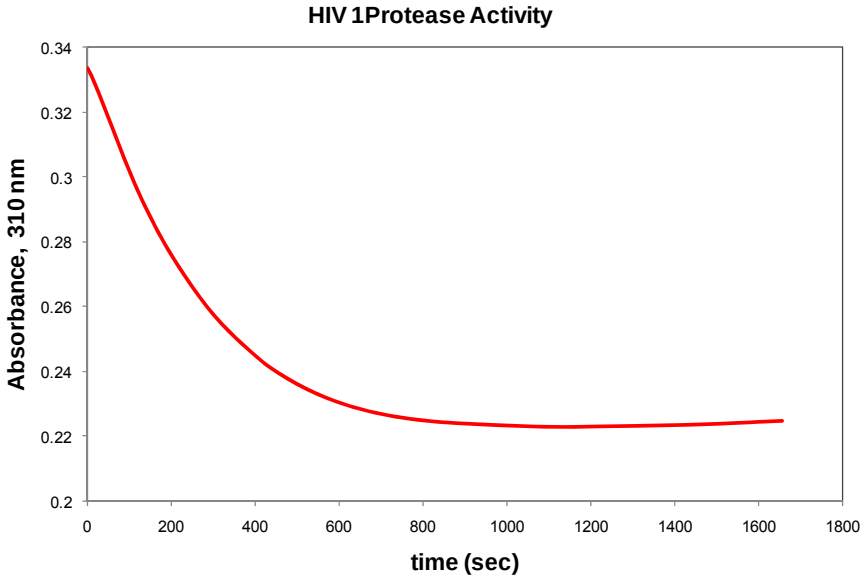

Absorbance-based assay vs FRET-based assay of HIV1 protease: which is the assay method to use?

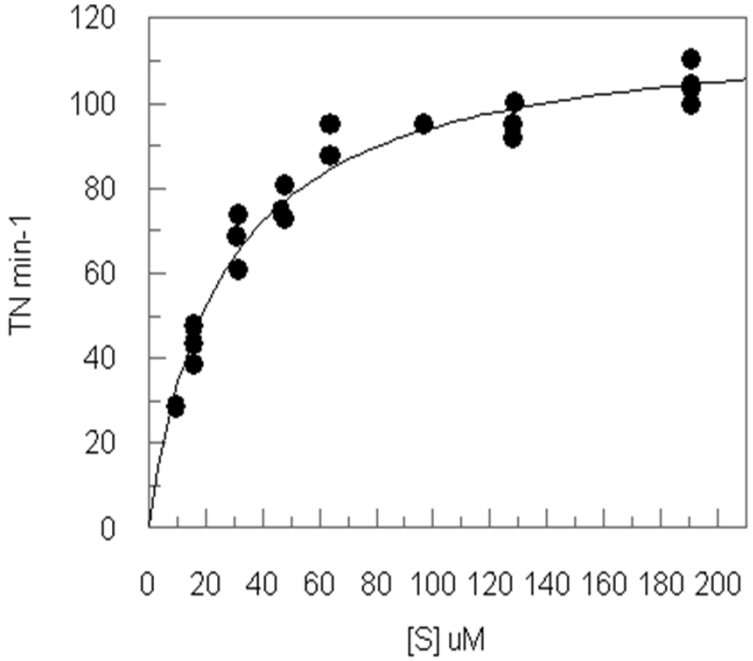

Parameter	Value	Std. Error
Vmax	118.5736	3.2182
Km	25.8217	2.4562

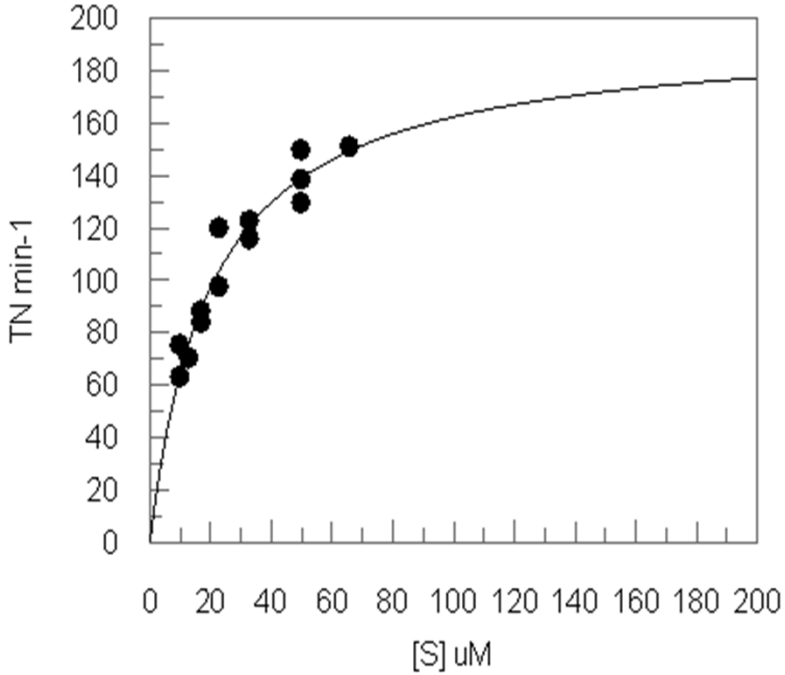

Parameter	Value	Std. Error
Vmax	195.2216	12.3678
Km	20.1679	3.2118

Buffer :100 mM Na Acetate, pH 5.00, 1mM EDTA, 1 mM DTT, 100 mM NaCl

Circular dichroism spectroscopy to measure:

- Folding/unfolding
- Conformational changes
- Reduction of redox center (e.g.: flavin coenzyme)

The principle: different absorption of left vs right circularly polarized light by chiral molecules as a function of environment

Warning: Signals are small; interference by air, solvents, solutes: high; but the technique is very sensitive

A few useful websites: the principle made easy?

http://www.photophysics.com/tutorials/circular-dichroism-cd-spectroscopy/1-understanding-circular-dichroism

Electromagnetic waves and circular dichroism: an animated tutorial

szilagyi.andras@ttk.mta.hu

Protein Circular Dichroism Data Bank: pcddb.cryst.bbk.ac.uk/home.php

Instrumentation

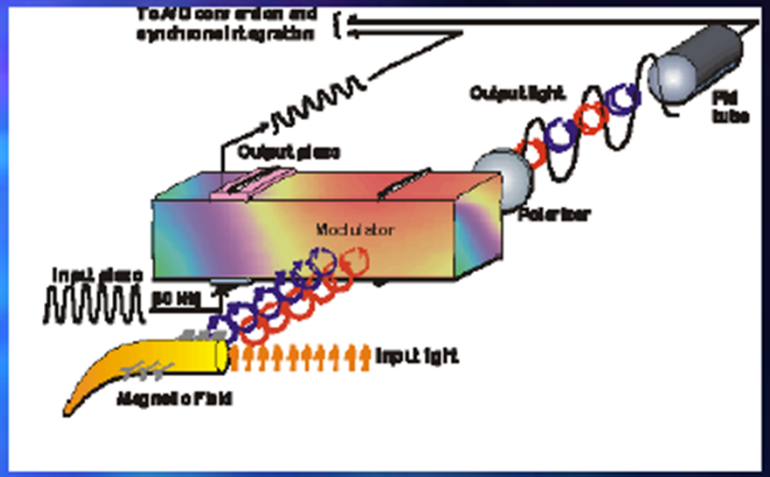

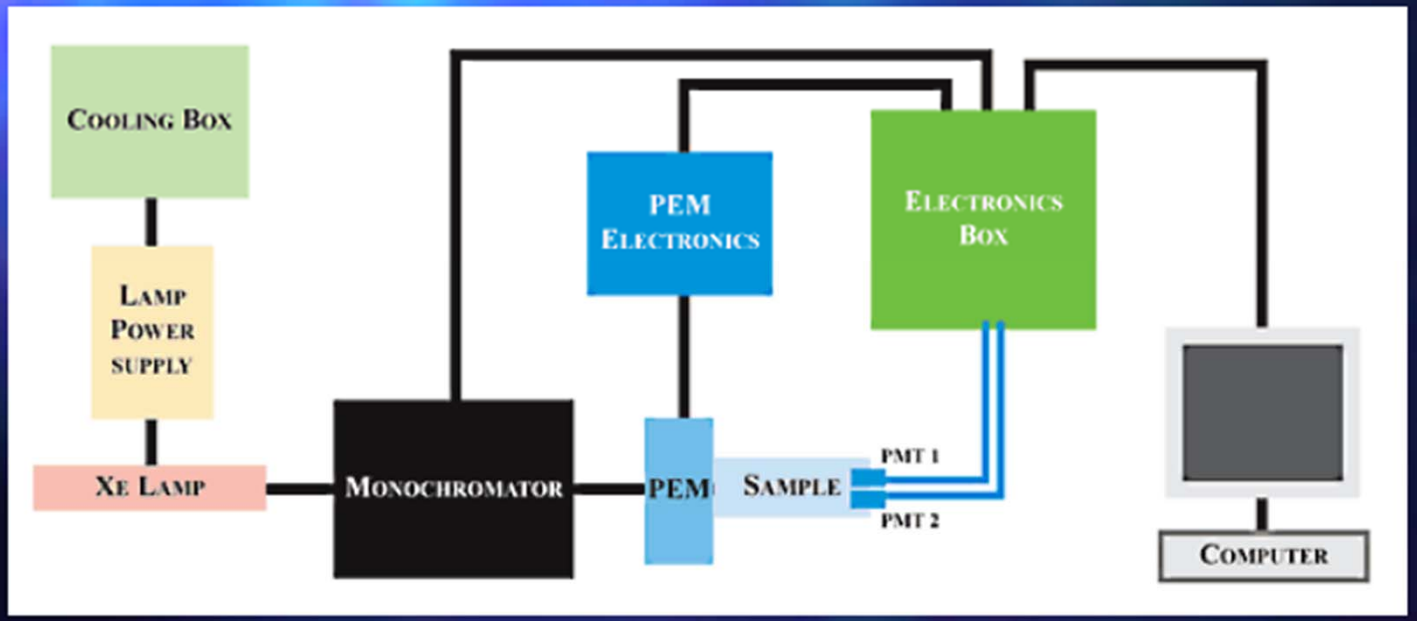

szilagyi.andras@ttk.mta.hu

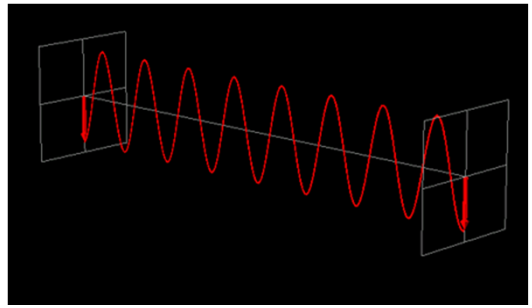

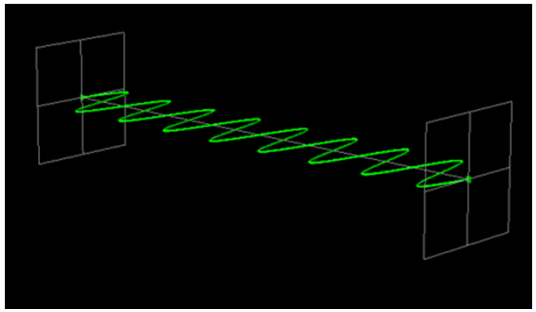

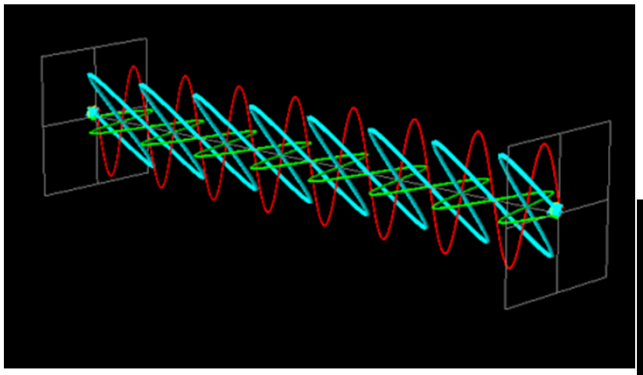

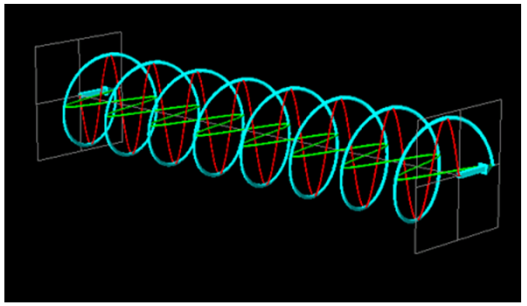

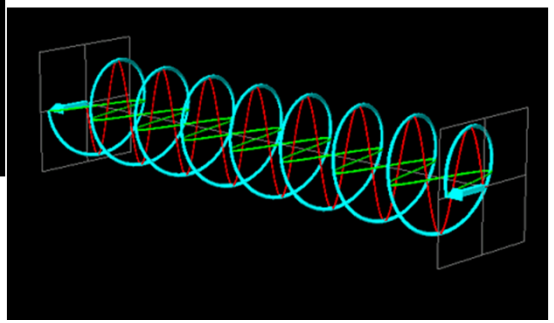

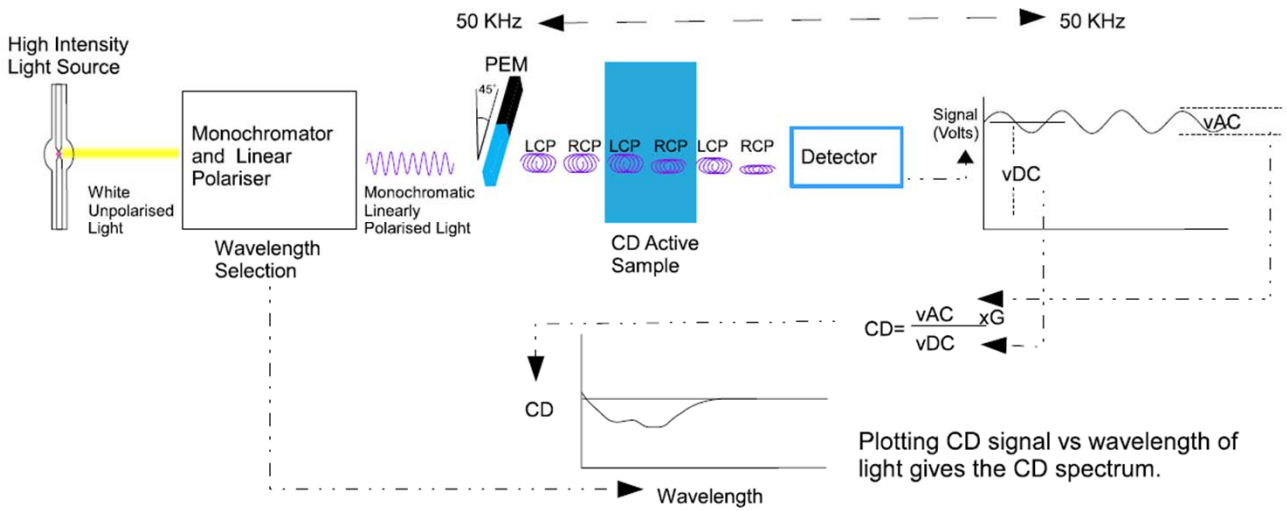

Applied Photophysics website

CD Data Analysis

The difference in absorption to be measured is very small. The differential absorption is usually a few 1/100ths to a few 1/10th of a percent, but it can be determined quite accurately. The raw data represent the ellipticity of the sample in millidegrees:

$$\theta_d = \frac{2.303}{4} \cdot (A_L - A_R) \cdot \frac{180}{\pi} \cdot [\text{deg}]$$

To be able to compare these ellipticity values they have to be converted into a normalized value, the mean molar ellipticity per residue. We need to consider path length *l*, concentration *c*, molecular mass *M* and number of residues n_r:

$$\theta_{mr} = \theta_d \cdot \frac{M}{c \cdot l \cdot n_r}$$

Expected signals from secondary structure elements

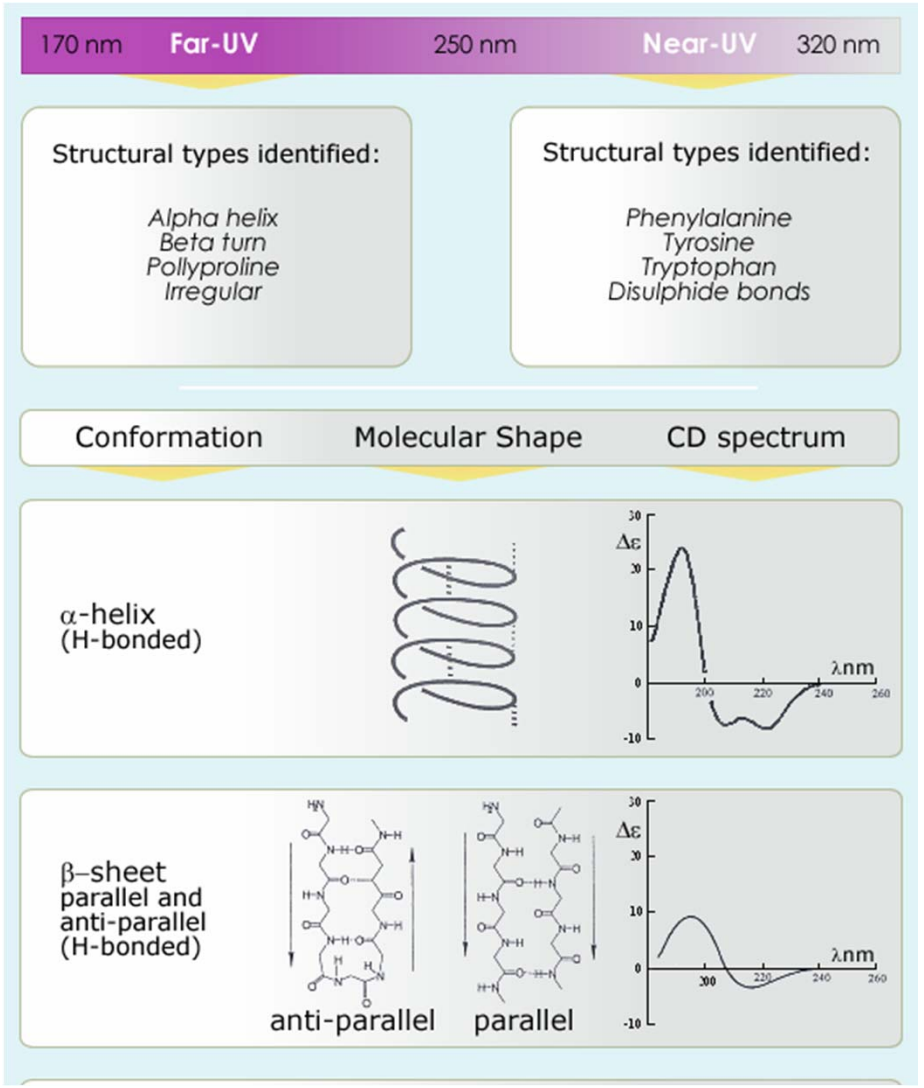

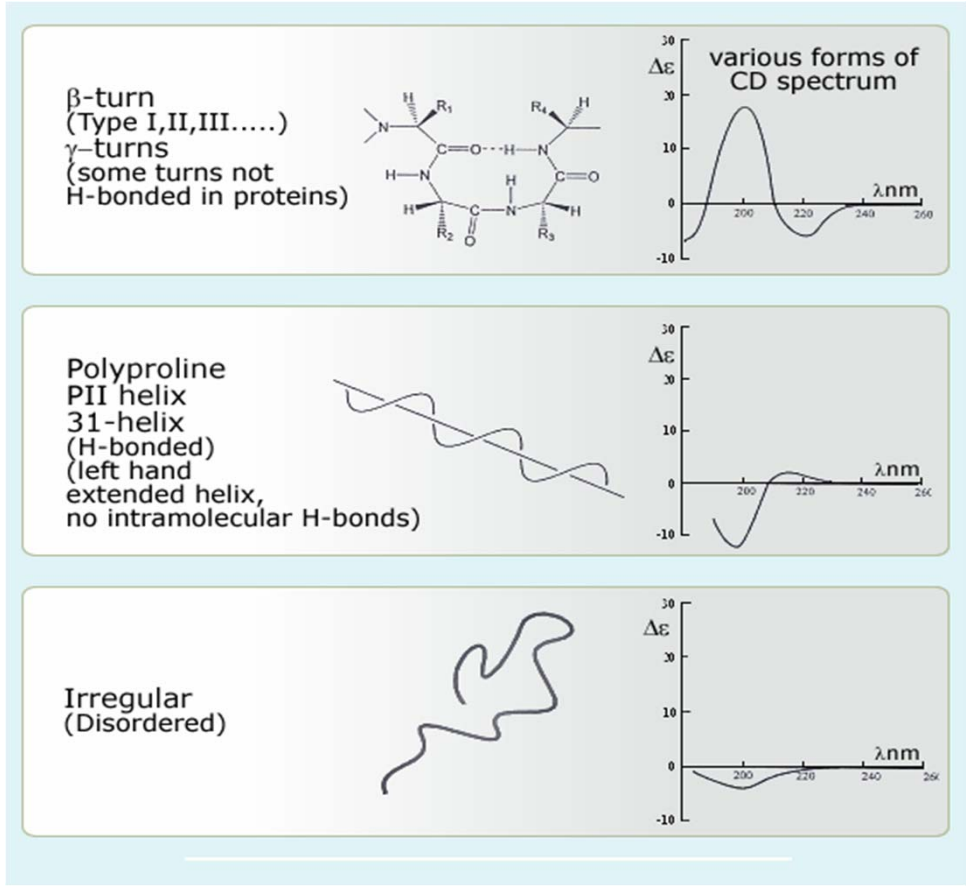

Applied Photophysics website

CD is often used to study folding – unfolding, often in conjunction with fluorescence

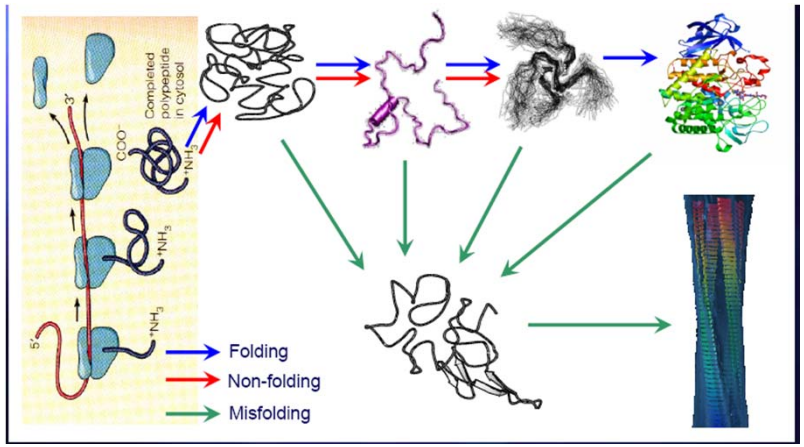

Example: HIV protease

Published in final edited form as:
J Mol Biol. 2009 April 10; 387(4): 1002–1016. doi:10.1016/j.jmb.2008.12.061.

The Folding Free Energy Surface of HIV-1 Protease: Insights into the Thermodynamic Basis for Resistance to Inhibitors

Amanda F. Noel, Osman Bilsel, Agnita Kundu, Ying Wu, Jill A. Zitzewitz*, and C. Robert Matthews*
Department of Biochemistry and Molecular Pharmacology, University of Massachusetts Medical School, Worcester, MA 01605, USA

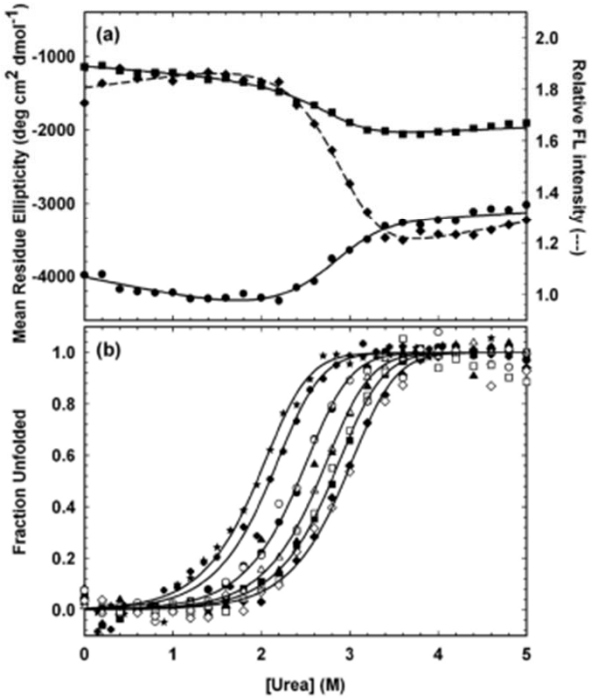

Figure 3.
Equilibrium folding properties of HIV-PR*. (a) Equilibrium unfolding monitored by CD at 220 nm (circles) and at 230 nm (squares) and by FL at 350 nm (diamonds) at 30 μM HIVPR*. Lines represent local fits to the two-state model, 2U ⇌ N_2. Protein concentration in monomer units was 30 μM. (b) Fraction unfolded protein (F_{app}) plots of the SVD vectors extracted from equilibrium unfolding CD (open symbols) and FL (filled symbols) spectra fit globally to the two-state model, 2U ⇌ N_2. Protein concentrations, expressed in terms of monomer, are 0.5 μM (stars), 1 μM (crosses), 5 μM (circles), 15 μM (triangles), 30 μM (squares), and 60 μM (diamonds). Buffer conditions are described in the caption to Figure 2.

Use CD to monitor activatory conformational changes in PBP2a (Penicillin Binding Protein 2a) the peptidyl transferase responsible of methicillin resistance in *Staphylococcus aureus* (MRSA), in the presence of peptidoglycan.

THE JOURNAL OF BIOLOGICAL CHEMISTRY
© 2004 by The American Society for Biochemistry and Molecular Biology, Inc.
Vol. 279, No. 39, Issue of September 24, pp. 40802–40806, 2004
Printed in U.S.A.

The Basis for Resistance to β-Lactam Antibiotics by Penicillin-binding Protein 2a of Methicillin-resistant *Staphylococcus aureus**

Received for publication, March 31, 2004, and in revised form, June 1, 2004
Published, JBC Papers in Press, June 28, 2004, DOI 10.1074/jbc.M403589200

Cosimo Fuda, Maxim Suvorov, Sergei B. Vakulenko, and Shahriar Mobashery‡

J|A|C|S COMMUNICATIONS

Published on Web 02/01/2005

Activation for Catalysis of Penicillin-Binding Protein 2a from Methicillin-Resistant *Staphylococcus aureus* by Bacterial Cell Wall

Cosimo Fuda, Dusan Hesek, Mijoon Lee, Ken-ichiro Morio, Thomas Nowak, and Shahriar Mobashery*

Published in final edited form as:
J Am Chem Soc. 2008 July 23; 130(29): 9212–9213. doi:10.1021/ja8029448.

Co-opting the Cell Wall in Fighting Methicillin-Resistant *Staphylococcus aureus*: Potent Inhibition of PBP 2a by Two Anti-MRSA β-Lactam Antibiotics

Adriel Villegas-Estrada, Mijoon Lee, Dusan Hesek, Sergei B. Vakulenko, and Shahriar Mobashery*
Department of Chemistry and Biochemistry, University of Notre Dame, Notre Dame, Indiana 46556

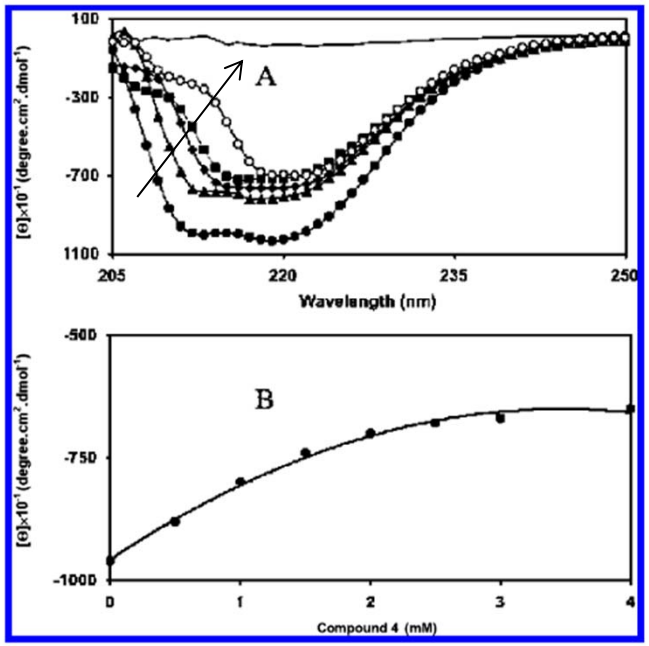

Figure 1. (A) Far-UV circular dichroic spectra of compound **4** by itself (4.0 mM, —), of PBP 2a by itself (3 μM, ●), and of PBP 2a (3 μM) in the presence of **4** at 1.0 mM (▲), 2.0 mM (◆), 3.0 mM (■), and 4.0 mM (○). The lines connect the data points and were not fitted to any specific model. (B) Change in molar ellipticity of PBP 2a at 222 nm as a function of the concentrations of compound **4**.

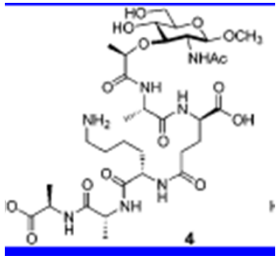

Eventually discover allosteric regulatory site in PBP2a as a novel drug target to combat MRSA

Crystallography shows the location of an allosteric site where peptidoglycan binds

How allosteric control of *Staphylococcus aureus* penicillin binding protein 2a enables methicillin resistance and physiological function

Lisandro H. Otero[a,1], Alzoray Rojas-Altuve[a,1], Leticia I. Llarrull[b], Cesar Carrasco-López[a], Malika Kumarasiri[b], Elena Lastochkin[b], Jennifer Fishovitz[b], Matthew Dawley[b], Dusan Hesek[b], Mijoon Lee[b], Jarrod W. Johnson[b], Jed F. Fisher[b], Mayland Chang[b], Shahriar Mobashery[b,2], and Juan A. Hermoso[a,2]

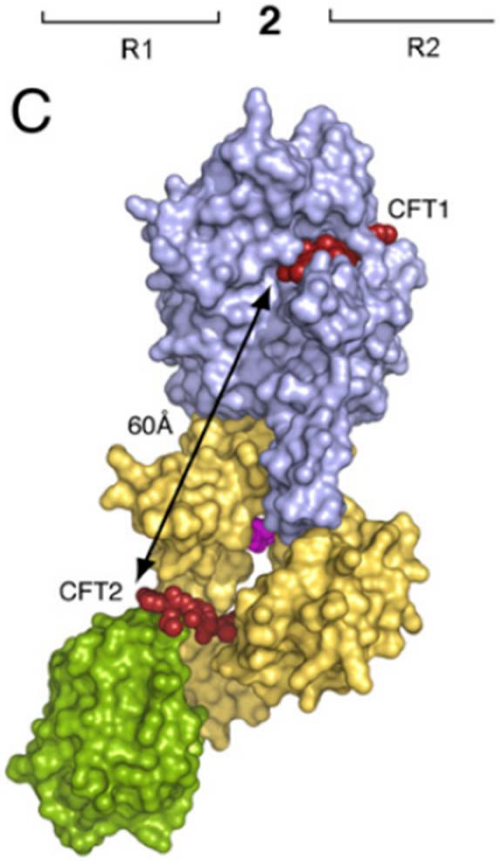

Fig. 1. Domains of PBP2a and I

Fluorescence anisotropy

The principle:
Excite fluorophor with polarized light. The emitted light will be polarised or depolarised depending on speed of tumbling (which is in turn related to mass).

Applications: measure binding

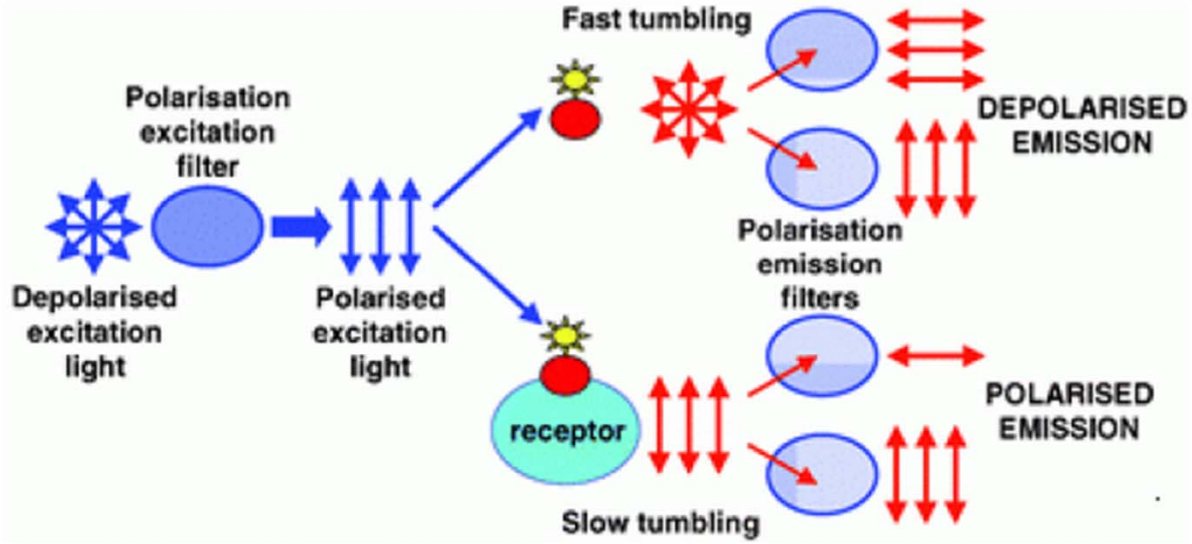

Example: Characterize interaction between p53 and peptides mimicking one of its interactors to stabilize oncogenic mutants

A peptide that binds and stabilizes p53 core domain: Chaperone strategy for rescue of oncogenic mutants

Assaf Friedler, Lars O. Hansson, Dmitry B. Veprintsev, Stefan M. V. Freund, Thomas M. Rippin, Penka V. Nikolova, Mark R. Proctor, Stefan Rüdiger, and Alan R. Fersht*

Cambridge University Chemical Laboratory and Cambridge Centre for Protein Engineering, Medical Research Council Centre, Hills Road, Cambridge CB2 2QH, United Kingdom

Contributed by Alan R. Fersht, November 27, 2001

Conformationally compromised oncogenic mutants of the tumor known complexes of p53 with its binding proteins, and so avoid

www.pnas.org/cgi/doi/10.1073/pnas.241629998 PNAS | January 22, 2002 | vol. 99 | no. 2 | 937–942

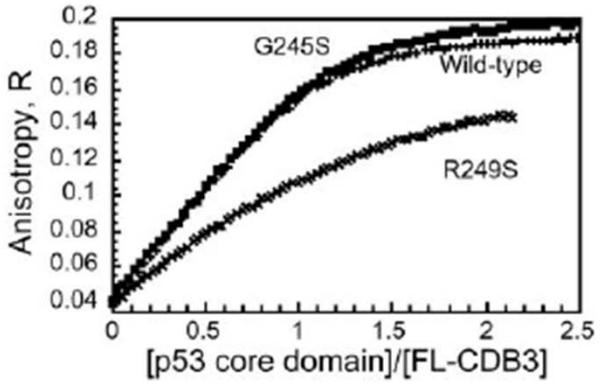

Fig. 3. CDB3 binding to p53C analyzed by fluorescence anisotropy. Wild-type and mutant p53C were titrated into a fluorescein-labeled CDB3 (4.6 μM; see *Materials and Methods* for details).

shown).

The binding of FL-CDB3 to two p53C mutants was measured: to G245S, which is 95% folded at 37°C and is destabilized by 1.21 kcal/mol at 10°C; and to R249S, which is 85% folded at 37°C and is distorted and destabilized by 1.92 kcal/mol at 10°C (3, 7). At 10°C both mutants are expected to be in a native-like conformation. K_d values, from fluorescence anisotropy (see Fig. 3), were 0.57 ± 0.09 μM for G245S and 3.3 ± 0.5 μM for R249S.

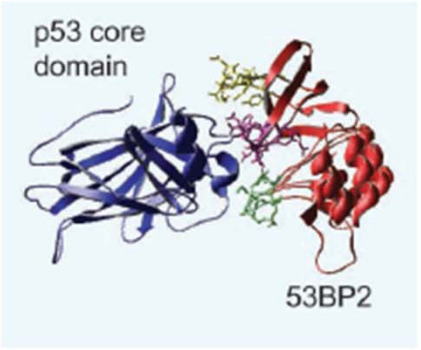

Fig. 1. Crystal structure of the p53C (blue)–53BP2 (red) complex (coordinates taken from ref. 10) with the three 53BP2-derived peptides synthesized for this study highlighted: CDB1 (residues 422–428), green; CDB2 (residues 469–477), yellow; CDB3 (residues 490–498), purple. The picture was generated using SWISSPDB VIEWER (23).

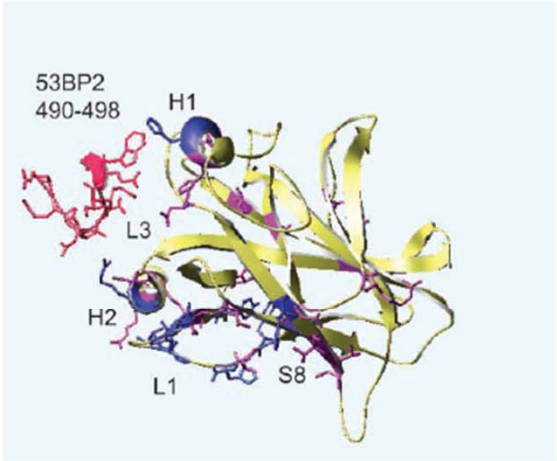

Fig. 2. Chemical shift changes ($\Delta\partial$) in p53C on binding to CDB3. Deviations above five times the standard deviation ($\Delta\partial > 0.25$ ppm for ^{15}N and $\Delta\partial > 0.05$ ppm for ^{1}H) were considered significant (color-coded blue). $\Delta\partial$ differences between 2.5 times and 5 times the standard deviation ($0.125 < \Delta\partial < 0.25$ ppm for ^{15}N, $0.025 < \Delta\partial < 0.05$ ppm for ^{1}H) were considered as minor (color-coded purple), and $\Delta\partial$ differences below 2.5 times the standard deviation ($\Delta\partial < 0.125$ ppm for ^{15}N and $\Delta\partial < 0.025$ ppm for ^{1}H) were considered insignificant (color-coded yellow). See text for residue number details. CDB3 in its original position in the 53BP2-p53 complex is shown in red (coordinates taken from ref. 10). The picture was generated using SWISSPDB VIEWER.

Use of absorbance and fluorescence to characterize enzyme mechanisms:

- Enzyme activity assays
- Binding studies
- Redox titrations
- Rapid reaction kinetics

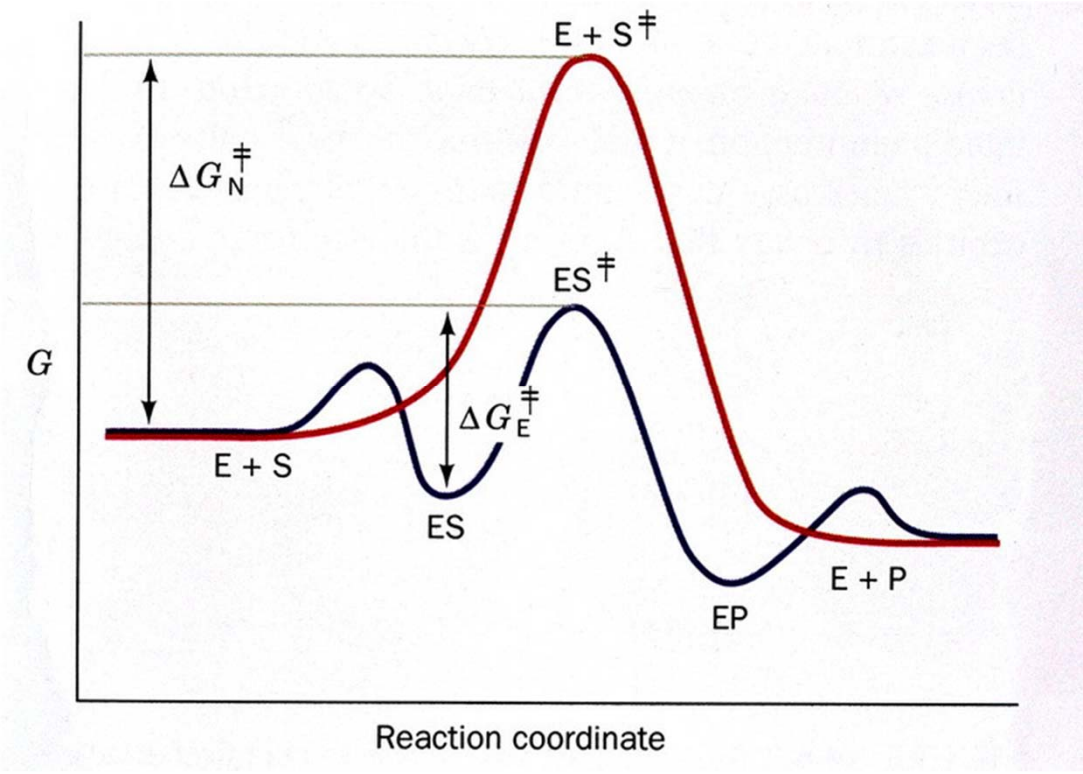

$$E + S \underset{k_2}{\overset{k_1}{\rightleftharpoons}} ES \underset{k_4}{\overset{k_3}{\rightleftharpoons}} EP \underset{k_6}{\overset{k_5}{\rightleftharpoons}} E+P$$

Enzymes catalyze chemical reactions with:

- High (stereo)specificity with respect to the substrates and products
- High acceleration rates (versus the uncatalysed reaction)

Enzymes do not alter the reaction equilibrium

The high acceleration rates are achieved by combining:

- Orientation and proximity effects
- Acid-base catalysis
- Electrostatic catalysis
- Covalent catalysis
- Metal-assisted catalysis
- Preferential stabilization of the transition-state

The study of enzyme catalytic properties complements structural studies and is essential for (e.g.) drug design: rational drug design and inhibitor characterization.

Initial velocity measurements under steady-state conditions allow to determine the kinetic parameters V and K_M for the substrates, which depend on the rate constants that govern the individual reaction steps.

$$E + S \underset{k_2}{\overset{k_1}{\rightleftharpoons}} ES \underset{k_4}{\overset{k_3}{\rightleftharpoons}} EP \underset{k_6}{\overset{k_5}{\rightleftharpoons}} E+P$$

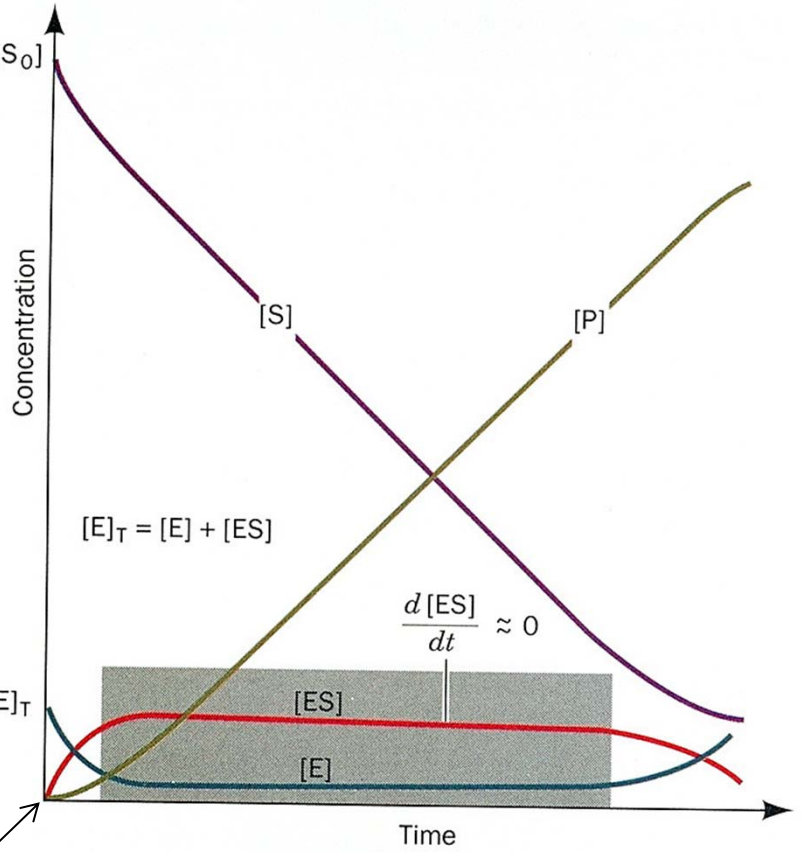

Velocity measurements under pre-steady-state conditions allow to determine directly the values of the rate constants that govern the individual reaction steps

Initial velocity measurements of the enzyme-catalyzed reaction are carried out, under a variety of conditions,

- to quantify the enzyme and
- to obtain information on the reaction mechanism, regulatory mechanisms, the active enzyme form.

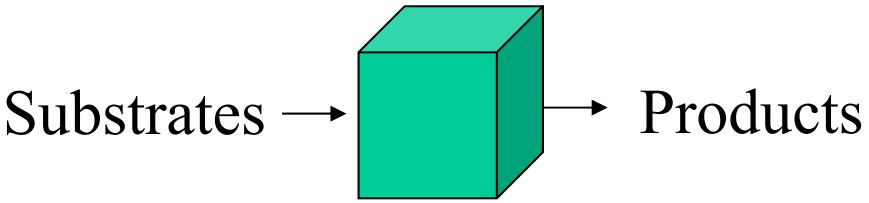

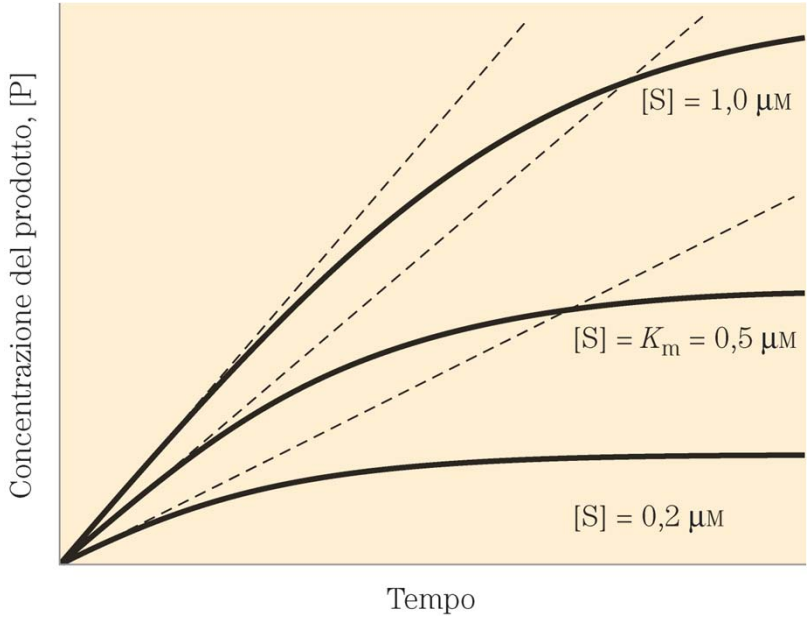

$$v = -\frac{d[S]}{dt} = \frac{d[P]}{dt}$$

The Michaelis-Menten Equation.

$$v_o = \frac{V_{max}[S]}{K_m + [S]}$$

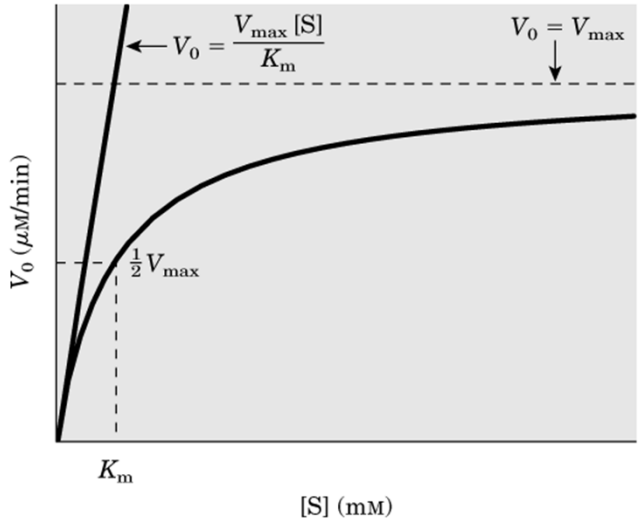

for the Simple Model: $E + S \underset{k_2}{\overset{k_1}{\rightleftharpoons}} ES \xrightarrow{k_3} E+P$

The Assumptions of the model

- $[E] << [S_o]$
- Measure v_o (initial velocity) when $[P] = 0$
- $v = k_3 * [ES]$
- $[ES]$ = constant

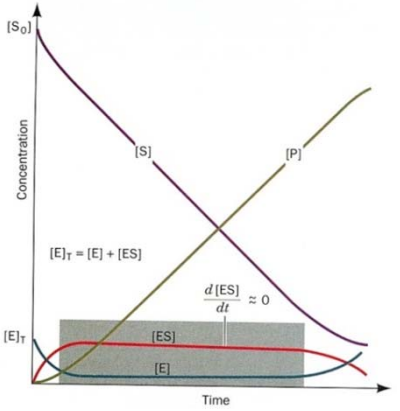

The expression of v: $$v = \frac{k_3 [Etot] * [S]}{\frac{k_2+k_3}{k_1} + [S]}$$

$$V_{max} = k_3[E_t]$$

$$K_m = \frac{k_2 + k_3}{k_1}$$

The Michaelis-Menten Equation.

for the Simple Model: $E + S \underset{k_2}{\overset{k_1}{\rightleftharpoons}} ES \xrightarrow{k_3} E+P$

$$v = \frac{k_3\,[Etot] * [S]}{\frac{k_2+k_3}{k_1} + [S]}$$

$$V_{max} = k_3[E_t]$$

$$K_m = \frac{k_2 + k_3}{k_1}$$

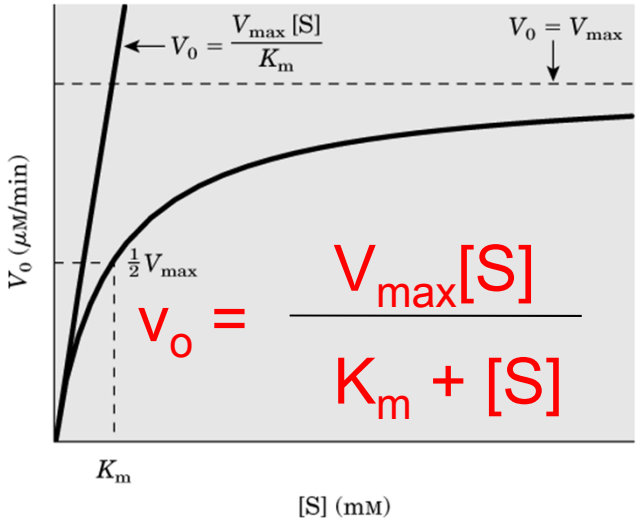

$$v_o = \frac{V_{max}[S]}{K_m + [S]}$$

Simplifying....

k_1, k_2, k_3 will depend on , e.g., temperature; isotopic substitution of S and solvent; ionic strength of the medium, solvent viscosity

«Active» enzyme form with respect to S or P binding will depend on, e.g., pH, presence of inhibitors

Thus, V and V/K values as a function of T, pH, I, isotopic substitutions, inhibitors will give information on E, on the catalytic mechanism and on the relative magnitude of little k's

$$v = -\frac{d[S]}{dt} = \frac{d[P]}{dt}$$

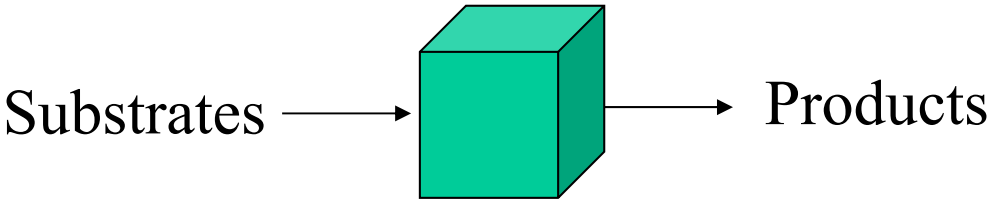

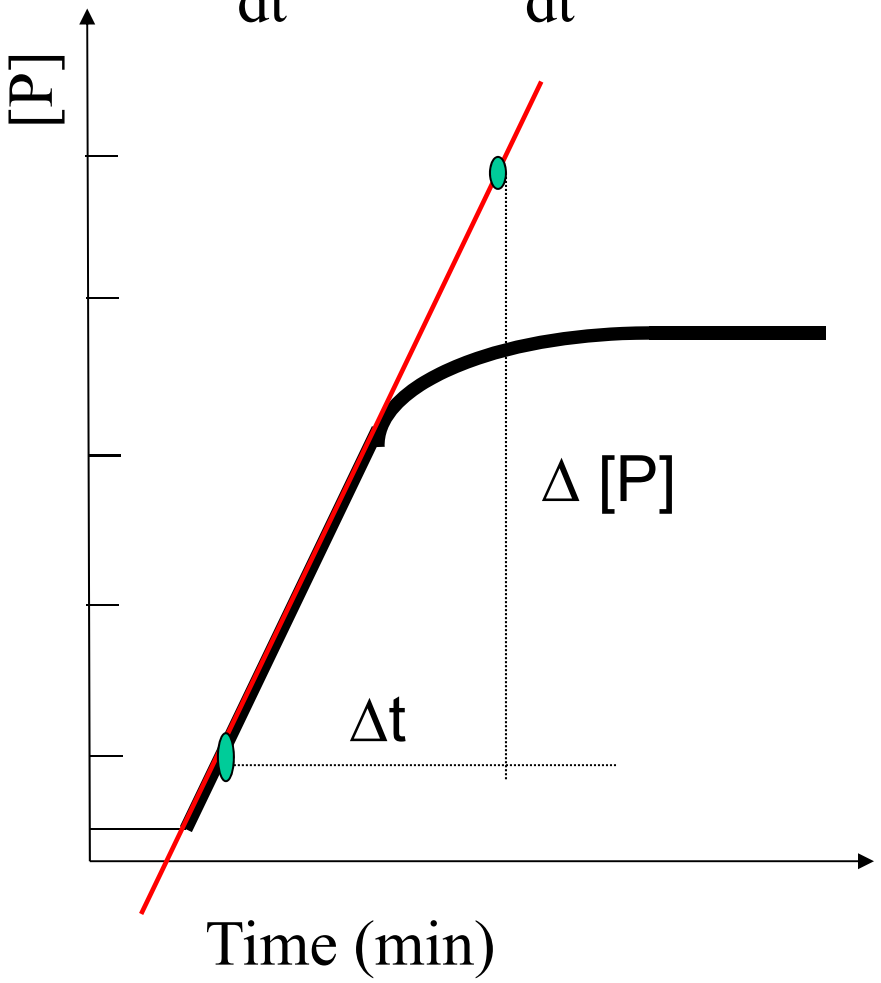

Continuous spectrophotometric assays are very handy: no sample manipulation, direct observations, often high sensitivity, reproducibility.

Information we can extract from steady-state kinetics:

Reaction mechanism,

Steady-state kinetic mechanism,

Position and structure of the transition state

Relative magnitude of rate constants

What may we miss?

Conformational changes part of the reaction mechanism

Reaction intermediates

Values of individual rate constants

Substrate/product/inhibitor binding constants

Direct Observation of the Enzyme or the ligand using an intrinsic spectroscopic probe:

Determination of equilibrium (or dissociation) constants

$$A + B \underset{k_2}{\overset{k_1}{\rightleftharpoons}} C$$

$$K_d = \frac{[A]*[B]}{[C]} \qquad K_{eq} = \frac{[C]}{[A]*[B]}$$

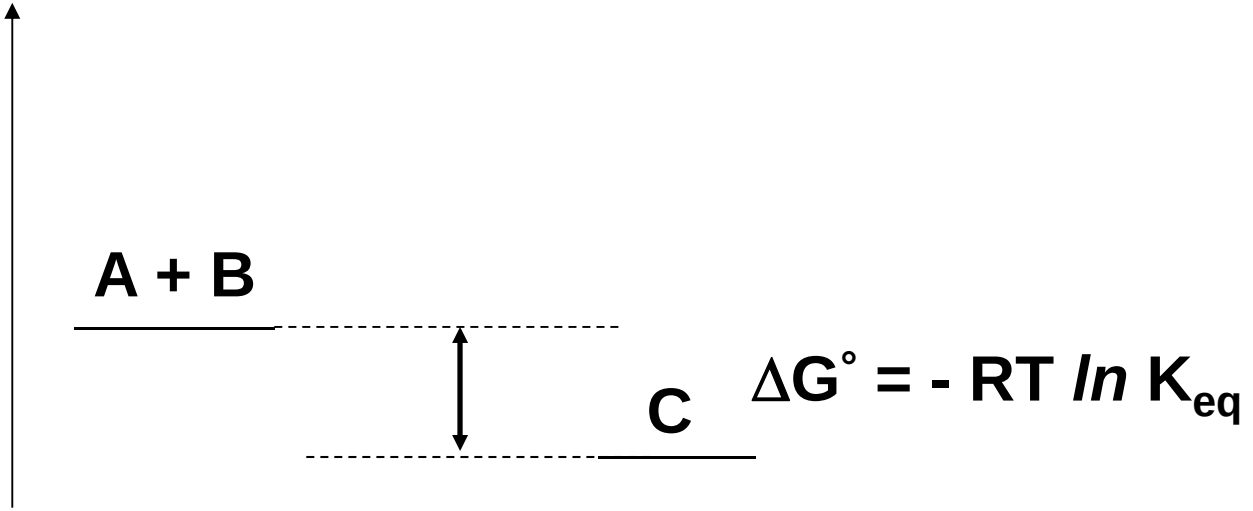

Flavin-dependent enzymes contain FMN or FAD as the coenzyme

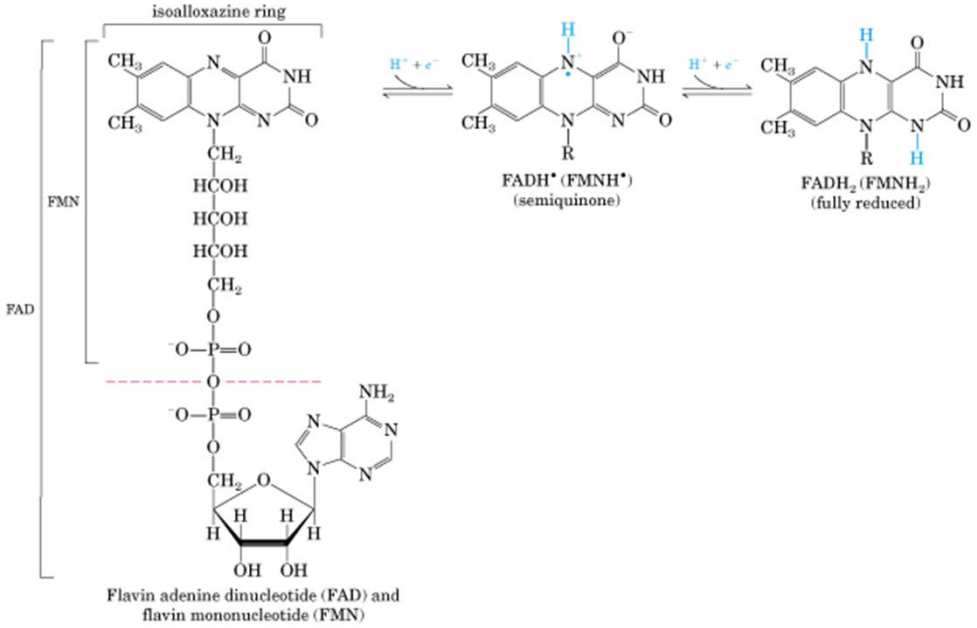

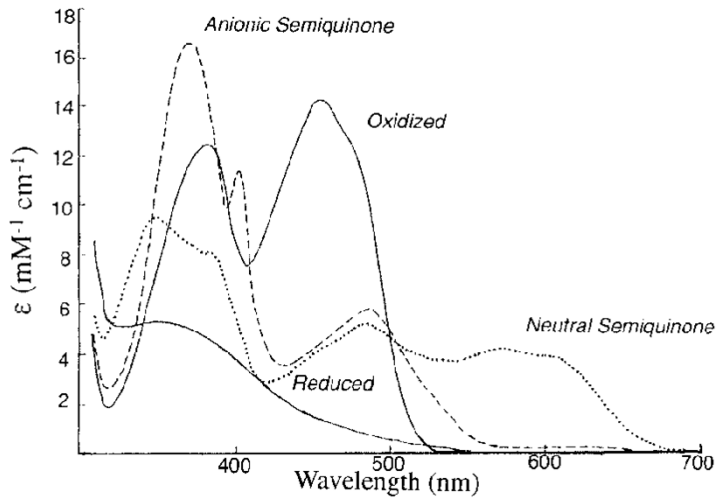

Scheme 2

Reductive and oxidative half-reactions of flavoproteins

Fl, flavin; ox, oxidized; red, reduced. See the text for details.

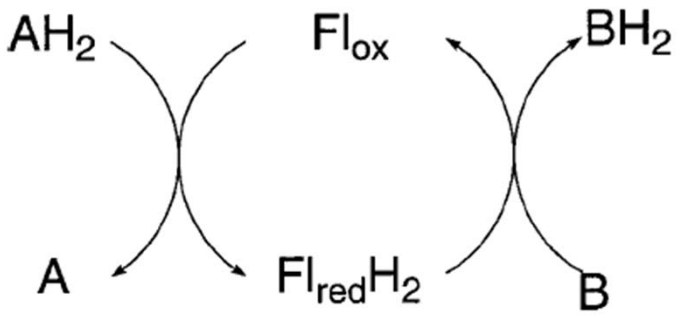

The flavin cofactor acts as an intermediate electron acceptor between the substrate/product couple: (can study reductive and oxidative half reaction, under anaerobiosis).

The flavin absorbance spectrum is sensitive to:

Redox state

Data are from [23].

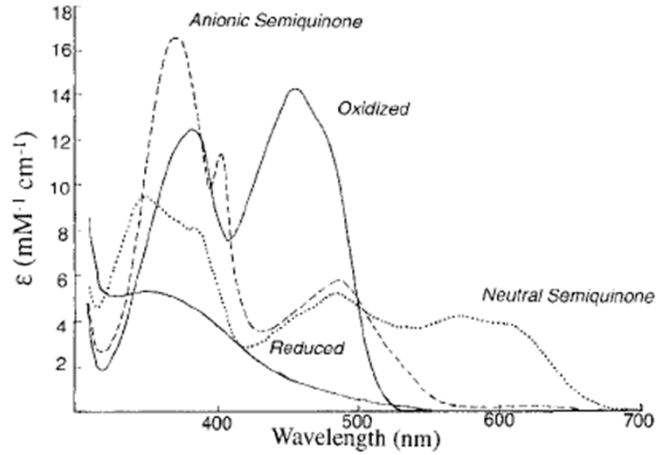

Flavin ox (Yellow)

Flavin hydroquinone (leuco)

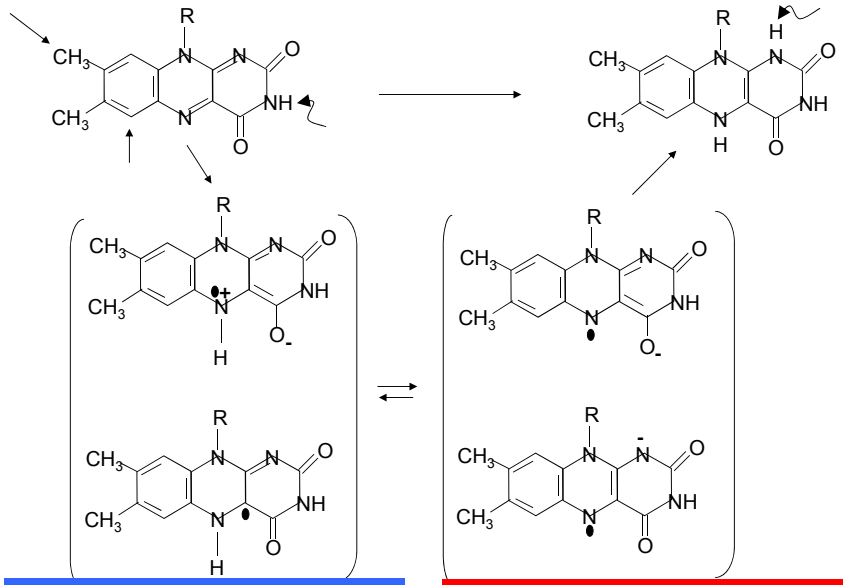

Neutral semiquinone (Blue)

Anionic semiquinone (Red)

Ionization state of isoalloxazine positions, which is in turn sensitive to environment (protein, ligands, ...)

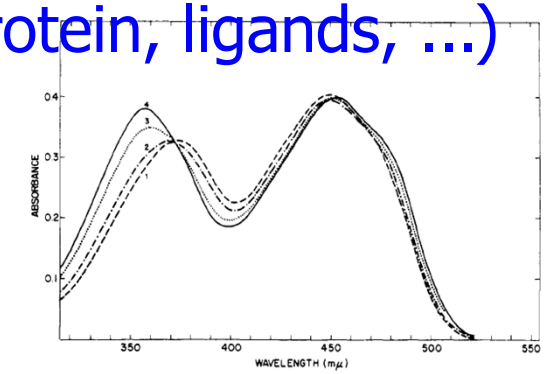

FIGURE 10: Effect of *p*H on the spectrum of FAD in 0.1 M pyrophosphate, 7°. Curve 1, *p*H 8.70; curve 2, *p*H 10.04; curve 3, *p*H 10.60; curve 4, *p*H 12.1.

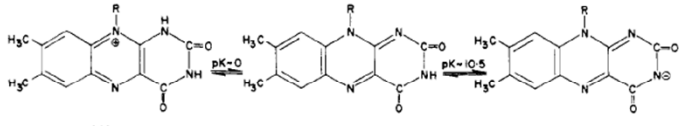

FIGURE 9: Ionic forms of the isoalloxazine moiety of flavins (after Hemmerich and Müller, 1965).

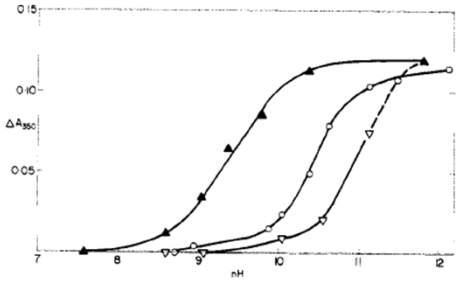

FIGURE 11: Ionization of the 3-imino group of the isoalloxazine moiety in FAD (○), D-amino acid oxidase (▲), and the benzoate complex of D-amino acid oxidase (△).

The flavin absorption spectrum is sensitive to the «environment»:

Binding of Benzoate (an inhibitor of D-amino acid oxidase that mimicks the iminoacid intermediate) causes large absorbance changes, which can be used to calculate Kd

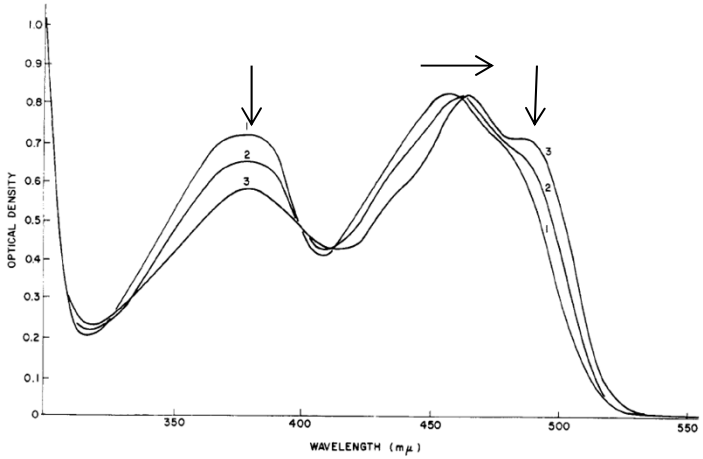

FIGURE 1: Effect of benzoate on the spectrum of D-amino acid oxidase. Curve 1, benzoate-free enzyme (4.85 mg/ml) in 0.1 M pyrophosphate, *p*H 8.5; curve 2, after 0.46 mole benzoate per mole enzyme FAD; curve 3, after 4.33 moles benzoate.

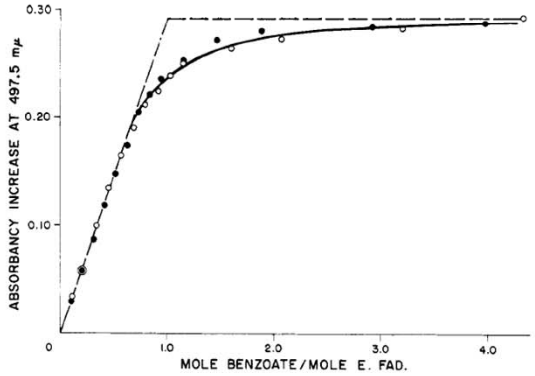

FIGURE 2: Increase in absorbancy at 497.5 mμ on titration of D-amino acid oxidase with benzoate. Conditions as in Figure 1. (○), Results obtained in the absence of added FAD (FAD content of the preparation used was 15.4 mμmoles/mg protein); (●), results obtained on enzyme dialyzed to equilibrium against 2×10^{-4} M FAD (bound FAD content 20 mμmoles/mg protein). The concentration of enzyme-bound FAD in each experiment was 7.3×10^{-5} M.

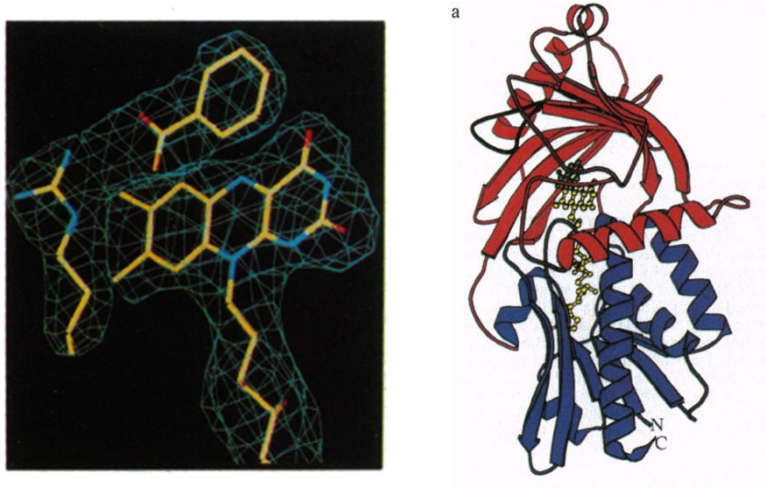

FIG. 1. Electron density for FAD, benzoate, and Arg-283 calculated at 3.0 Å after phase extension by eightfold averaging. The contour level is 1σ. The refined final model is colored by atom type: C, yellow; N, blue; O; red. Produced with program O (17).

Mattevi et al. PNAS

Some flavoproteins can form a Flavin-N(5)-sulfite adduct

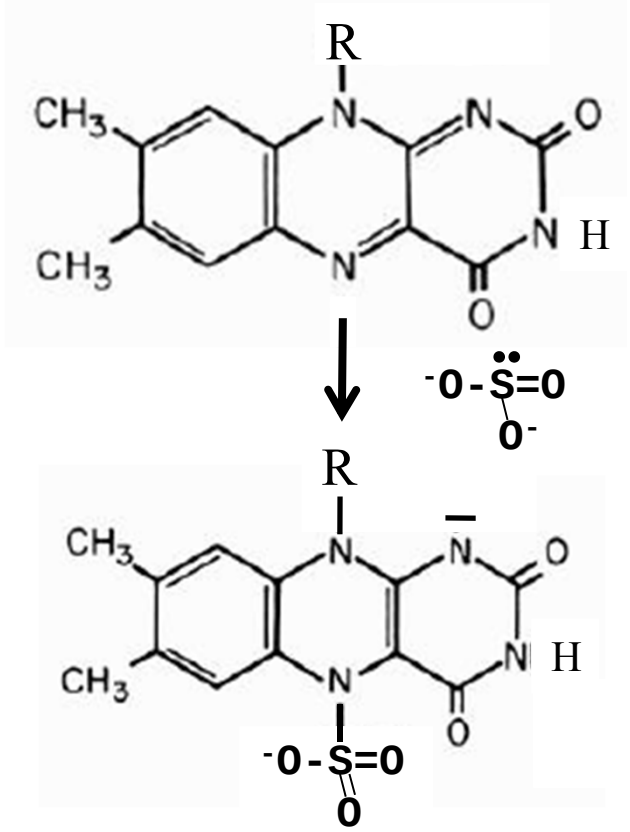

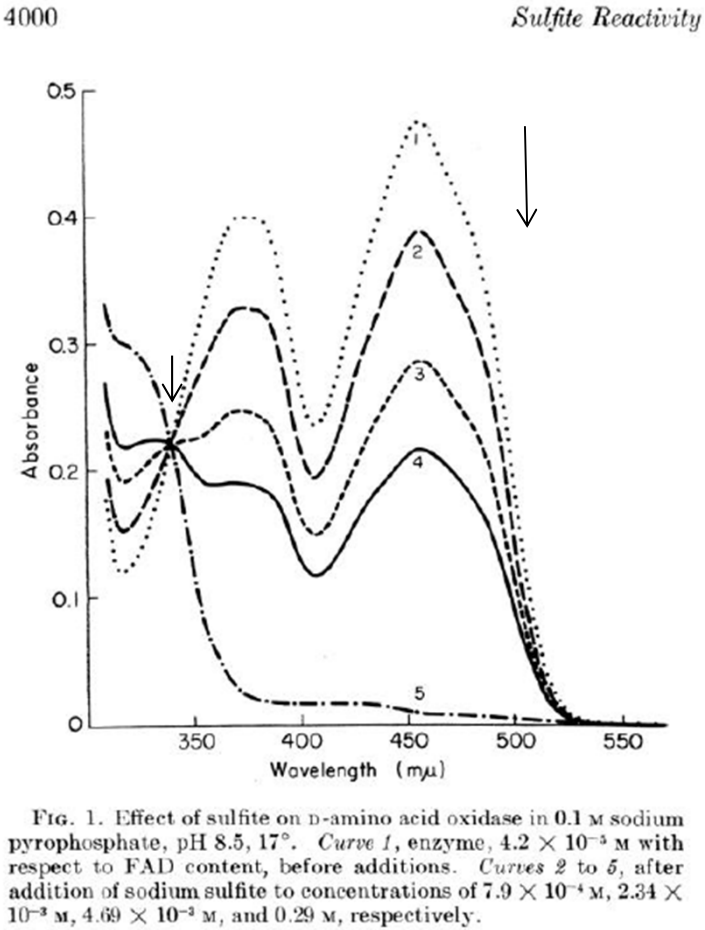

FIG. 1. Effect of sulfite on D-amino acid oxidase in 0.1 M sodium pyrophosphate, pH 8.5, 17°. *Curve 1*, enzyme, 4.2×10^{-5} M with respect to FAD content, before additions. *Curves 2* to *5*, after addition of sodium sulfite to concentrations of 7.9×10^{-4} M, 2.34×10^{-3} M, 4.69×10^{-3} M, and 0.29 M, respectively.

The formation of the flavin N(5) sulfite adduct gives information on the electronic distribution of the bound flavin coenzyme, which depends on the flavin environment.

Typically: flavin in oxidases reacts with sulfite, in oxidoreductases does not.

Determination of the midpoint potential of bound flavin coenzymes

Data are from [23].

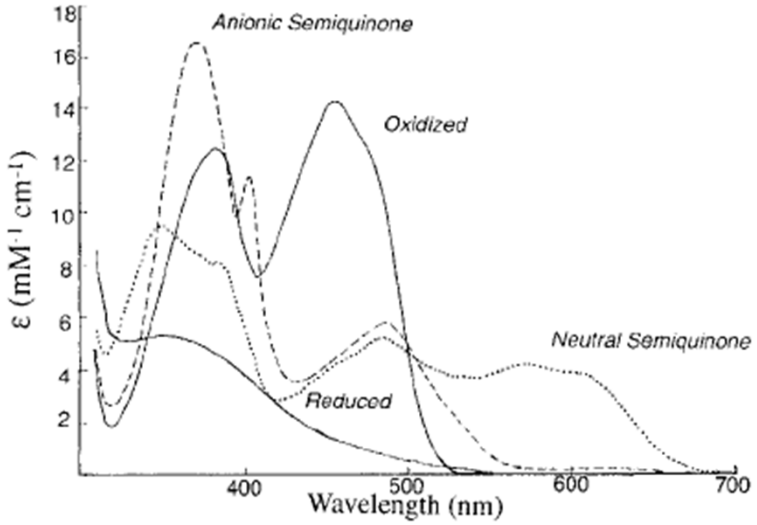

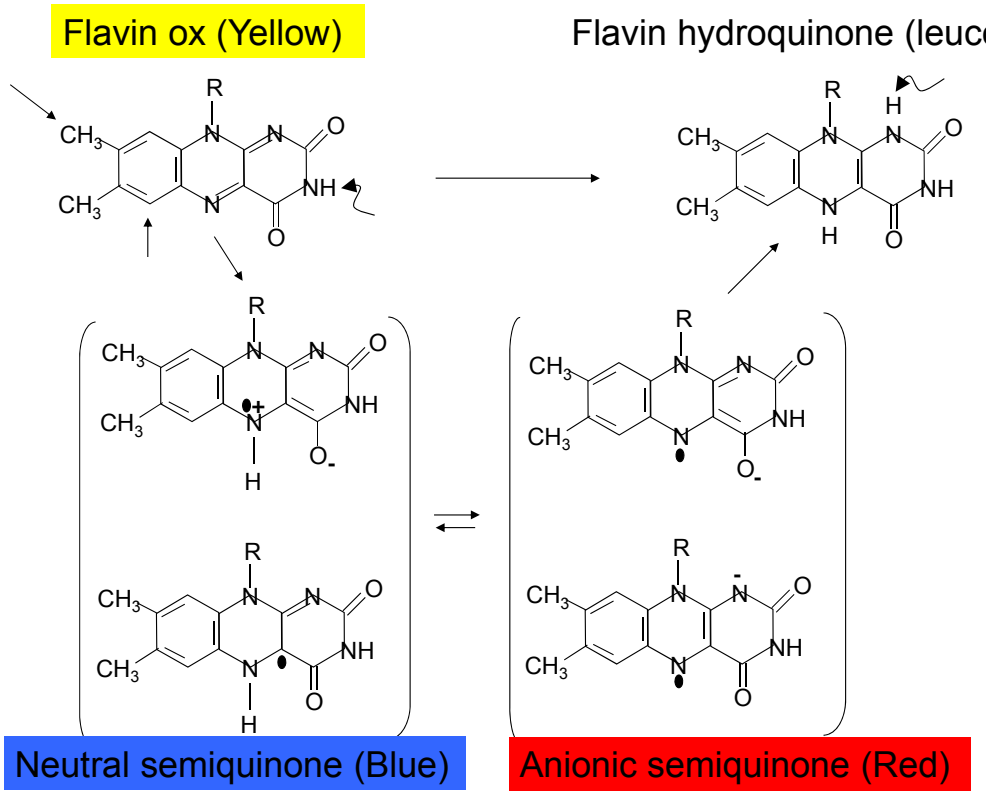

Several important reactions are oxidoreductions

The E° of a redox couple indicates the tendency of the species to accept/donate electrons.

In redox reactions electrons flow from species with lower E_m to species with higher E_m

Fundamental equation:
Nernst equation

$$E_A = E_A° - (RT/nF) \ln(A_{red}/A_{ox})$$

$$\Delta G = - nF\Delta E$$

table 14–7

Standard Reduction Potentials of Some Biologically Important Half-Reactions, at 25 °C and pH 7

Half-reaction	$E'°$ (V)
$\frac{1}{2}O_2 + 2H^+ + 2e^- \longrightarrow H_2O$	0.816
$Fe^{3+} + e^- \longrightarrow Fe^{2+}$	0.771
$NO_3^- + 2H^+ + 2e^- \longrightarrow NO_2^- + H_2O$	0.421
Cytochrome *f* $(Fe^{3+}) + e^- \longrightarrow$ cytochrome *f* (Fe^{2+})	0.365
$Fe(CN)_6^{3-}$ (ferricyanide) $+ e^- \longrightarrow Fe(CN)_6^{4-}$	0.36
Cytochrome a_3 $(Fe^{3+}) + e^- \longrightarrow$ cytochrome a_3 (Fe^{2+})	0.35
$O_2 + 2H^+ + 2e^- \longrightarrow H_2O_2$	0.295
Cytochrome *a* $(Fe^{3+}) + e^- \longrightarrow$ cytochrome *a* (Fe^{2+})	0.29
Cytochrome *c* $(Fe^{3+}) + e^- \longrightarrow$ cytochrome *c* (Fe^{2+})	0.254
Cytochrome c_1 $(Fe^{3+}) + e^- \longrightarrow$ cytochrome c_1 (Fe^{2+})	0.22
Cytochrome *b* $(Fe^{3+}) + e^- \longrightarrow$ cytochrome *b* (Fe^{2+})	0.077
Ubiquinone $+ 2H^+ + 2e^- \longrightarrow$ ubiquinol $+ H_2$	0.045
$Fumarate^{2-} + 2H^+ + 2e^- \longrightarrow succinate^{2-}$	0.031
$2H^+ + 2e^- \longrightarrow H_2$ (at standard conditions, pH 0)	0.000
Crotonyl-CoA $+ 2H^+ + 2e^- \longrightarrow$ butyryl-CoA	−0.015
$Oxaloacetate^{2-} + 2H^+ + 2e^- \longrightarrow malate^{2-}$	−0.166
$Pyruvate^- + 2H^+ + 2e^- \longrightarrow lactate^-$	−0.185
Acetaldehyde $+ 2H^+ + 2e^- \longrightarrow$ ethanol	−0.197
FAD $+ 2H^+ + 2e^- \longrightarrow FADH_2$	−0.219*
Glutathione $+ 2H^+ + 2e^- \longrightarrow$ 2 reduced glutathione	−0.23
$S + 2H^+ + 2e^- \longrightarrow H_2S$	−0.243
Lipoic acid $+ 2H^+ + 2e^- \longrightarrow$ dihydrolipoic acid	−0.29
$NAD^+ + H^+ + 2e^- \longrightarrow NADH$	−0.320
$NADP^+ + H^+ + 2e^- \longrightarrow NADPH$	−0.324
Acetoacetate $+ 2H^+ + 2e^- \longrightarrow$ β-hydroxybutyrate	−0.346
α-Ketoglutarate $+ CO_2 + 2H^+ + 2e^- \longrightarrow$ isocitrate	−0.38
$2H^+ + 2e^- \longrightarrow H_2$ (at pH 7)	−0.414
Ferredoxin $(Fe^{3+}) + e^- \longrightarrow$ ferredoxin (Fe^{2+})	−0.432

$$A^{n+}_{ox} + B_{red} \leftrightarrow A_{red} + B^{n+}_{ox}$$

An oxidoreduction reaction is formally the sum of two half-reactions.

$$A^{n+}_{ox} + ne^- = A_{red} \qquad E_A = E_A° - (RT/nF)\ \ln(A_{red}/A_{ox})$$

$$B_{red} = B^{n+}_{ox} + ne^- \qquad E_B = E_B° - (RT/nF)\ \ln(B_{red}/B_{ox})$$

n= no. transferred electrons; $\mathcal{F}$ = Faraday constant= 96494 JV^{-1}; R, 8.341 $Jmol^{-1}K^{-1}$; T, 20°C = 293K n Log N = 2.303 Ln N; 2.302RT/nF with n = 2 = 0.029V at 20°C

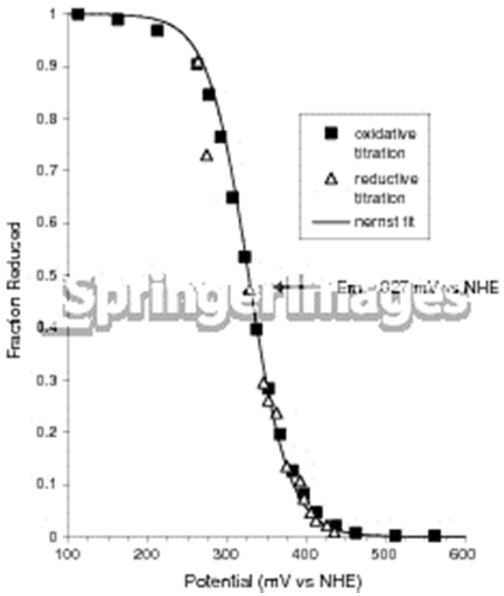

With a Redox titration we can determine E°

E = E° (E_m) when $A_{red} = A_{ox}$

But we need to know E (in V)

Experimental set-up (anerobiosis conditions):

$$E_{ox} + \text{Dye}_{ox} \xrightarrow{e^-} \begin{cases} E_{ox} + ne^- \leftrightarrow E_{red} \\ \text{Dye}_{ox} + ne^- \leftrightarrow \text{Dye}_{red} \end{cases}$$

Let equilibrate WELL with the help of a mediator; quantify species; then add more reducing agent, and repeat

Use Dye redox state to measure E (V)

$$E = E_{Dye} = E_{Dye}^{\circ} - (RT/nF)\ \ln(\text{Dye}_{red}/\text{Dye}_{ox})$$

Known values

Determine during titration

Calculate Em of enzyme bound cofactor

$$E = E_{E}^{\circ} - (RT/nF)\ \ln(E_{red}/E_{ox})$$

Known from E_{Dye}

Determine during titration

Spectrophotometric determination of the midpoint potential of FMN:

(1) Anaerobic reductive titrations of FMN; Dye; FMN+Dye under conditions that guarantee equilibrium

(2) Determine λ and ε useful to measure FMNox/red and Dye ox/red

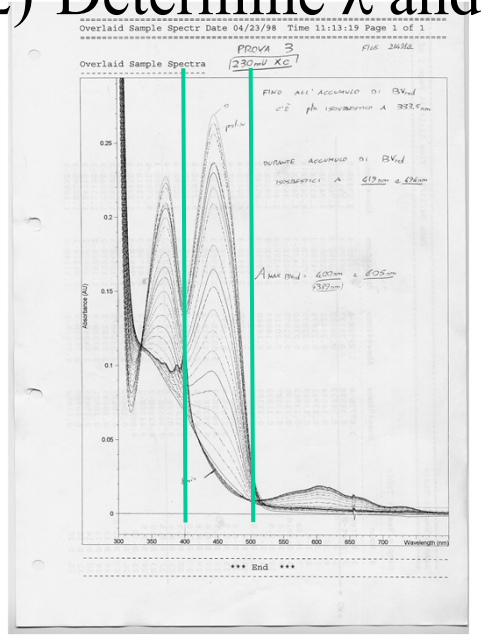

20 μM FMN

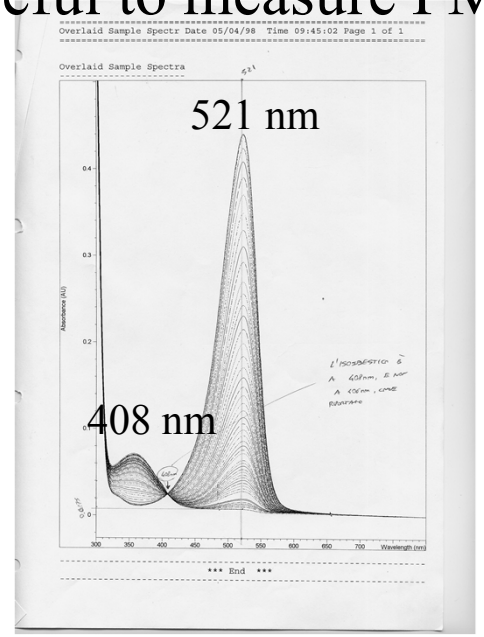

17 μM Phenosafranine, E°=-252mV

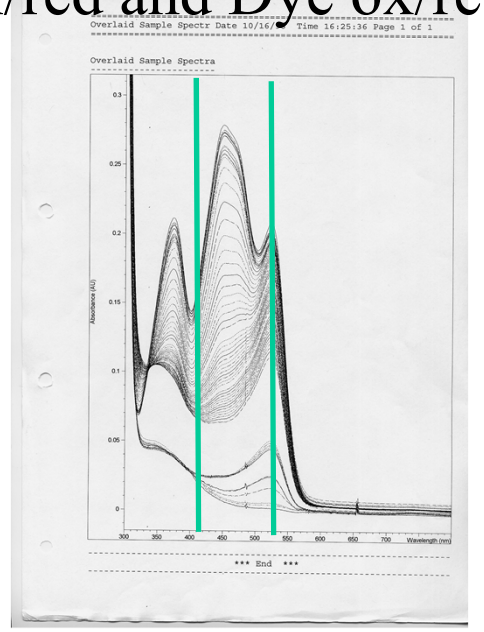

20 μM FMN + 17 μM PS

(3) Monitor A_{408} to determine FMN_{red}/FMN_{total} and A_{521} to determine PS_{red}/Ps_{tot} during an equilibrium redox titration

(4) Apply Nernst equation to determine $E°_{FMN}$

Spectrophotometric determination of the midpoint potential of FMN: rearrange Nernst equation

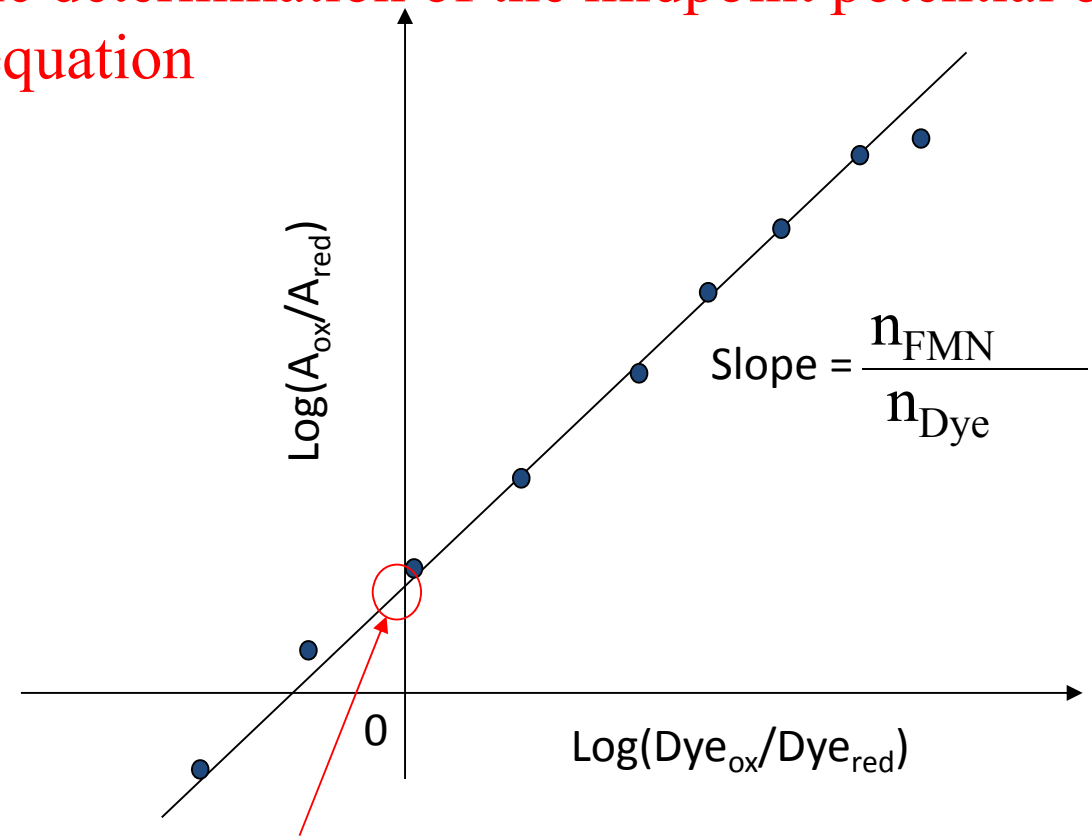

$$\text{Log}\ \frac{FMN_{ox}}{FMN_{red}} = (E_{m,Dye} - E_{m,FMN}) * \frac{n_{FMN} * F}{2.303RT} + \frac{n_{FMN}}{n_{Dye}} \text{Log}\ \frac{Dye_{ox}}{Dye_{red}}$$

- 0.99

-252 mV

-222 mV

2

0.9 ≈1!

Determine the mid-point potential of FAD, FMN and of the 3Fe/4S center of NADPH-GltS

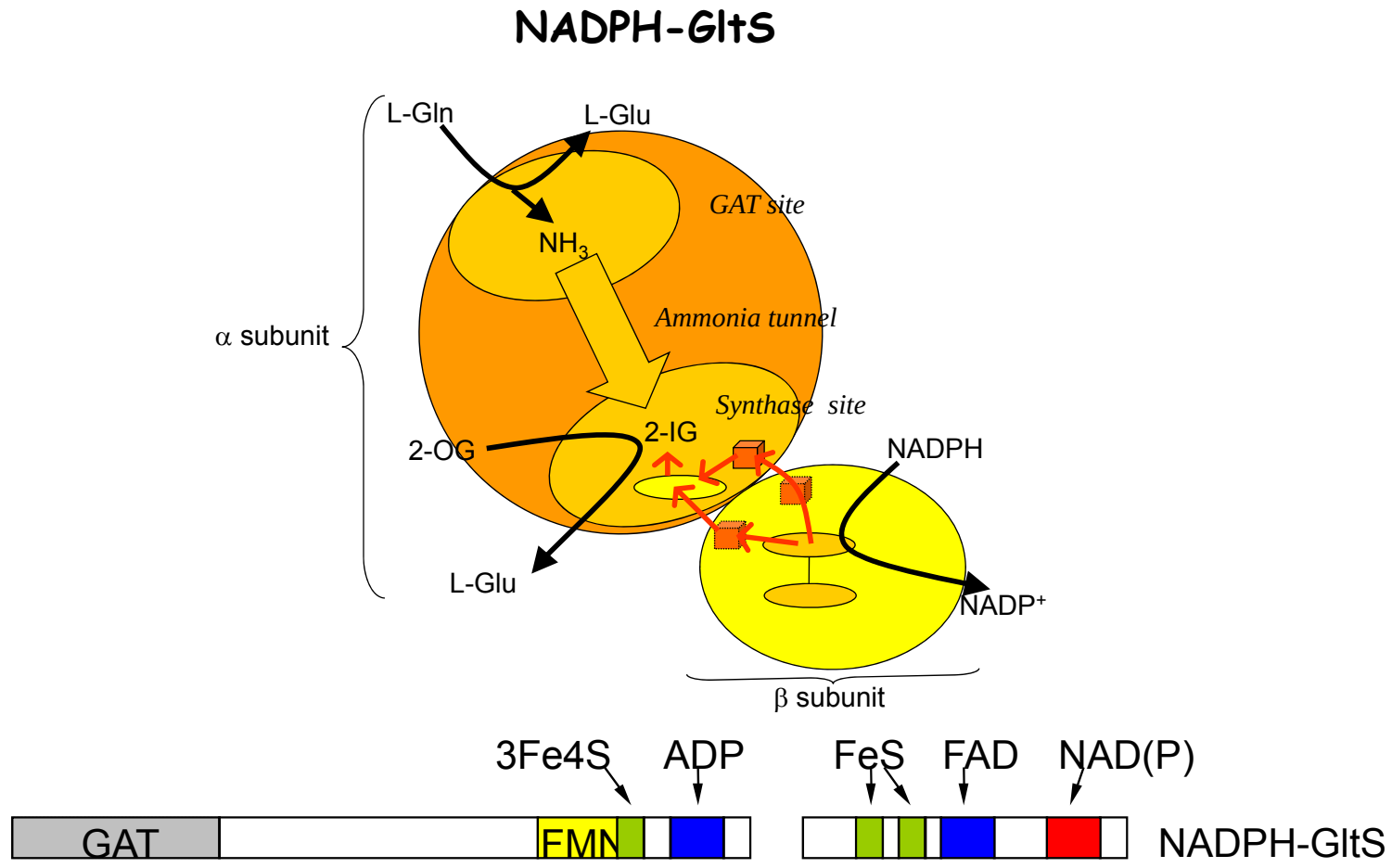

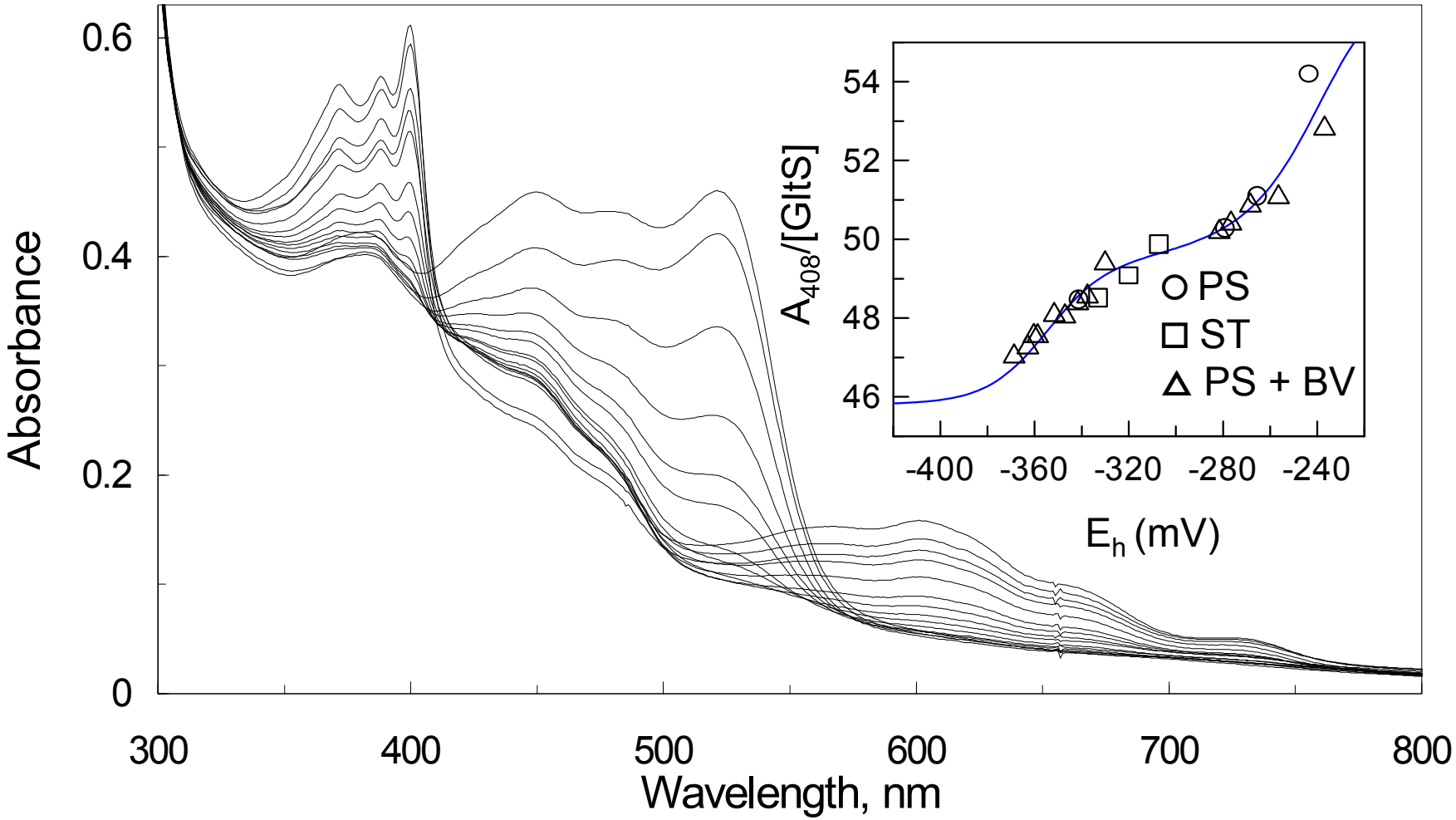

Enzyme	E_m, mV FAD (n = 2)	FMN (n=2)	Fe/S_I (n = 1)
α		-235.0 ± 1.9	-260.0 ± 3.5
β	-339.8 ± 1.5		
αβ	-354.7 ± 2.5	-238.9 ± 7.5	-245.0 ± 12.0

Propose electron transfer pathway in NADPH-GltS from measurement of E_m of FAD, FMN coenzymes and 3Fe/4S cluster and a model of GltS protomer from Small Angle X-ray Scattering (SAXS) and low-temperature electron microscopy (cryoEM)

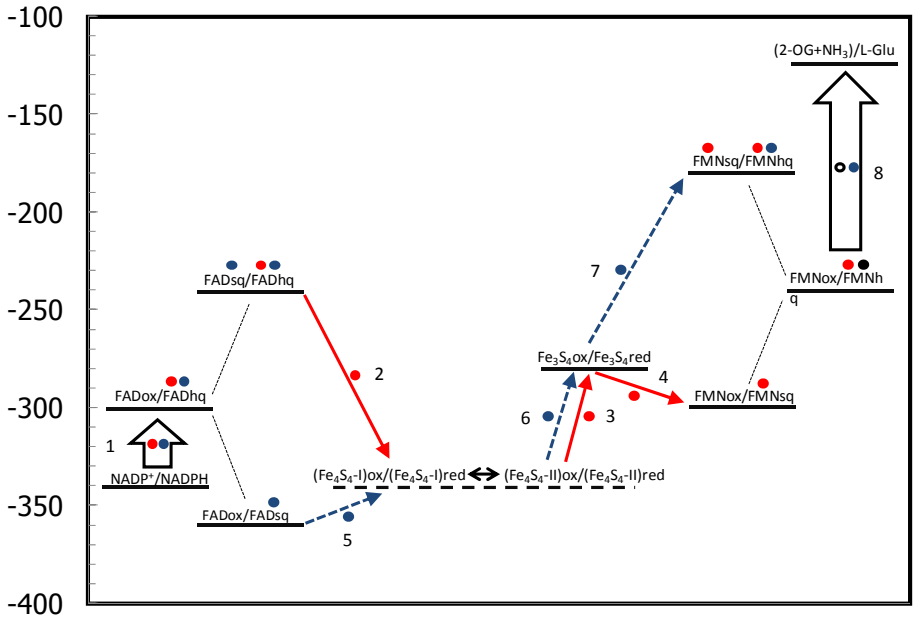

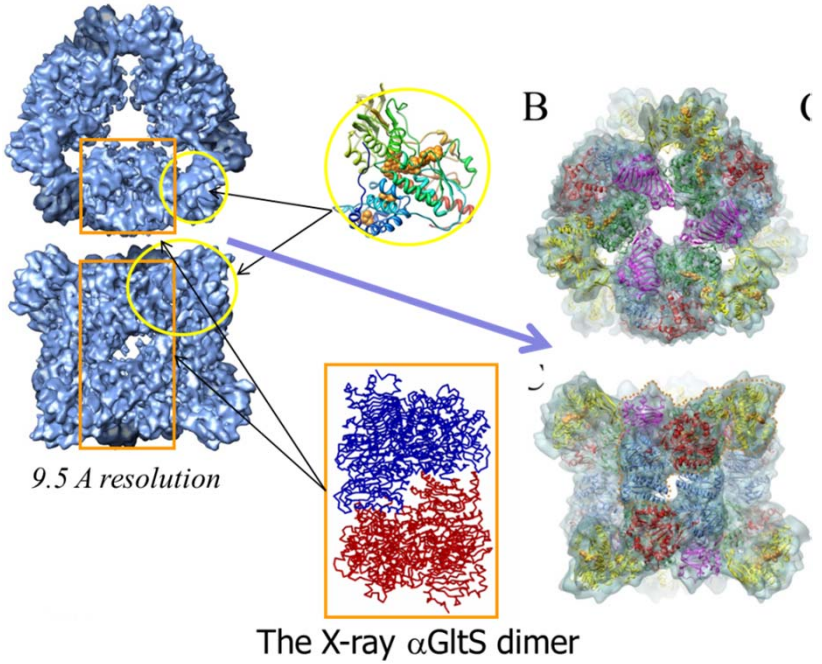

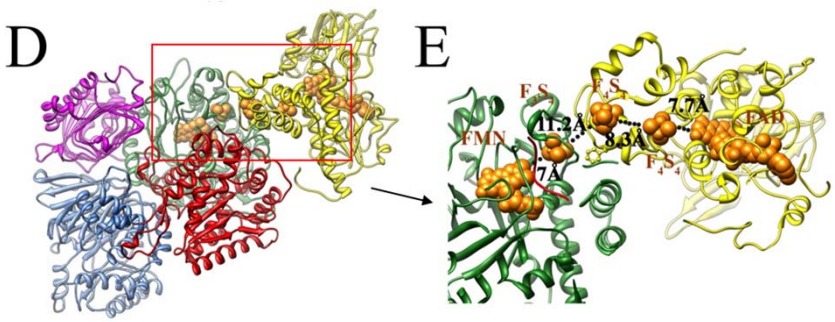

•Cottevieille et al. (2008) JBC The subnanometer resolution structure of the glutamate synthase 1.2 MDa hexamer by cryo-electron microscopy and its oligomerization behavior in solution: functional implications.

NADPH titrations to study the properties of GltS Site 1, the NADPH oxidising site on NADPH-GltS β subunit

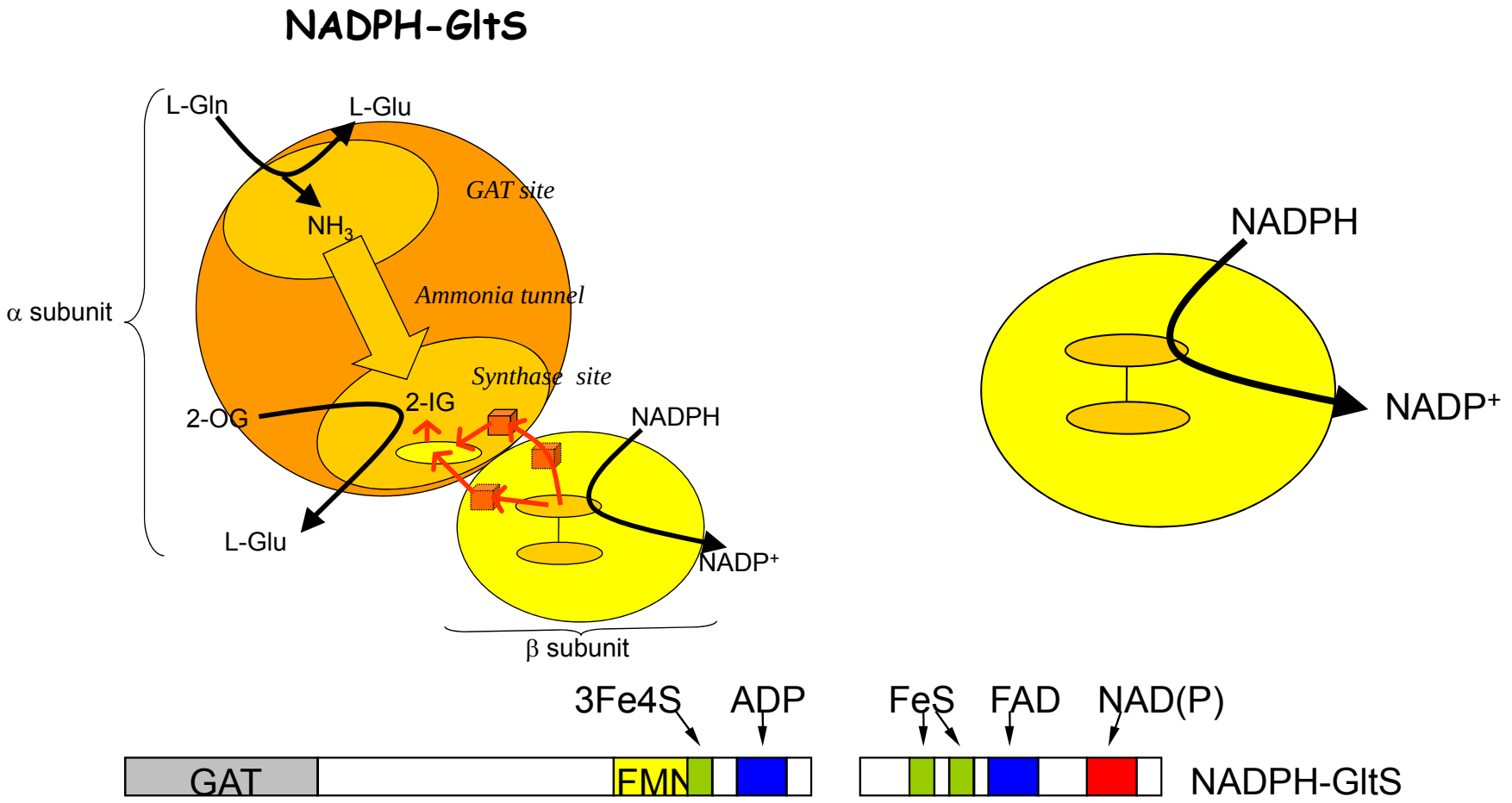

1) Express, purify and characterize the GltS β subunit
2) Identify the NADPH-binding site by characterizing the G298A variant

Anaerobic NADPH titration of β-GltS and the G298A variant

Wild-type: bound FAD is reduced by NADPH with formation of a stable FAD_{red}-$NADP^+$ charge-transfer complex

The substitution of the second G of the GXGXXA motif of the binding site of the adenylate portion of NADP

- weakens NADPH binding,
- prevents the formation of the CT complex, thus it
- alters the positioning of the nicotinamide ring

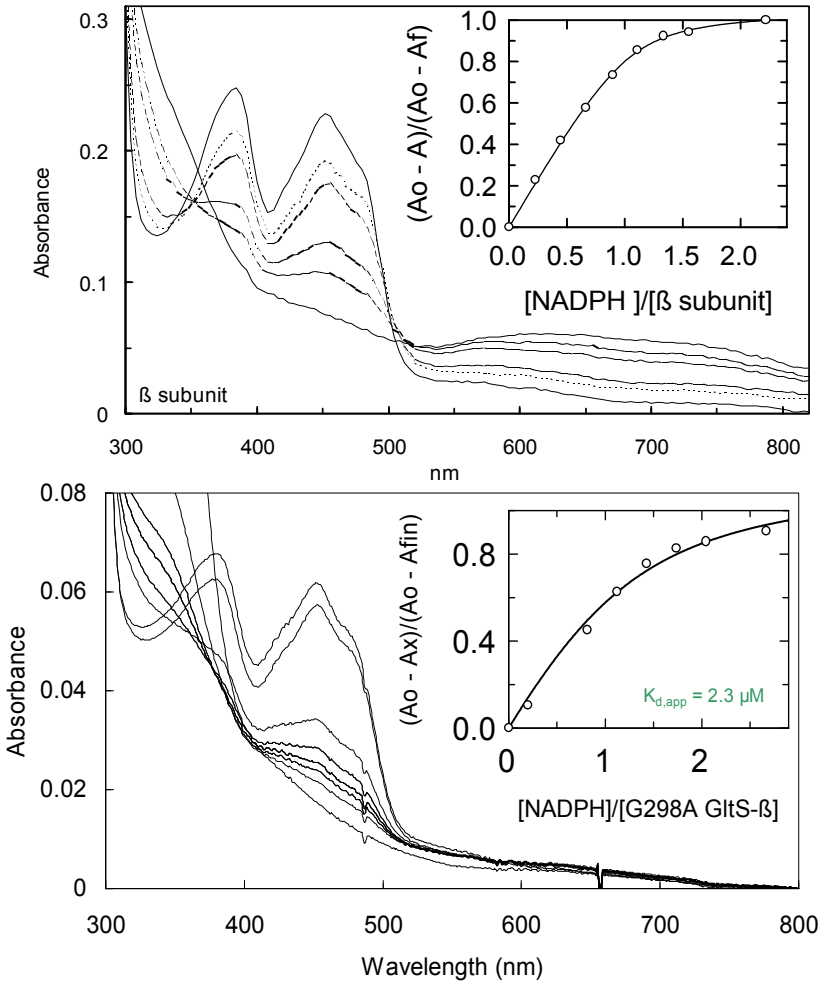

$$E\text{-}FAD + NADPH \rightleftharpoons E\text{-}FAD.NADPH \rightleftharpoons (E\text{-}FAD_{red}.NADP^+)CT$$

$$\rightleftharpoons E\text{-}FAD_{red}.NADP^+ \rightleftharpoons E\text{-}FAD_{red} + NADP^+$$

The structure of a charge-transfer complex betwen NAD(H) and FAD

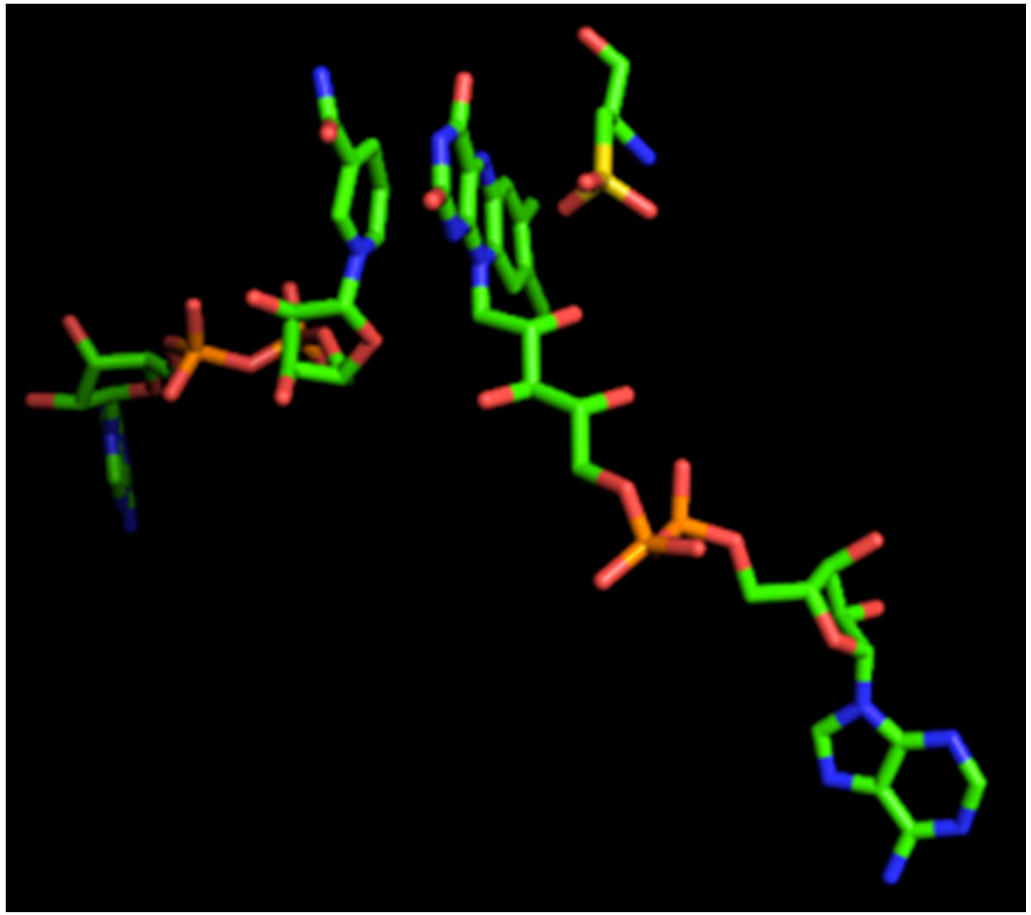

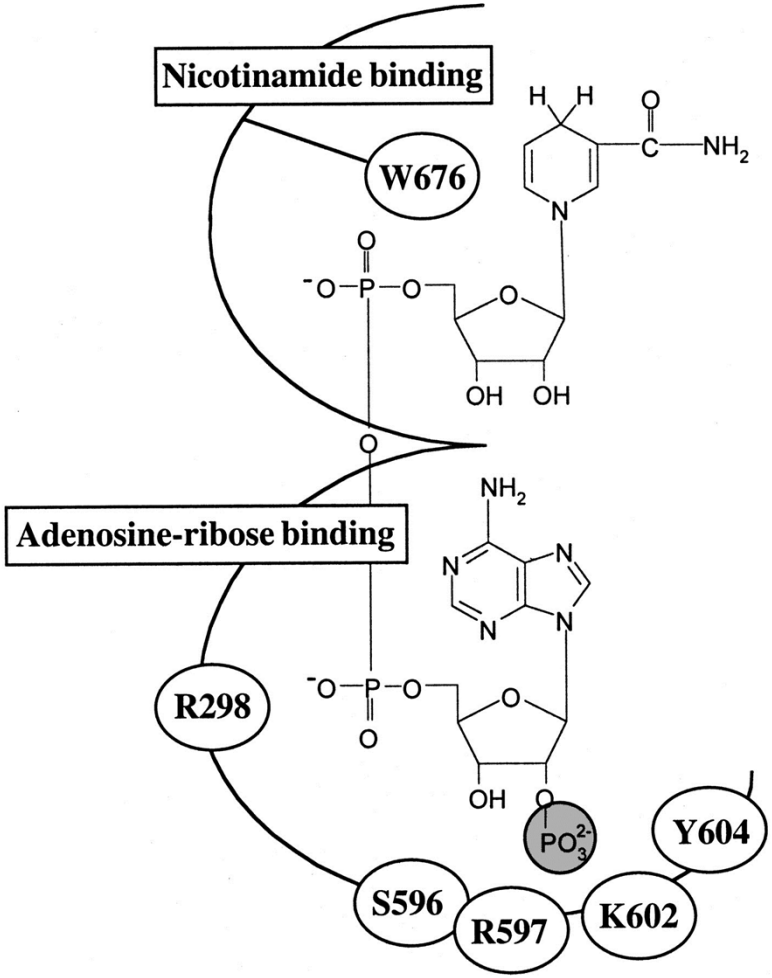

Scheme of «bipartite binding mechanism» of NADPH to spinach Ferredoxin NADPH reductase.

Information we can extract from steady-state kinetics:

Reaction mechanism,

Steady-state kinetic mechanism,

Position and structure of the transition state

Relative magnitude of rate constants

What may we miss?

Conformational changes part of the reaction mechanism

Reaction intermediates

Values of individual rate constants

Substrate/product/inhibitor binding constants

Rapid Reaction Kinetics.

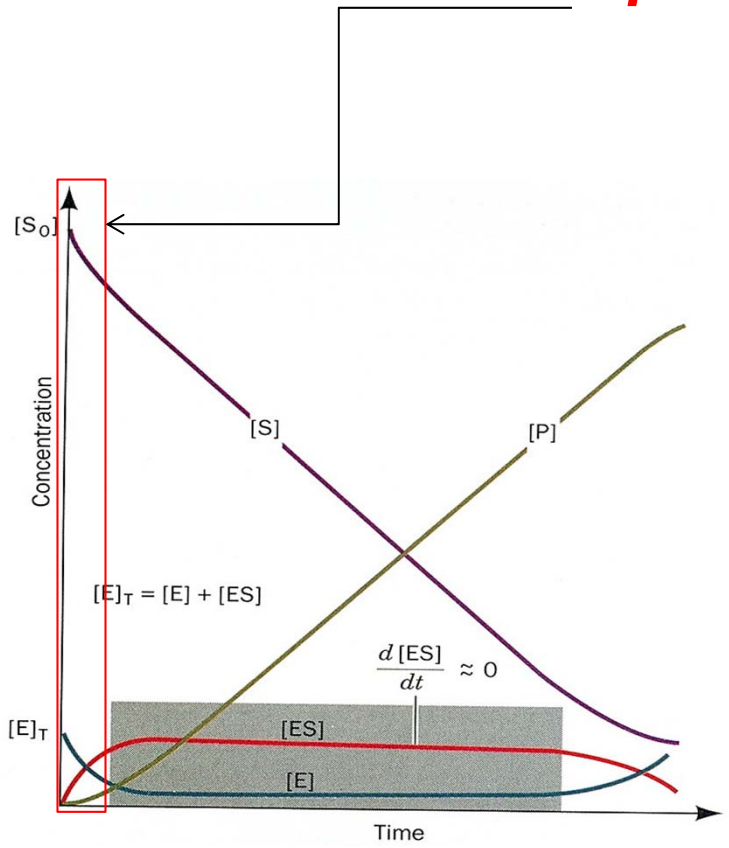

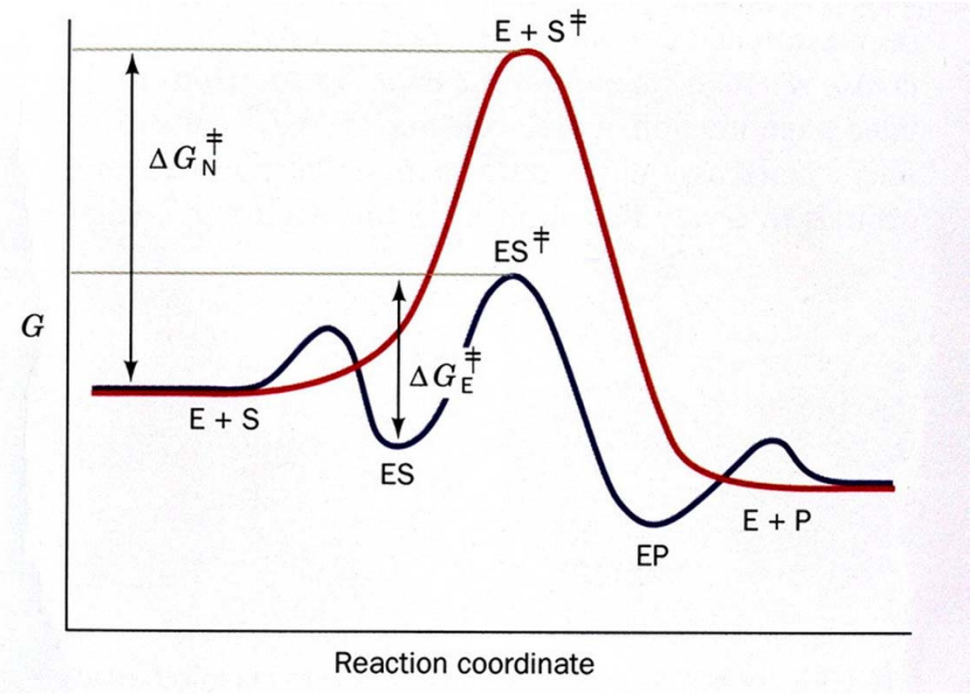

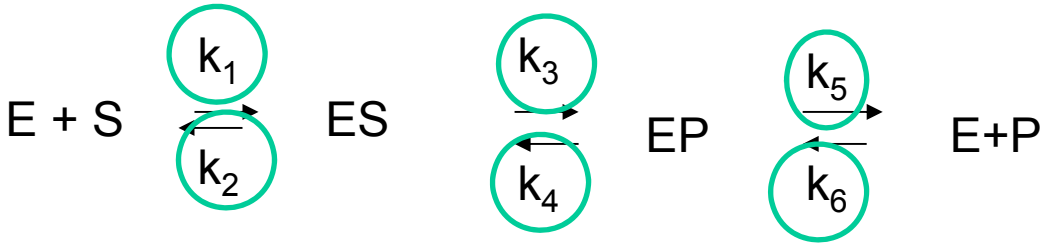

What can be measured by RR Kinetics?

Chemical reactions

Folding/Unfolding

Protein-protein, Protein-ligand interactions

Conformational changes

Rapid Reaction Kinetics - Pre-Steady-State Kinetics

[Enzyme] : μM, mM vs nM, μM for steady-state

[Substrate] : μM, mM

([S]> 10x [E] for pseudo-first order conditions)

Measuring Times: msec-sec vs sec-min for steady-state

Thus, need:

- large amounts of enzyme/protein & substrate/ligand
- highly concentrated protein/ligand solutions
- rapid mixing device
- rapid measuring times (in continuous methods)
- rapid data acquisition
- software (expertize) for data analysis

Stopped-flow set-up for rapid reaction studies and absorbance or fluorescence detection (also continuous flow and setups for chemical quench/freeze quench)

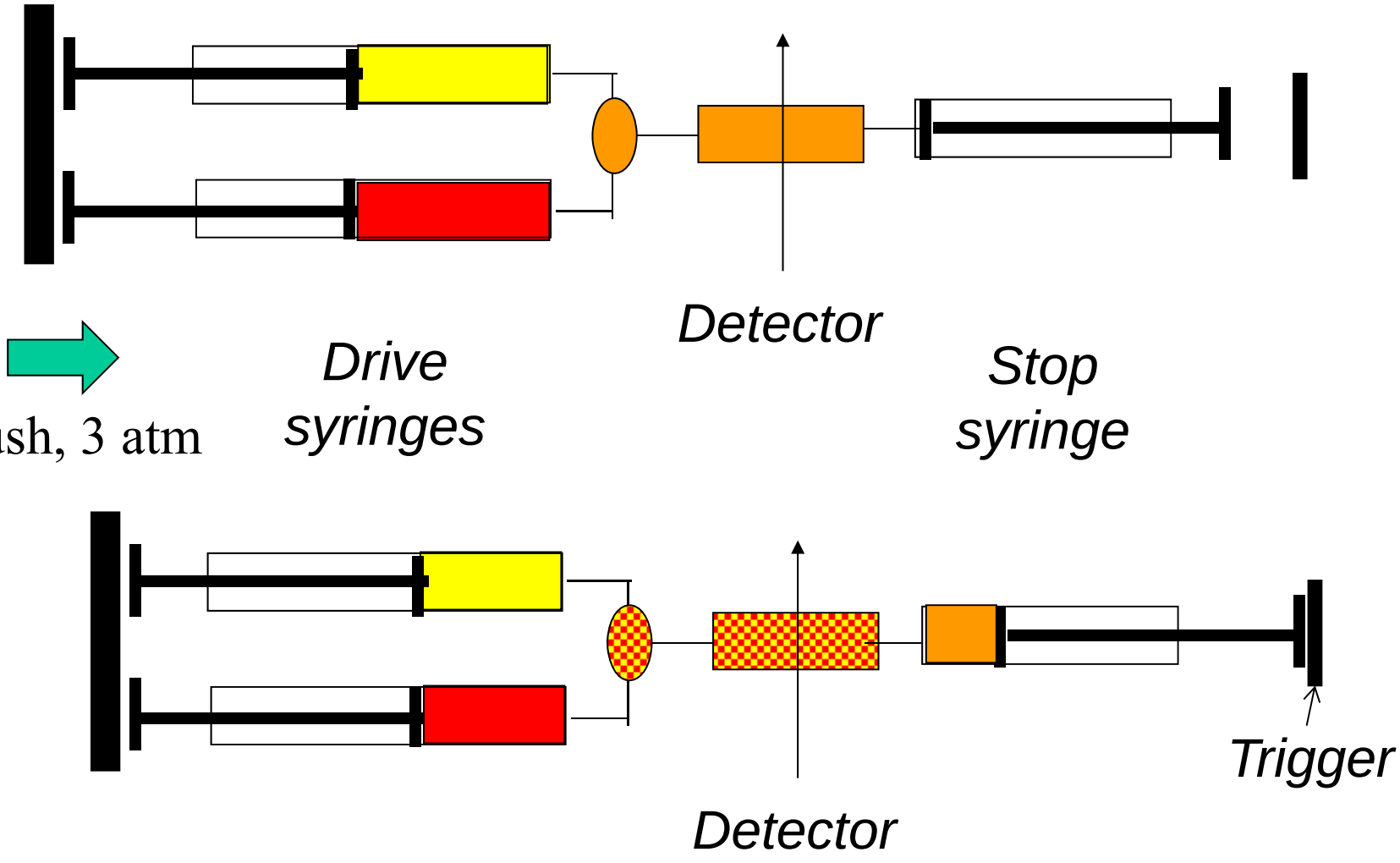

Rapid Mixing device

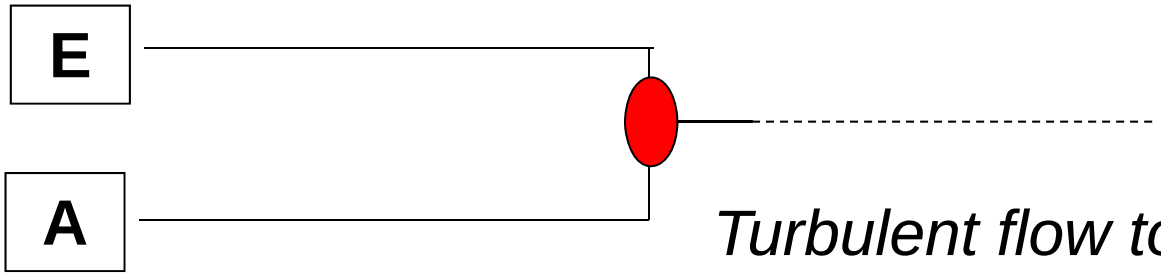

Turbulent flow to ensure constant velocity across tubing

High flow rate (e.g.:10 m/s = 1 cm/msec)

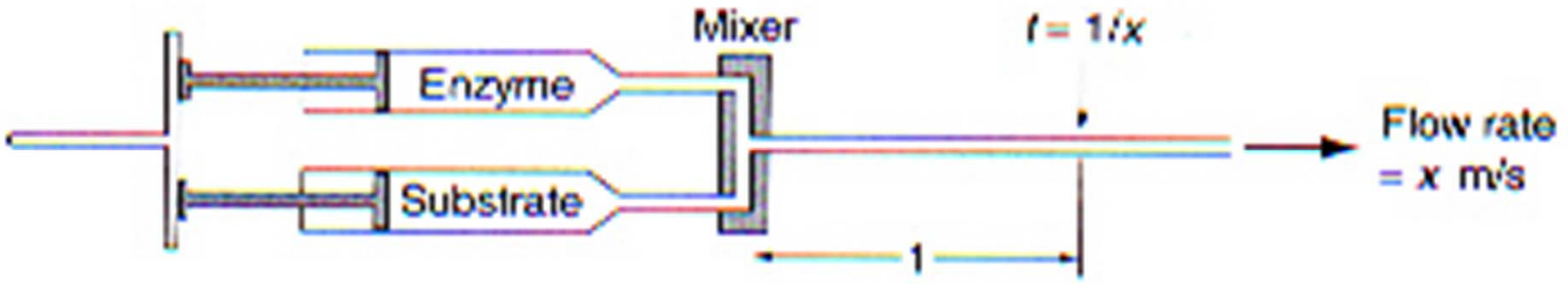

Figure 4.1 Continuous-flow apparatus.

Detection

Continuous methods:

Absorbance, Fluorescence, Circular Dichroism, Fluorescence anisotropy, conductivity, X-ray scattering (?)

Discontinuous methods:

EPR (freeze-quench)

Mossbauer (freeze-quench)

HPLC separation of reaction components and chemical analysis (chemical quench)

The upper limit of measured rates is set by:

Dead-time, Time-constant (Time Resolution), Sensitivity of detector

Dead-time

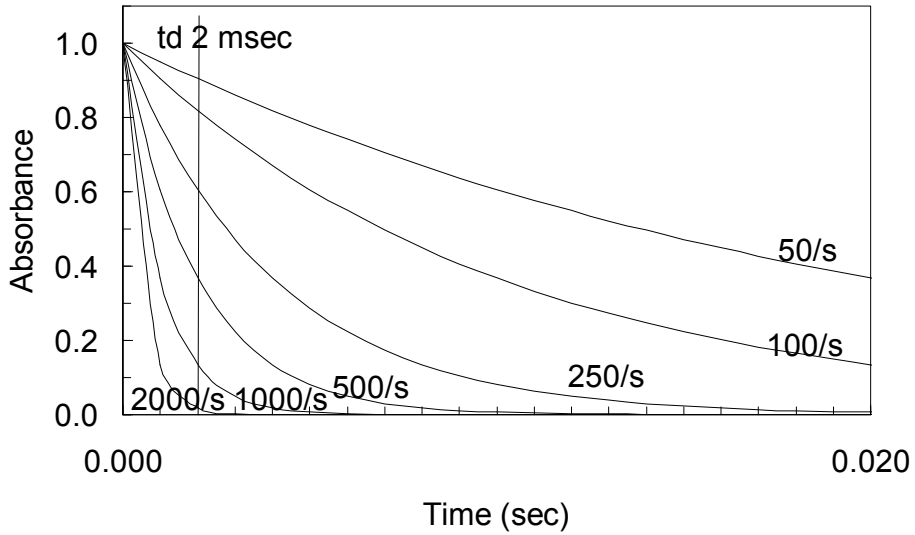

Time-constant (Resolution)

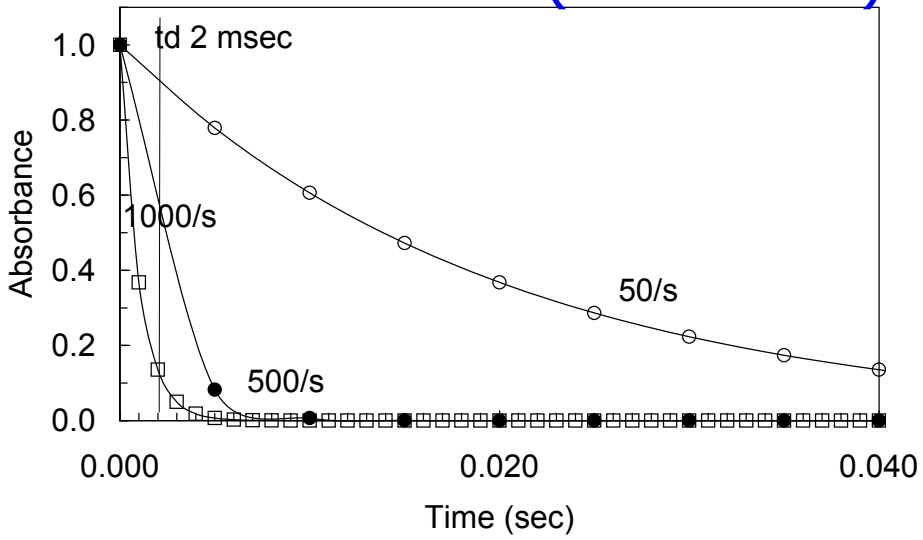

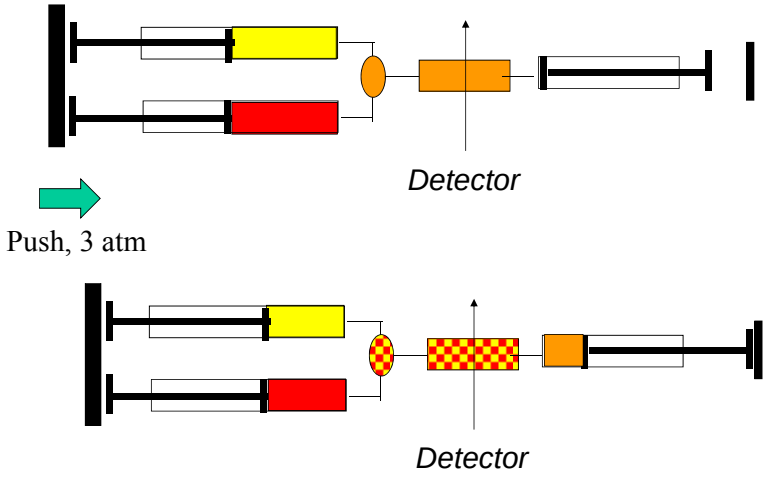

Single Mixing Stopped-flow

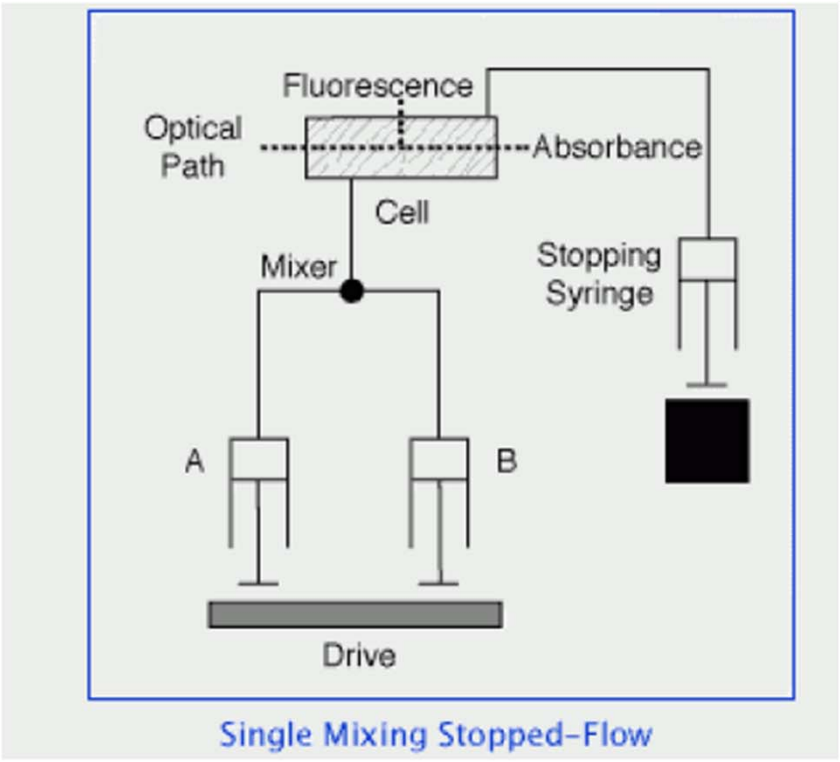

Single Mixing Stopped-Flow

$E + S \longrightarrow$

Double Mixing Stopped-flow

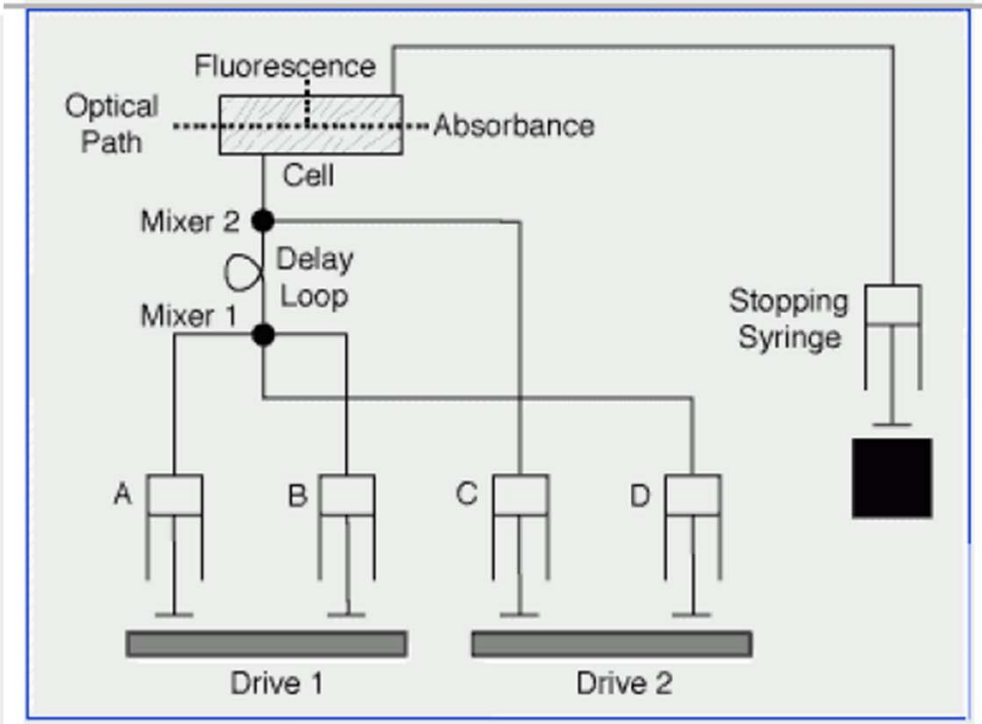

Double Mixing Stopped-Flow

$E + S_1 \longrightarrow ES_1$

Aging time, varies

$ES_1 + S_2$ (or I, or ....) $\longrightarrow$

To directly measure the rates of formation/decay of the various species we need to identify suitable wavelengths for analyses

$$A \xrightarrow{k_1} B \xrightarrow{k_2} C$$

$$A = A_o\, e^{-k1t}$$

$$B = A_o k_1/(k_2-k_1)(e^{-k1t} - e^{-k2t})$$

$$C = A_o[1 + 1/(k_1 - k_2)(k_2 e^{-k1t} - k_1\, e^{-k2t})$$

$$I_{\lambda,A} = [A]^* \varepsilon_{\lambda,A}$$

$$I_{\lambda B} = [B]^* \varepsilon_{\lambda,B}$$

$$I_{\lambda C} = [C]^* \varepsilon_{\lambda,C}$$

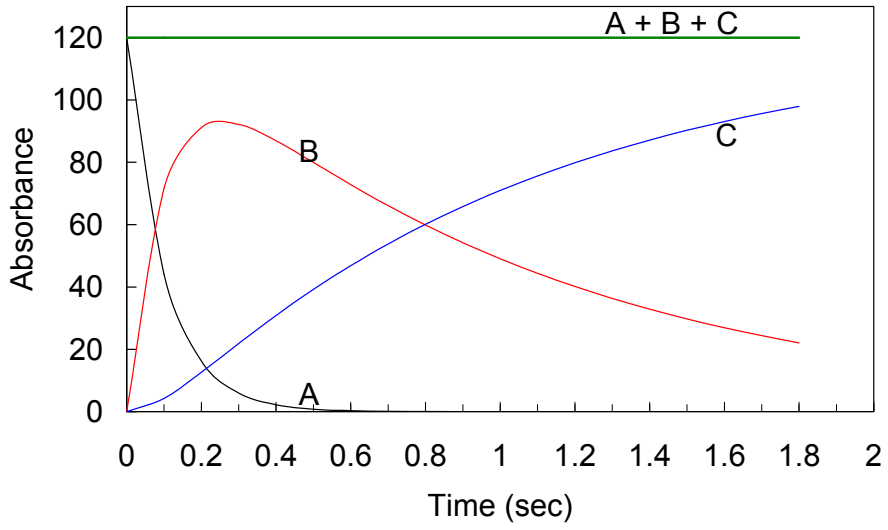

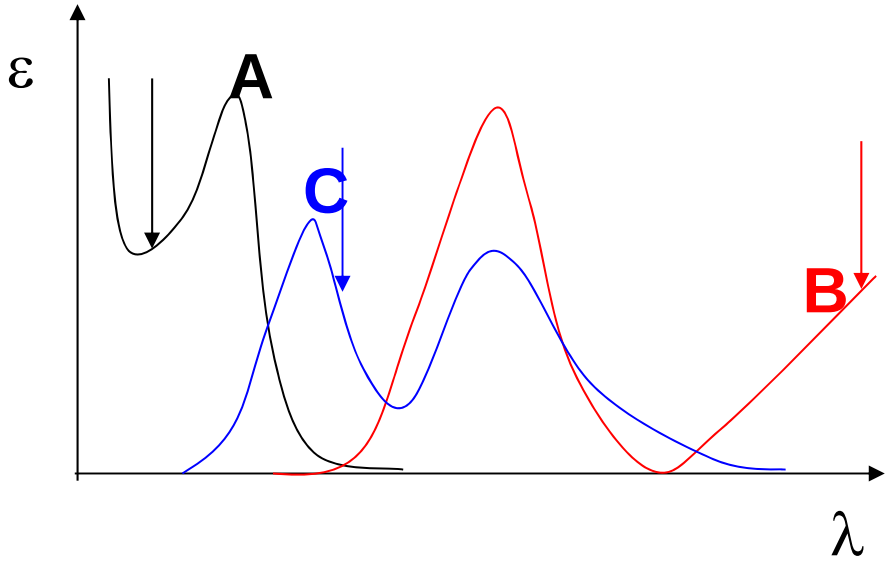

Green: At a given wavelength A, B, C have the same extinction coefficient

At different wavelengths: we can distinguish A from B from C

Catalytic competence of the NADPH oxidising site of the isolated GltS β subunit

Measurement of the rate of FAD reduction by NADPH in the stopped-flow

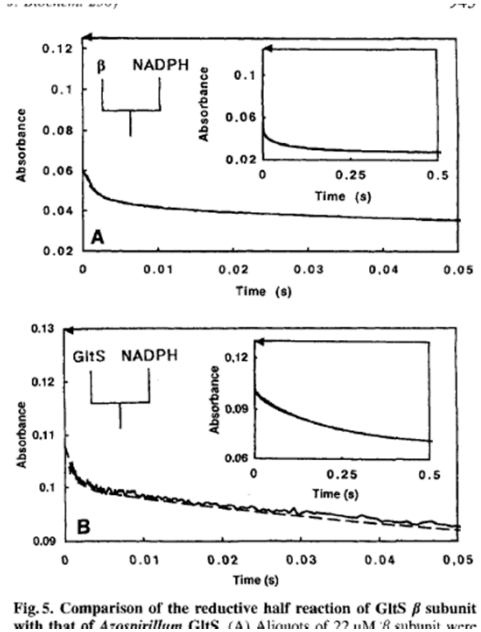

Fig. 5. Comparison of the reductive half reaction of GltS β subunit with that of *Azospirillum* GltS. (A) Aliquots of 22 μM β subunit were

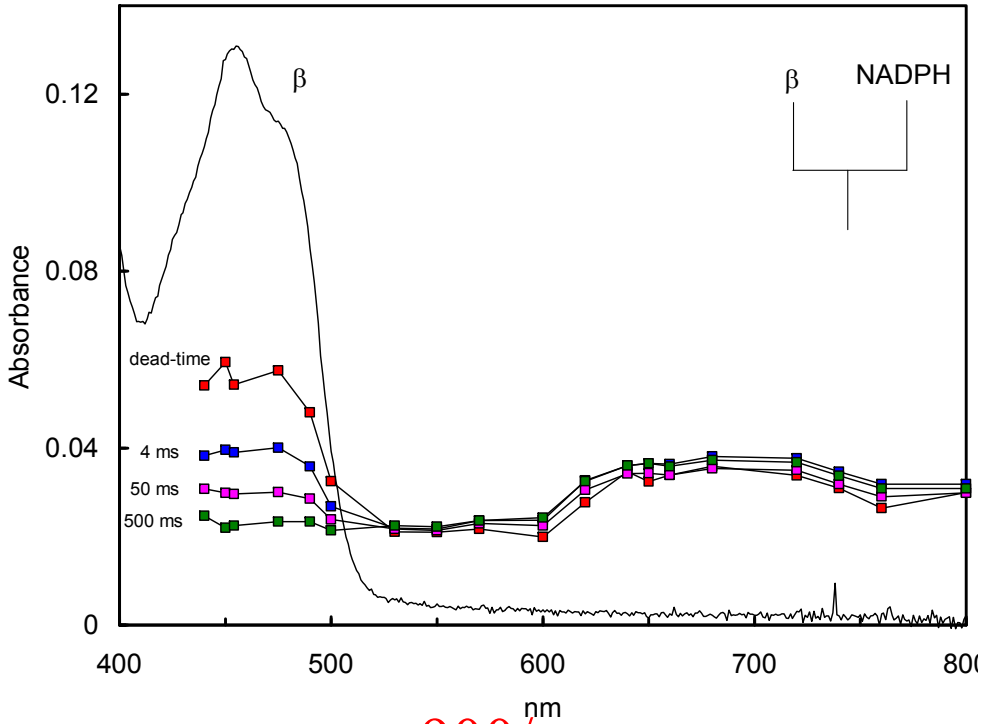

$$\textbf{E-FAD} + \text{NADPH} \rightleftharpoons \text{E-FAD.NADPH} \overset{900/s}{\rightleftharpoons} \textbf{(E-FAD}_{\textbf{red}}\textbf{.NADP}^{+}\textbf{)}_{\textbf{CT}}$$

$$\rightleftharpoons \text{E-FAD}_{red}\text{.NADP}^{+} \rightleftharpoons \text{E-FAD}_{red} + \text{NADP}^{+}$$

Is there a charge-transfer complex between E_{ox} and NADPH prior to electron transfer? Enzyme reduction is too fast to detect such a CT.

Diode array set-up is slower than PMT mode but monitors entire spectrum:

- Interesting/informative wavelengths can be selected later ;
- global analysis can be applied also combining data from rapid reaction and static experiments (starting/final spectra of Eox, Ered)

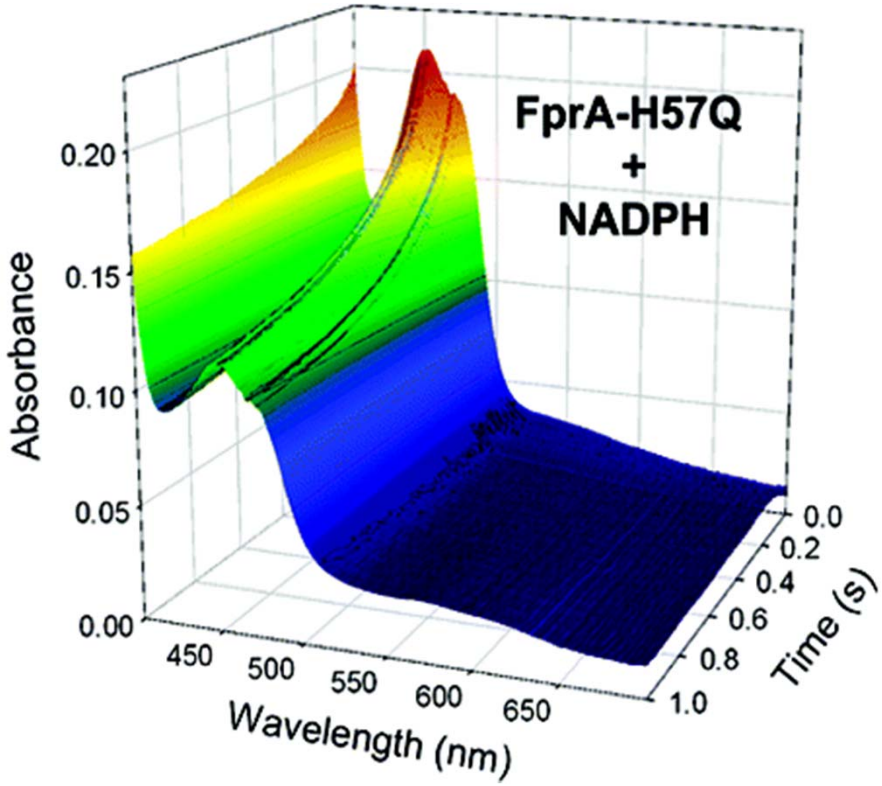

Software for global analysis

- Import data from spectrophotometers and stopped-flow
- Built in mechanisms
- Can write your own mechanism

KinSim
Spectfit
Reacti-Lab,
etc

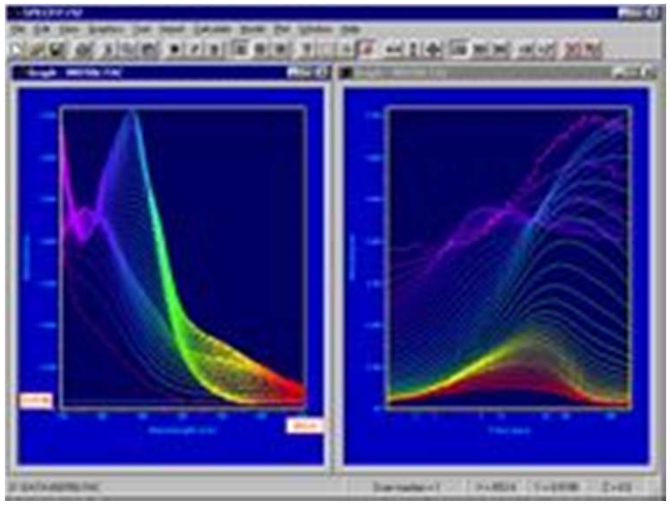

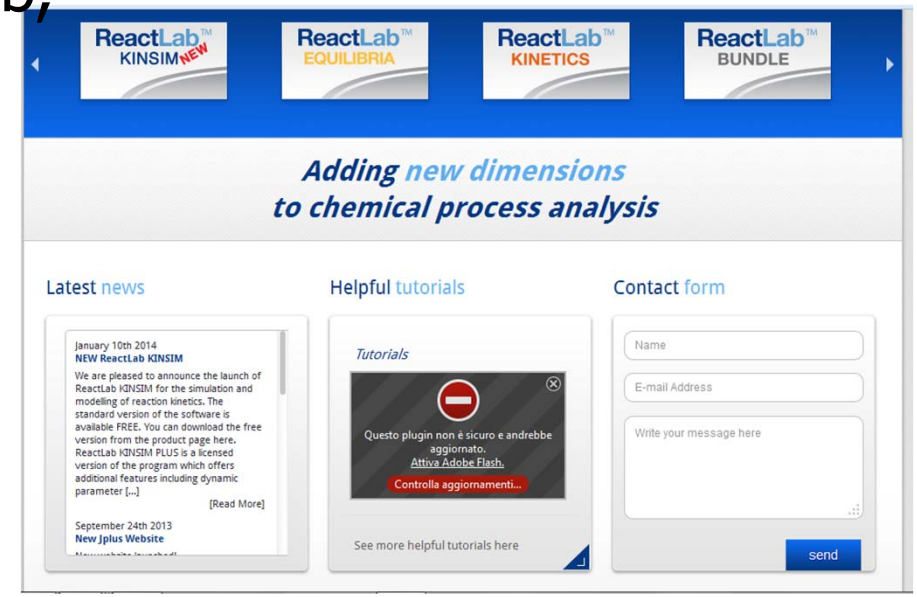

http://jplusconsulting.com/support/videos/

Video Article

Monitoring the Reductive and Oxidative Half-Reactions of a Flavin-Dependent Monooxygenase using Stopped-Flow Spectrophotometry

Elvira Romero, Reeder Robinson, Pablo Sobrado
Department of Biochemistry, Virginia Polytechnic Institute and State University

Correspondence to: Pablo Sobrado at psobrado@vt.edu

URL: http://www.jove.com/video/3803/
DOI: 10.3791/3803

calculated. The slow rate of the reoxidation obtained (0.006 s^{-1}) indicates that the C4a-hydroperoxyflavin is very stable in absence the ornithine.

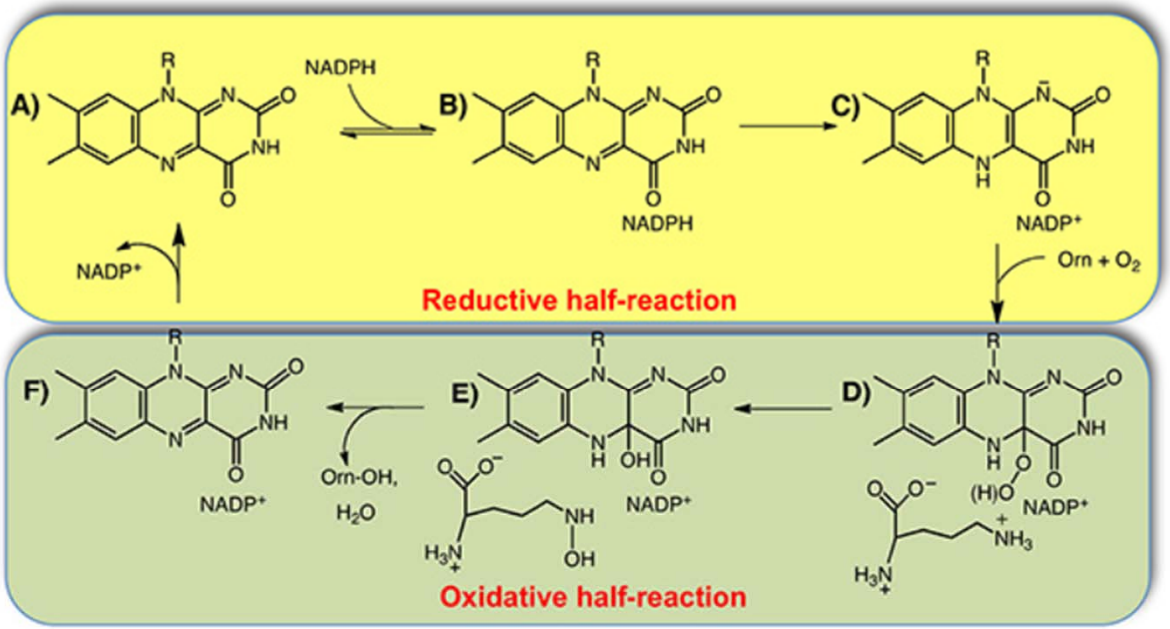

Scheme 1. Mechanism of *Af* SidA. The isoallozaxine ring of the FAD cofactor is shown. The oxidized flavin (A) binds to NADPH (B) and reacts to form reduced flavin and $NADP^+$ (C). After reaction with molecular oxygen and binding of ornithine, the C4a-hydroperoxyflavin is formed (D). This is the hydroxylating species. After hydroxylation of ornithine, the hydroxyflavin (E) must be dehydrated to form the oxidized enzyme. $NADP^+$ remains bound throughout the catalytic cycle and is the last product to be released (F).

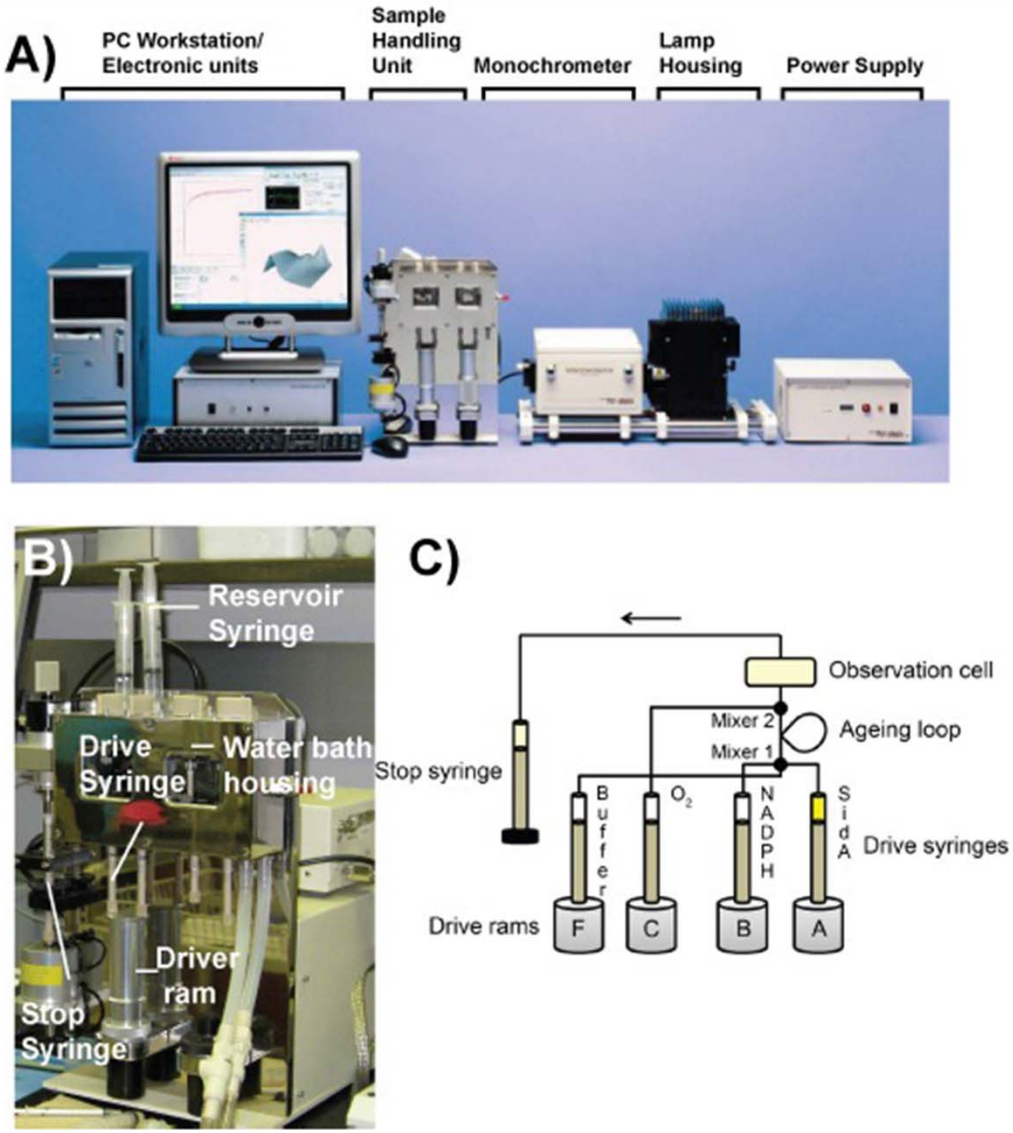

Figure 1. The stopped-flow instrument. A) Picture of the components of the Applied Photophysics SX20 stopped-flow spectrophotometer. B) Picture of the sample handling unit. C) Scheme of the flow circuit in double mixing mode.

Reductive half-reaction of SidA (in the absence of the ornithine substrate and oxygen)

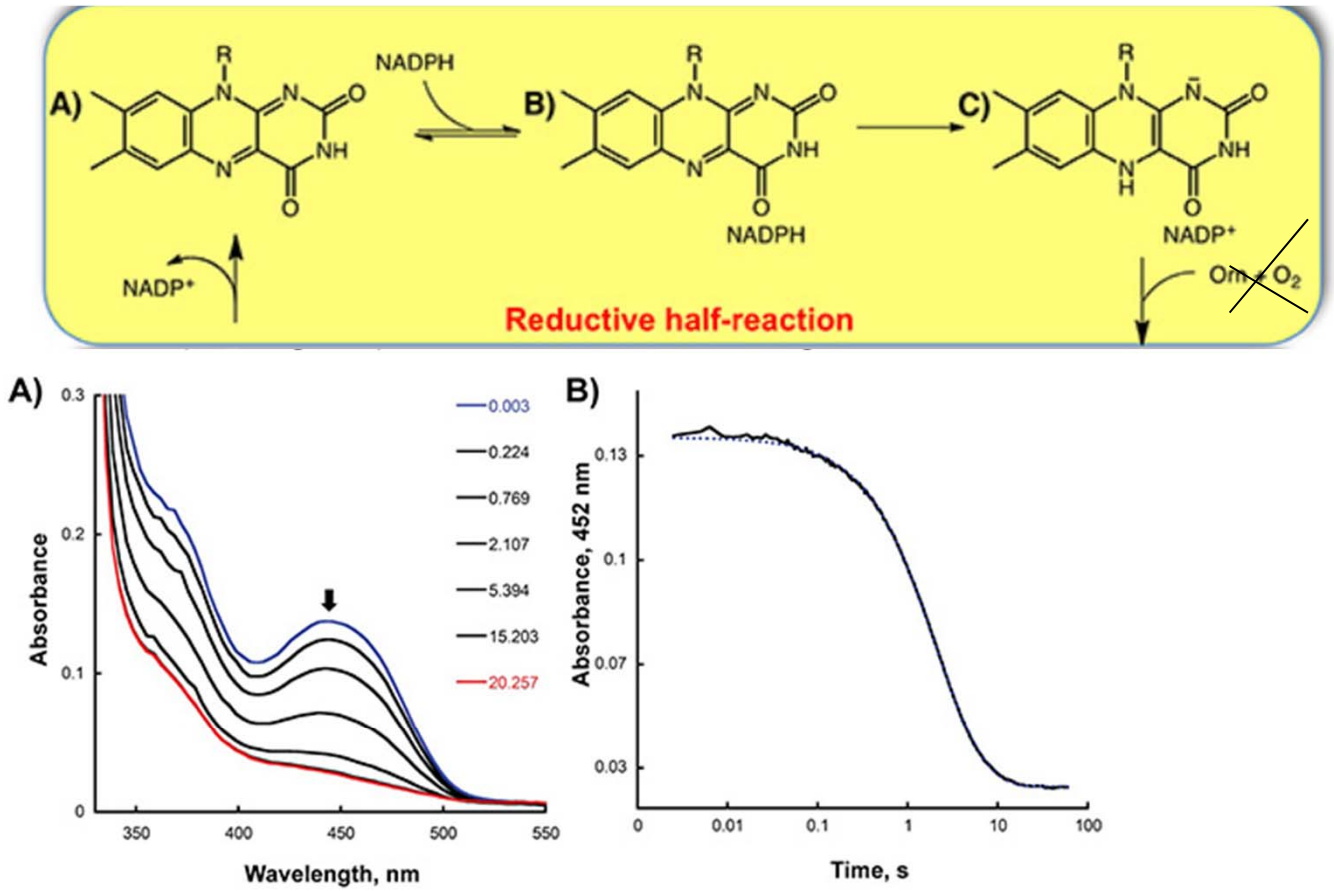

Figure 2. Anaerobic reduction of SidA with NADPH in the stopped-flow instrument. A) Spectral changes recorded after mixing equal volumes of 30 μM SidA and 45 μM NADPH. The first spectrum (oxidized SidA) and last spectrum (fully reduced SidA) is highlighted in blue and red, respectively. B) Absorbance trace at 452 nm recorded as a function of time.

$SidA_{red}$ $Ornithine + O_2$

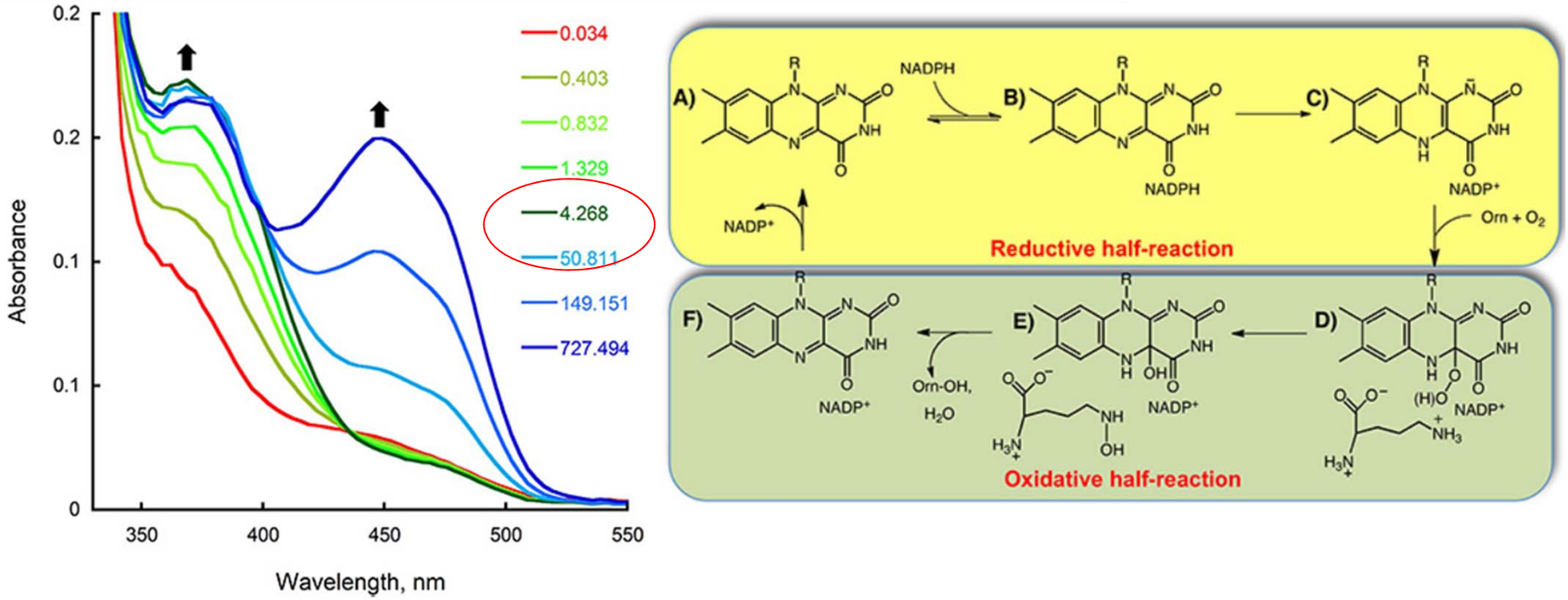

Figure 3. Oxidation of SidA in the stopped-flow instrument. A) Spectral changes recorded after mixing equal volumes of the fully reduced SidA and oxygenated buffer. The final concentrations were 15 µM SidA, 22.5 µM NADPH, and 0.95 mM oxygen. The spectrum recorded at 0.034, 4.268, and 727.494 s corresponds to the fully reduced enzyme, the C4a-hydroperoxyflavin intermediate (λ_{max} of 380 nm), and the oxidized enzyme (λ_{max} of 450 nm), respectively. B) Absorbance trace at 382 and 452 nm recorded as a function of time.

Reaction of reduced 3HB6H enzyme in the presence of 3HB

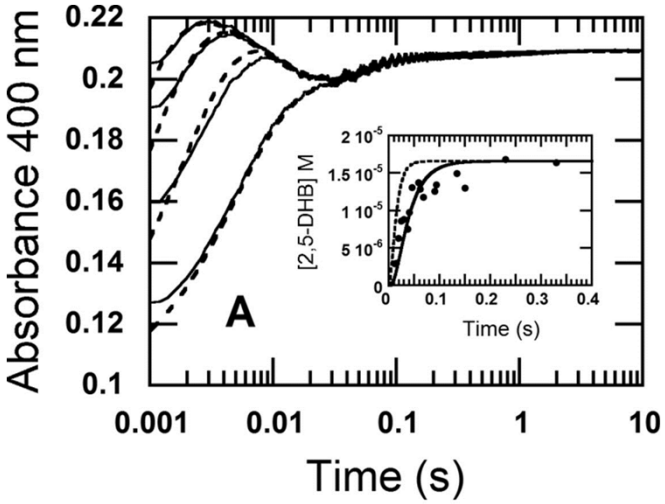

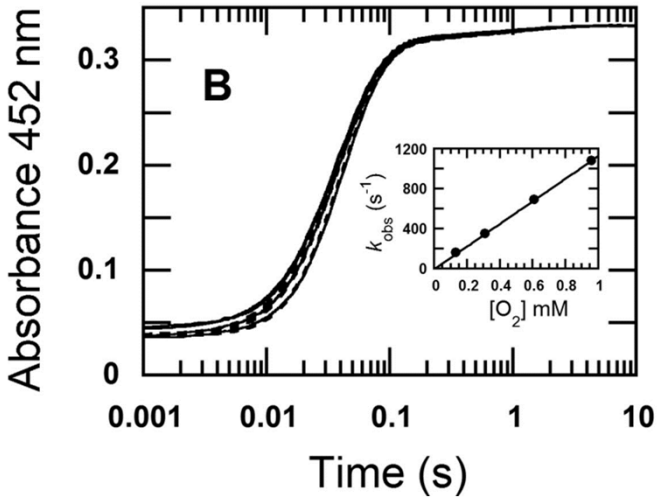

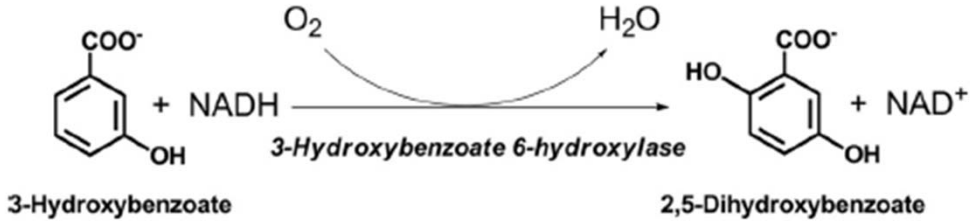

FIGURE 1. **Catalytic reaction of 3HB6H.**

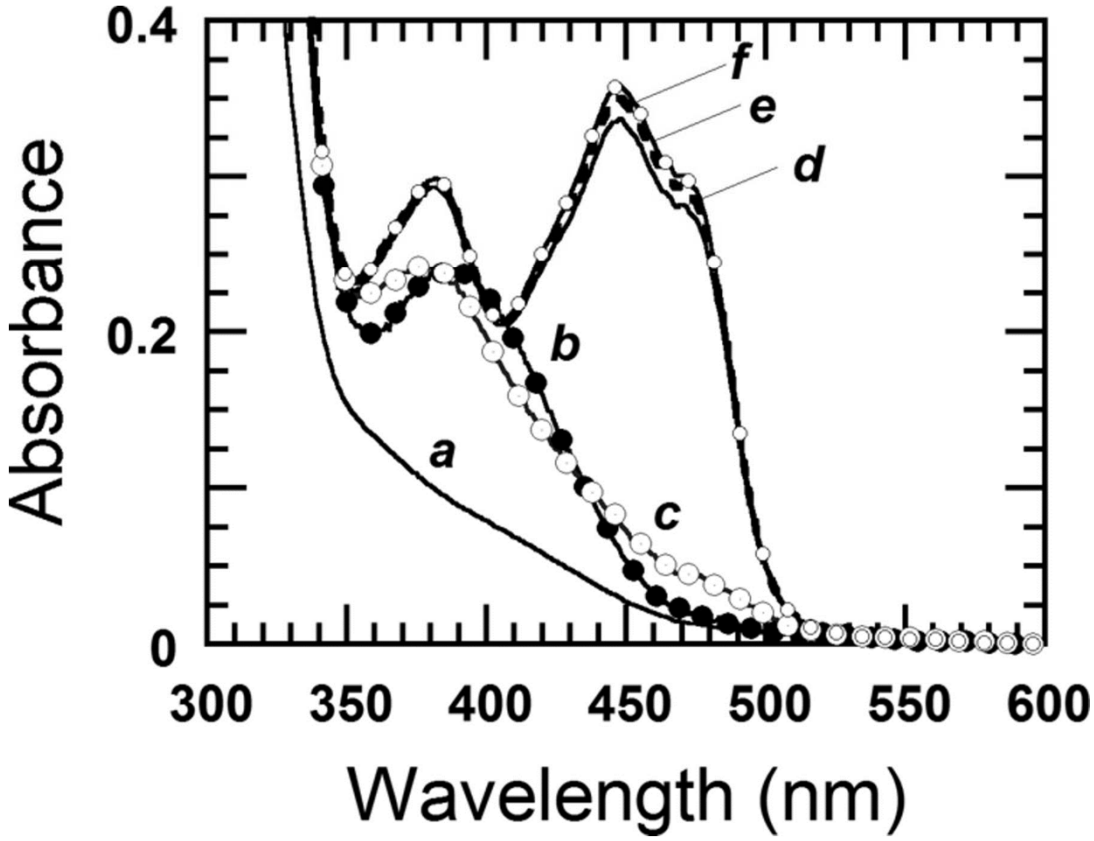

Sucharitakul J et al. J. Biol. Chem. 2013;288:35210-35221

jbc

The kinetic mechanism for the overall reaction of 3HB6H.

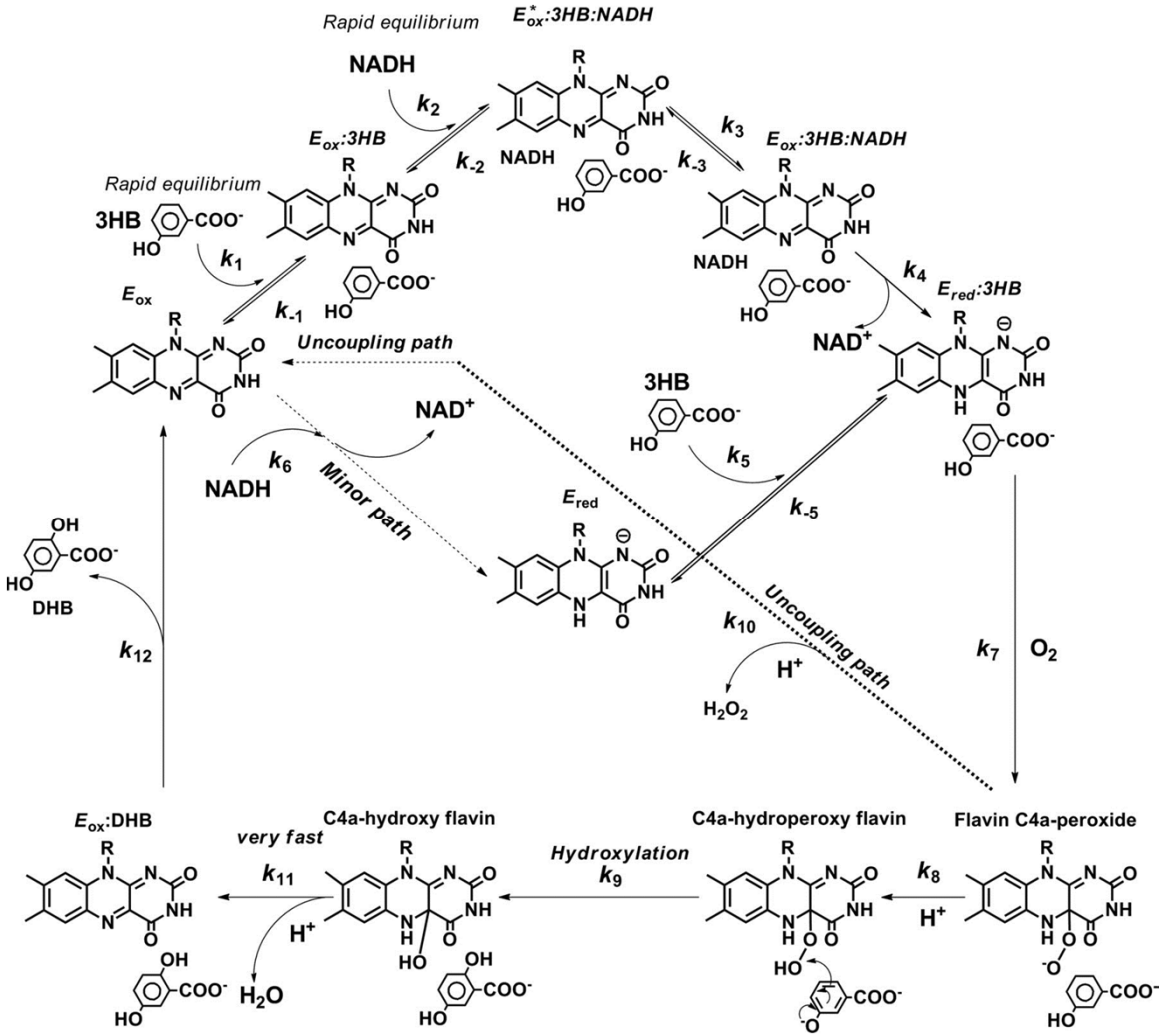

Sucharitakul J et al. J. Biol. Chem. 2013;288:35210-35221

jbc

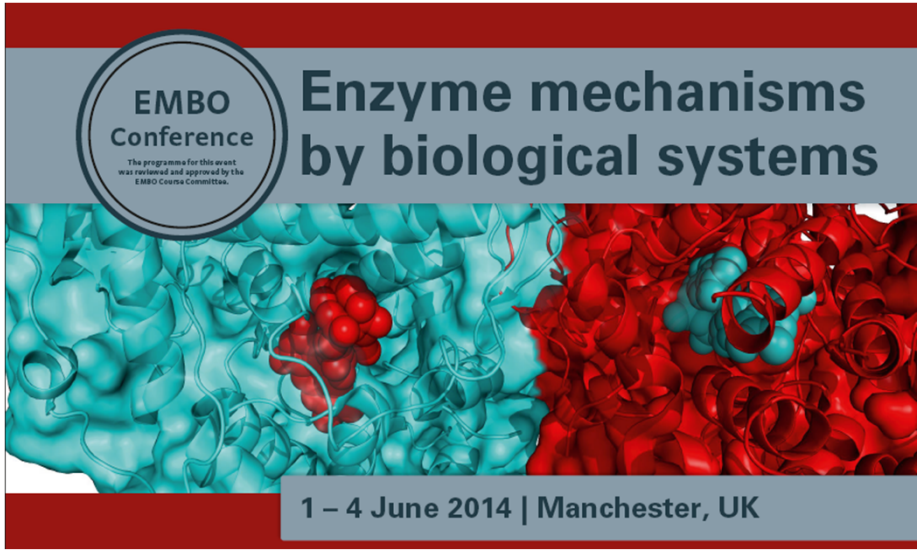
EMBO
Conference
The programme for this event was reviewed and approved by the EMBO Course Committee.
Enzyme mechanisms by biological systems
1 – 4 June 2014 | Manchester, UK

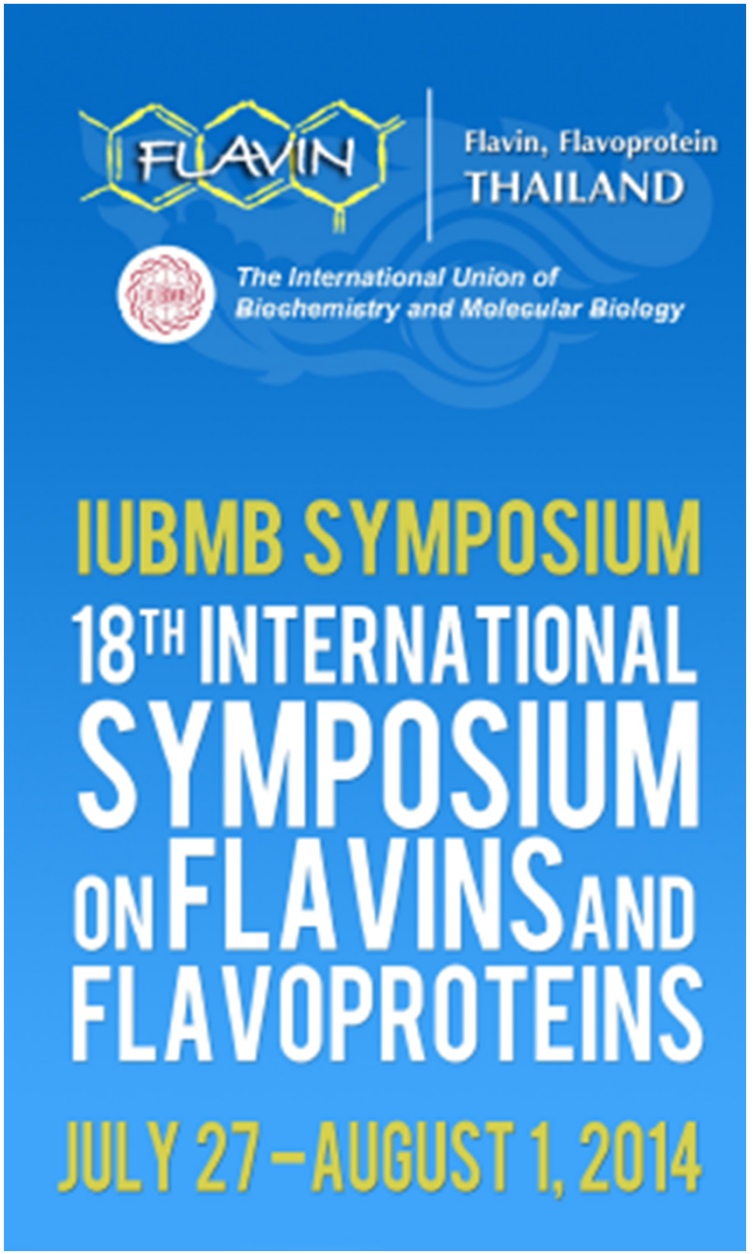
FLAVIN
Flavin, Flavoprotein
THAILAND
The International Union of Biochemistry and Molecular Biology
IUBMB SYMPOSIUM
18TH INTERNATIONAL
SYMPOSIUM
ON FLAVINS AND
FLAVOPROTEINS
JULY 27 – AUGUST 1, 2014